

Doctorate Program in Molecular Oncology and Endocrinology

XVIII cycle - 2002–2006
Coordinator: Prof. Giancarlo Vecchio

“New genes involved in the neoplastic transformation of the thyroid gland”

Pierlorenzo Pallante

University of Naples Federico II
Dipartimento di Biologia e Patologia Cellulare e Molecolare
“L. Califano”

Administrative Location

Dipartimento di Biologia e Patologia Cellulare e Molecolare “L. Califano”
Università degli Studi di Napoli Federico II

Partner Institutions

Italian Institutions

Università di Napoli “Federico II”, Naples, Italy
Istituto di Endocrinologia ed Oncologia Sperimentale “G. Salvatore”, CNR, Naples, Italy
Seconda Università di Napoli, Naples, Italy
Università del Sannio, Benevento, Italy
Università di Genova, Genoa, Italy
Università di Padova, Padova, Italy

Foreign Institutions

Johns Hopkins University, Baltimore, MD, USA
National Institutes of Health, Bethesda, MD, USA
Ohio State University, Columbus, OH, USA
Université Paris Sud XI, Paris, Francia

Supporting Institutions

Università di Napoli “Federico II”, Naples, Italy
Ministero dell’Istruzione, dell’Università e della Ricerca
Istituto Superiore di Oncologia (ISO)
Polo delle Scienze e delle Tecnologie per la Vita, Università di Napoli “Federico II”
Polo delle Scienze e delle Tecnologie, Università di Napoli “Federico II”
Terry Fox Foundation
Istituto di Endocrinologia ed Oncologia Sperimentale “G. Salvatore”, CNR, Naples, Italy
Centro Regionale di Competenza in Genomica (GEAR)

Faculty

Italian Faculty

Giancarlo Vecchio, MD, Co-ordinator

Francesco Beguinot, MD

Angelo Raffaele Bianco, MD

Francesca Carlomagno, MD

Gabriella Castoria, MD

Angela Celetti, MD

Fortunato Ciardiello, MD

Sabino De Placido, MD

Pietro Formisano, MD

Massimo Imbriaco, MD

Paolo Laccetti, MD

Antonio Leonardi, MD

Barbara Majello, PhD

Rosa Marina Melillo, MD

Claudia Miele, PhD

Pacelli Roberto, MD

Giuseppe Palumbo, PhD

Silvio Parodi, MD

Renata Piccoli, PhD

Giuseppe Portella, MD

Antonio Rosato, MD

Massimo Santoro, MD

Giampaolo Tortora, MD

Donatella Tramontano, PhD

Giancarlo Troncone, MD

Bianca Maria Veneziani, MD

Foreign Faculty

National Institutes of Health (USA)

Michael M. Gottesman, MD

Silvio Gutkind, PhD

Derek LeRoith, MD

Stephen Marx, MD

Ira Pastan, MD

Johns Hopkins University (USA)

Vincenzo Casolaro, MD

Pierre Coulombe, PhD

James G. Herman MD

Robert Schleimer, PhD

Ohio State University, Columbus (USA)

Carlo M. Croce, MD

Université Paris Sud XI, Paris, Francia

Martin Schlumberger, MD

**“New genes involved in
the neoplastic
transformation of the
thyroid gland”**

TABLE OF CONTENTS

LIST OF PUBLICATIONS	4
ABSTRACT	5
1. BACKGROUND	6
1.1 The thyroid gland.....	6
1.2 Thyroid follicular cell carcinomas.....	7
1.3 Microarray analysis of human carcinomas.....	9
1.4 UbcH10 and the Ubiquitin-Proteasome proteolytic pathway.....	10
1.5 UbcH10 involvement in cancer.....	12
1.6 CBX7 and Polycomb group genes.....	15
2. AIMS OF THE STUDY	19
3. MATERIALS AND METHOD	20
3.1 Cell culture and transfections.....	20
3.2 Human thyroid tissue samples.....	20
3.3 RNA isolation.....	20
3.4 Microarray analysis.....	20
3.5 Reverse transcriptase and PCR analysis.....	21
Reverse transcription.....	21
Selection of primers and probes for qRT-PCR.....	21
qRT-PCR.....	22
3.6 Protein extraction, Western blotting, and antibodies.....	22
3.7 Immunohistochemistry.....	22
Tissue samples.....	22
Immunostaining: technique, evaluation and statistical analysis.....	23
3.8 Thyroid Fine-Needle Aspiration Biopsies (FNAB).....	23
3.9 Loss-of-heterozygosity (LOH) analysis.....	24
3.10 Methylation analysis using bisulphite genomic sequencing.....	24
3.11 Plasmid constructs and cell colony-forming assay.....	24
3.12 Preparation of recombinant adenovirus and infection protocol.....	25
3.13 RNA interference.....	25
3.14 Assay of the transformed state.....	25
4. RESULTS AND DISCUSSION	27
4.1 Gene expression profile analysis of six thyroid carcinoma cell lines compared to normal human thyroid primary cells.....	27
4.2 Expression of UbcH10 gene in normal human thyroid cells and thyroid carcinoma cell lines.....	29
4.3 Analysis of UbcH10 expression in normal and neoplastic thyroid tissues by immunohistochemistry, Western blot and RT-PCR.....	30
4.4 UbcH10 expression in experimental models of thyroid carcinogenesis.....	34
4.5 Suppression of the UbcH10 synthesis inhibits thyroid carcinoma cell growth.....	35
4.6 UbcH10 overexpression is not sufficient to transform rat thyroid cells.....	37

4.7 UbcH10 involvement in ovarian carcinoma.....	38
4.8 CBX7 gene expression is down-regulated in human thyroid carcinoma cell lines.....	39
4.9 The loss of CBX7 expression correlates with a more aggressive phenotype of thyroid carcinomas.....	40
4.10 Analysis of CBX7 expression in normal and neoplastic thyroid tissues by semiquantitative RT-PCR and quantitative Real-Time PCR.....	41
4.11 Analysis of human thyroid fine-needle aspiration biopsy.....	43
4.12 LOH at CBX7 locus (22q13.1).....	44
4.13 Methylation status of the CBX7 gene.....	44
4.14 CBX7 expression in rat thyroid cells transformed by viral oncogenes.....	46
4.15 CBX7 expression in experimental mouse models of thyroid carcinogenesis.....	47
4.16 Restoration of CBX7 gene expression inhibits the growth of thyroid carcinoma cell lines.....	48
4.17 Generation of an adenovirus carrying the CBX7 gene.....	49
4.18 CBX7 deregulation in other cancers.....	49
5. CONCLUSIONS.....	52
6. ACKNOWLEDGEMENTS.....	54
7. REFERENCES.....	55

LIST OF PUBLICATIONS

This dissertation is based upon the following publications:

- ◆ Pallante P, Berlingieri MT, Troncone G, Kruhoffer M, Orntoft TF, Viglietto G, Caleo A, Migliaccio I, Decaussin-Petrucci M, Santoro M, Palombini L, Fusco A. UbcH10 overexpression may represent a marker of anaplastic thyroid carcinomas. *Br J Cancer*. 2005 Aug 22;93(4):464-71.
- ◆ Berlingieri MT, Pallante P, Guida M, Nappi C, Masciullo V, Scambia G, Ferraro A, Leone V, Sboner A, Barbareschi M, Ferro A, Troncone G, Fusco A. UbcH10 expression may be a useful tool in the prognosis of ovarian carcinomas. *Oncogene*. 2006 Oct 2; [Epub ahead of print].
- ◆ Pallante P, Berlingieri MT, Troncone G, Ferraro A, Pierantoni GM, Kruhoffer M, Iaccarino A, Russo M, Berger N, Leone V, Sacchetti S, Chiariotti L, Palombini L, Santoro M, Fusco A. Loss of the CBX7 gene correlates with a more malignant phenotype in thyroid cancer. (Manuscript submitted to *The Journal of Clinical Investigation*).
- ◆ Visconti R, Federico A, Coppola V, Pentimalli F, Berlingieri MT, Pallante P, Kruhoffer M, Orntoft TF, Fusco A. Transcriptional profile of Ki-Ras-induced transformation of thyroid cells. *Cancer Invest*. 2006 Accepted.

ABSTRACT

To identify the genes involved in the process of thyroid carcinogenesis we have analysed the gene expression profiles of six thyroid carcinoma cell lines compared with normal human thyroid primary cell culture using an Affymetrix HG_U95Av2 oligonucleotide array representing ~10.500 unique genes. These studies led to the identification of genes whose expression was up- or down-regulated in the carcinoma cell lines compared with a primary cell culture of normal thyroid origin.

We identified 510 up-regulated transcripts and 320 down-regulated transcripts with a fold change higher than 10 in all of the carcinoma cell lines. In particular our interest was focused on the genes whose expression was drastically (at least 10 fold) up- or down-regulated in all the cell lines, assuming that the genes altered in their expression in all of the thyroid carcinoma cell lines might represent candidate genes involved in thyroid cell transformation: these genes were UbcH10 (up-regulated) and CBX7 (down-regulated).

The UbcH10 gene, coding for a protein that belongs to the ubiquitin-conjugating enzyme family, was up-regulated by 150 fold in all of the carcinoma cell lines. CBX7, conversely, encodes a chromatin protein, probably involved in the compaction of heterochromatin: CBX7 resulted down-regulated about 20 fold in all the carcinoma cell lines analysed.

Expression analyses performed using several techniques such as RT-PCR and immunohistochemistry showed that the deregulation of these two genes was linked to the rising of a highly malignant phenotype of thyroid carcinomas. Moreover, functional studies performed on thyroid carcinoma cells clearly demonstrated that the deregulated expression of UbcH10 and CBX7 is really involved in the process of thyroid carcinogenesis and not only related to the malignant phenotype.

Taken together these results would indicate that UbcH10 and CBX7 expression is involved in thyroid cell proliferation and might represent a marker of thyroid malignant transformation, therefore, in conclusion, UbcH10 and CBX7 monitoring could contribute to thyroid cancer diagnosis and prognosis.

1. BACKGROUND

1.1 The thyroid gland

The thyroid gland is the largest endocrine organ in humans (Kondo et al. 2006). It is located in the neck region, on the anterior surface of the trachea, and is formed by two distinct cell types, the follicular cells (TFC) and the parafollicular or C cells (De Felice and Di Lauro 2004). The TFC constitute the most numerous cell population and form the thyroid follicles, spherical structures that store and release the thyroid hormones (Mauchamp et al. 1998). The C cells are located between follicles, mostly in a parafollicular position (Figure 1).

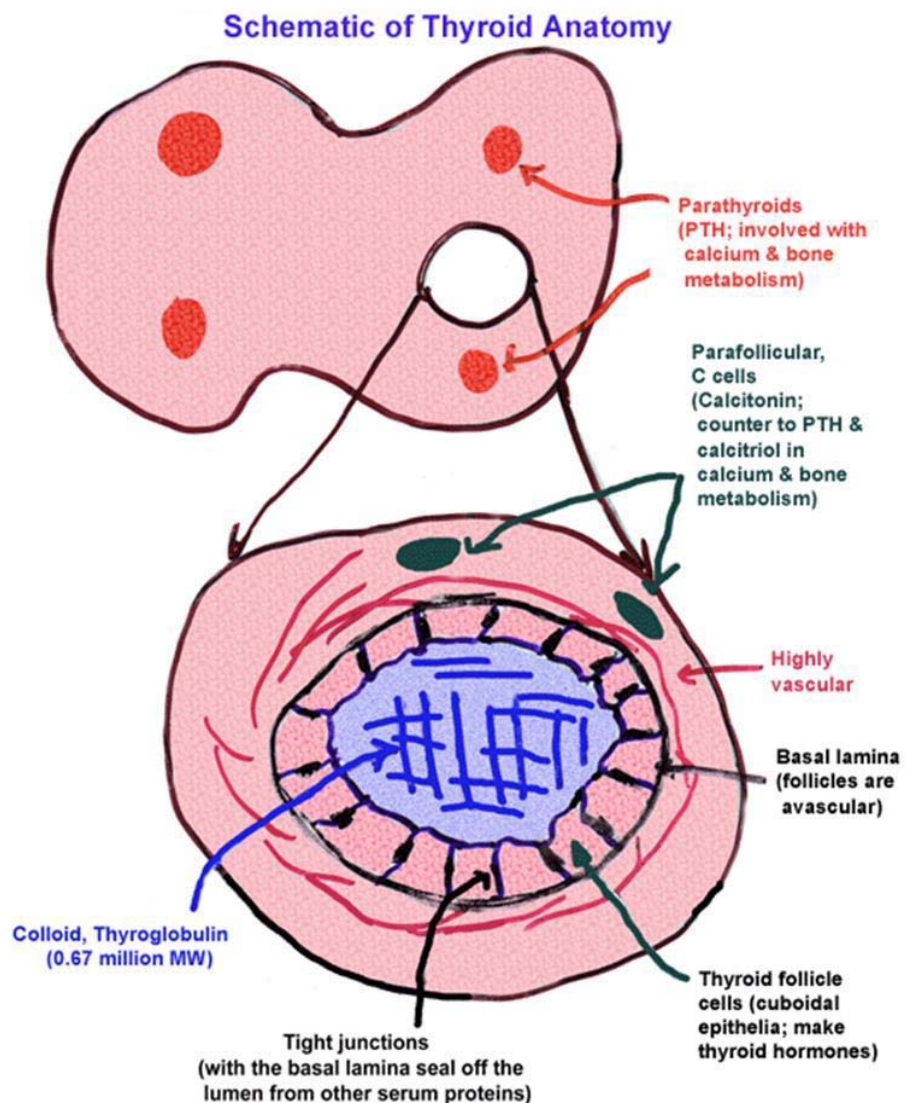


Figure 1 The general architecture of the thyroid gland. In the figure is shown the general architecture of the thyroid gland with the parafollicular cells interspersed in small groups among the follicles in the intermediate part of the thyroid lobes.

These two cell types take origine from two different embryological structures: the thyroid anlage for the TFC and the ultimobranchial bodies for the C cells. The thyroid anlage is an area enclosing a small group of endodermal cells, and it is located on the midline of the embryonic mouth cavity in its posterior part. The ultimobranchial bodies are a pair of transient embryonic structures derived from the fourth pharyngeal pouch and located symmetrically on the sides of the developing neck: C cell precursors migrate from the neural crest (Le Douarin et al. 1974) in these structures (Fontaine J 1979). The cells of the thyroid anlage and the ultimobranchial bodies migrate from their respective sites of origin and ultimately merge in the definitive thyroid gland. Once merged, the thyroid anlage and the ultimobranchial bodies disappear and their cells disperse in the adult thyroid gland. At this point the cells from the anlage continue to organize the thyroid follicles, whereas the C cells scatter within the interfollicular space. Interestingly, in some animals the ultimobranchial structures remain distinct from the rest of the thyroid gland (Gorbman A 1986).

In the adult human, the gland has a butterfly shape and has a weight 15–25 g. It is comprised of aggregates (lobules) of spherical follicles that are filled with colloid. The follicles range in size from 50–500 μm and are lined by cuboidal-to-flat follicular epithelial cells. The main functions of the thyroid gland are synthesis, storage and secretion of thyroid hormones, L-triiodothyronine (T3) and L-thyroxine (T4) (Kondo et al. 2006). This mechanism is under the control of the hypothalamic-pituitary axis with negative feedback by the thyroid hormones: thyrotropin releasing hormone (TRH), secreted from the hypothalamus, stimulates the release of thyroid-stimulating hormone (TSH) from the anterior pituitary gland. TSH, then, stimulates the follicular cells to synthesize and secrete thyroid hormones. Disruption of thyroid hormone homeostasis results in hypothyroidism, goiter and in childhood cretinism (Kondo et al. 2006).

The parafollicular C-cells secrete calcitonin, which is important for the bone formation. Its secretion is stimulated by elevate calcium concentration in the serum (Lin et al. 1991; Nicholson et al. 1986).

1.2 Thyroid follicular cell carcinomas

Thyroid carcinomas that originates from TFC are mainly divided into well-differentiated, poorly differentiated and undifferentiated carcinomas on the basis of clinico-pathological parameters such as prevalence, sex ratio, age, local/distant metastasis and survival rate (Kondo et al. 2006). Papillary (PTC) and follicular (FTC) thyroid carcinomas are considered well-differentiated carcinomas (Kondo et al. 2006). Although initially defined by architectural criteria, the histological diagnosis of PTC rests on a number of nuclear features that predict the propensity for metastasis to local lymph nodes (World Health Organization Classification of Tumours 2004). The diagnosis of this most frequent type of thyroid malignancy (85–90% of thyroid malignancies) has been increasing, possibly owing to the changing recognition of nuclear morphological criteria. On the other hand, FTC is characterized by haematogenous spread, and the frequency of its diagnosis has been decreasing (Li Volsi and Asa 1994). Most well-differentiated thyroid cancers behave in an indolent manner and have an excellent prognosis. By contrast, anaplastic (ATC) thyroid carcinoma (undifferentiated) is highly

aggressive and always fatal (World Health Organization Classification of Tumours 2004; Kebebew et al. 2005). For this type of cancer there is not an effective treatment and, usually, the prognosis is poor and death occurs within one year from the diagnosis. Finally, poorly differentiated (PDC) thyroid carcinomas are intermediate forms between well-differentiated and undifferentiated, morphologically and behavioural (World Health Organization Classification of Tumours 2004; Carcangiu et al. 1984; Rodriguez et al. 1998).

Thyroid neoplasms, therefore, represent a good model for studying the events involved in epithelial cell multistep carcinogenesis (Figure 2), because they comprise a broad spectrum of lesions with different degrees of malignancy from benign adenomas (FA) (not invasive and very well differentiated) to the ATC (very aggressive and always fatal), with the intermediate forms represented by PTC and FTC (differentiated and with a good prognosis) (Hedinger et al. 1989; Wynford-Thomas 1997; Kondo et al. 2006).

Multi-step tumorigenesis in thyroid carcinomas of follicular origin

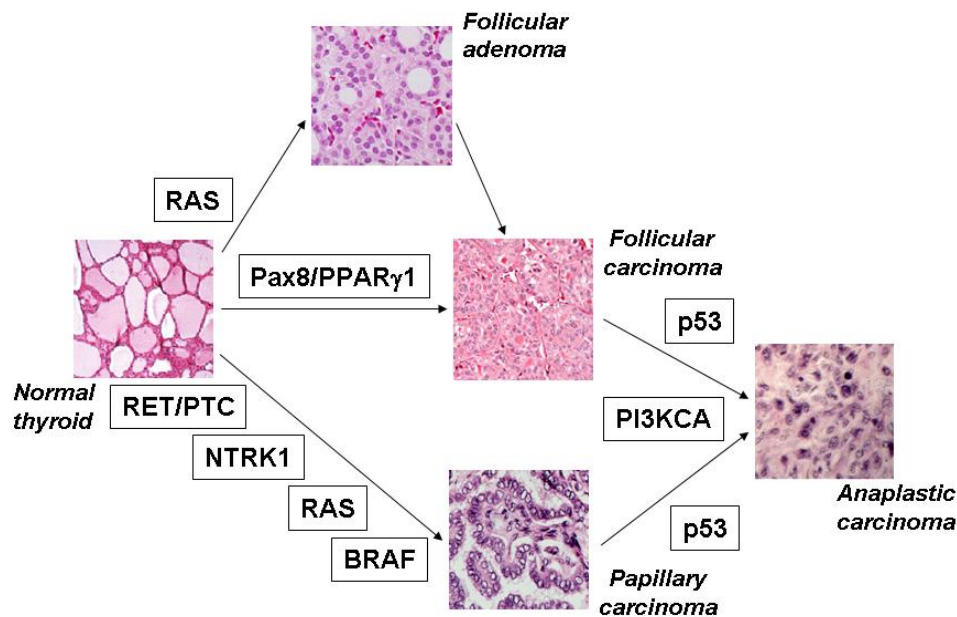


Figure 2 Model of multi-step carcinogenesis of thyroid neoplasms. On the basis of clinical, histological and molecular observations, three distinct pathways are proposed for neoplastic proliferation of thyroid follicular cells, including hyper-functioning follicular thyroid adenoma (tumours that are almost always benign lesions without a propensity for progression), follicular thyroid carcinoma and papillary thyroid carcinoma. Genetic defects that result in activation of RET or BRAF represent early, frequent initiating events that can be associated with radiation exposure. Most poorly differentiated and undifferentiated thyroid carcinomas are considered to derive from pre-existing well-differentiated thyroid carcinoma through additional genetic events, including p53 inactivation, but de novo occurrence might also occur.

Point mutations, rearrangements that activate proto-oncogenes, and loss-of-function in tumor suppressor genes have been identified in thyroid tumors (Kondo

et al. 2006). The involvement of several oncogenes has been demonstrated in PTC: activation of the RET/PTC oncogene, caused by rearrangements of the RET proto-oncogene, occurs in about 30% of cases (Kondo et al. 2006), whereas the B-RAF gene is mutated in about 40% of cases (Xing 2005). These tumors have also been associated with TRK gene rearrangements (Pierotti and Greco 2006) and MET gene overexpression (Di Renzo et al. 1992). RAS gene mutations (Suarez et al. 1990) and PAX8-PPAR- γ rearrangements (Kroll et al. 2000) are frequent in FTC, whereas impaired function of the p53 tumor suppressor gene is typical of ATC (Ito et al. 1992; Donghi et al. 1993; Fagin et al. 1993). Other genes have been implicated in thyroid neoplasias. Even though critical molecular mechanisms of thyroid carcinogenesis have been clarified, other molecular steps of neoplastic progression need to be investigated.

1.3 Microarray analysis of human carcinomas

Dna microarray technology was introduced in the scientific community in the mid-1990s as a mean to check the expression levels of thousands of genes simultaneously (Lipshutz et al. 1995; Schena et al. 1995). This kind of analysis was quickly adopted by the research community for the study of a wide range of biologic processes. Most of the early studies were performed simply to compare two biologic classes in order to identify the differential expression of the genes in them - genes with potential relevance to a wide range of biologic processes, such as the progression of cancer (De Risi et al. 1996; Welford et al. 1998; Khan et al. 1998; Agrawal et al. 2002), the causes of asthma (Rolph et al. 2006; Erle et al. 2003; Syed et al. 2005), heart disease (Heymans et al. 2005; Ohki et al. 2005; Li et al. 2003), neuropsychiatric disorders (Evans et al. 2003; Pierce et al. 2004; Zvara et al. 2005), and the analysis of factors associated with infertility (Chin et al. 2002; Zhang et al. 2005).

Soon after its introduction, microarray technology was used to find new subclasses in disease states (Alon et al. 1999; Perou et al. 1999) and to identify biologic markers (biomarkers) associated with disease (Moch et al. 1999) establishing that even the expression patterns of the genes could be used to distinguish subclasses of disease (Khan et al. 1998; Golub et al. 1999; Bloom et al. 2004; Eschrich et al. 2005).

This realization resulted in a proliferation of searches for patterns of expression that could be used to classify types of tumors (Sorlie et al. 2001) and predict the outcome (Beer et al. 2002; Van De Vijver et al. 2002) and response to chemotherapy (Van 't Veer et al. 2002; Kihara et al. 2001). In fact, gene expression profiling studies based upon this new technology has been successfully used to discover consistent gene expression patterns associated with a histological or clinical phenotype (Alizadeh et al. 2000; Van De Vijver et al. 2002; Bullinger et al. 2004; Dave et al. 2004; Lapointe et al. 2004; Valk et al. 2004; Lee et al. 2004; Roepman et al. 2005) and also to predict the clinical outcome and survival as well as to classify different types of cancer (Bittner et al. 2000; Beer et al. 2002; Van't Veer et al. 2002; Valk et al. 2004; Lee et al. 2004; Roepman et al. 2005). The research focus has now shifted toward identifying genetic determinants that are components of the specific regulatory pathways altered in cancers, leading to the discovery of novel therapeutic targets. In this view, our

group, recently, investigated the Ras-dependent modulation of gene expression in thyroid cells (Visconti et al. 2006 Accepted). However, it is not easy to select few candidate genes for further studies from the lengthy gene lists generated from gene expression profiling studies (Lee and Thorgeirsson 2006). This approach, however, promises to provide diagnostic and prognostic markers that can be clinically used in the near future (Lossos et al. 2004).

Therefore, to identify candidate genes involved in the process of thyroid carcinogenesis, we analysed a microarray, that represents 12.625 sequences, with RNAs extracted from normal human thyroid primary cell culture (NTPC), and six human thyroid carcinoma cell lines of different histotype (1 from a follicular carcinoma, 3 derived from papillary carcinomas and 2 from anaplastic carcinomas). We focused our interest on the genes whose expression was drastically (at least 10 fold) up- or down-regulated in all of the six thyroid carcinoma cell lines in comparison to the normal thyroid primary cell culture assuming that the genes altered in their expression in all of the thyroid carcinoma cell lines might represent candidate genes involved in thyroid cell transformation.

1.4 UbcH10 and the Ubiquitin-Proteasome proteolytic pathway

Among these genes, our attention was focused on the UbcH10 gene that was up-regulated about 150 fold in all of the cell lines tested by the cDNA microarray. The UbcH10 gene belongs to the E2 gene family and codes for a protein of 19.6 kDa that is involved in the ubiquitin-dependent proteolysis (Hershko et al. 1998; Joazeiro et al. 2000).

Like all macromolecular components of an organism, the proteome is in a dynamic state of synthesis and degradation. During proteolysis, the peptide bonds are hydrolyzed and free amino acids are released: the energy invested in the synthesis of the peptide bond is released. The process is carried out by a diverse group of enzymes termed proteases. Distinct proteolytic mechanisms serve different physiological requirements and allow the organism to accommodate to changing environmental and pathophysiological conditions (Glickman and Ciechanover 2002).

Degradation of a protein via the ubiquitin-proteasome pathway involves two discrete and successive steps: (1) tagging of the substrate by covalent attachment of multiple ubiquitin molecules and (2) degradation of the tagged protein by the 26S proteasome complex with release of free and reusable ubiquitin. This last process is mediated by deubiquitinating enzymes (DUB) that allow the recycling of the ubiquitin (Glickman and Ciechanover 2002). Ubiquitin is a highly evolutionarily conserved 76-residue polypeptide that is conjugated to the protein substrate via a cascade mechanism that involve three principal steps (Figure 3).

In the first step the ubiquitin activating enzyme E1 activates ubiquitin: this enzyme requires ATP and the reaction generates a high-energy thiol ester intermediate, E1-S-ubiquitin. Subsequently, several ubiquitin-carrier proteins E2 enzymes (or ubiquitin-conjugating enzymes, UBC) transfer the activated ubiquitin from E1, to the substrate that is specifically bound to a member of the ubiquitin-protein ligase family, E3. This reaction proceeds via an additional high-energy thiol ester intermediate, E2-S-ubiquitin (Peters et al. 1998; Hilt and Wolfe 2000). There are a number of different classes of E3 enzymes and they catalyze the last

step in the conjugation process: covalent attachment of ubiquitin to the substrate (Deshaies 1999; Jackson et al. 2000).

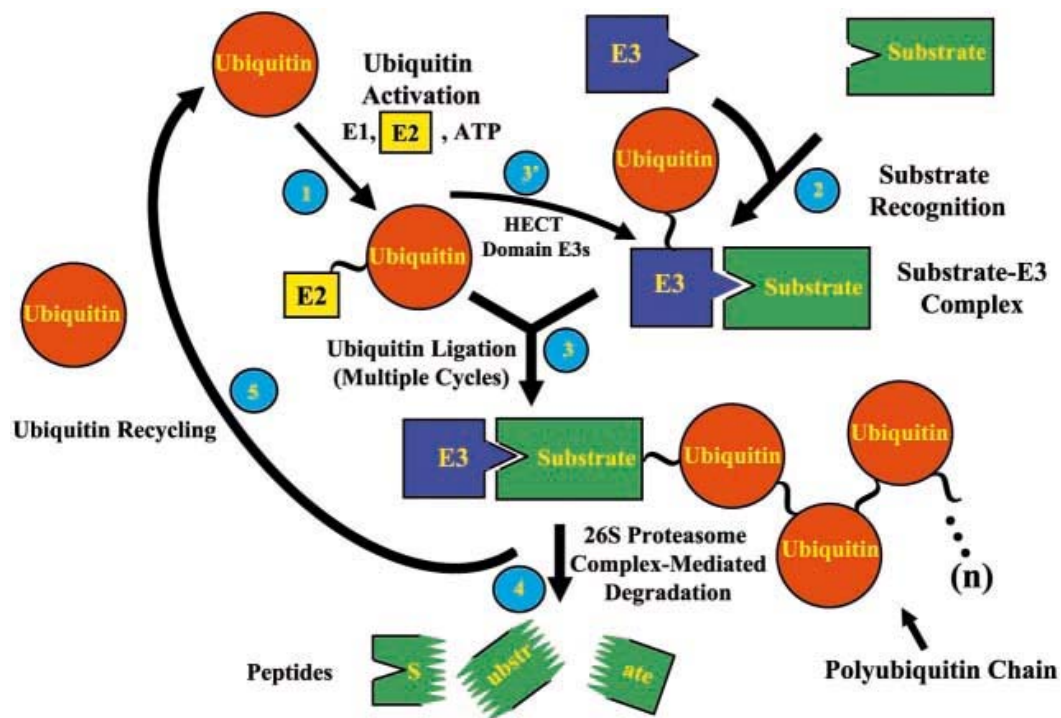


Figure 3 The ubiquitin proteolytic pathway. 1: Activation of ubiquitin by the ubiquitin-activating enzyme E1, a ubiquitin-carrier protein, E2 (ubiquitin-conjugating enzyme, UBC), and ATP. The product of this reaction is a high-energy E2-ubiquitin thiol ester intermediate. 2: Binding of the protein substrate, via a defined recognition motif, to a specific ubiquitin-protein ligase, E3. 3: Multiple (n) cycles of conjugation of ubiquitin to the target substrate and synthesis of a polyubiquitin chain. E2 transfers the first activated ubiquitin moiety directly to the E3-bound substrate, and in following cycles, to previously conjugated ubiquitin moiety. Direct transfer of activated ubiquitin from E2 to the E3-bound substrate occurs in substrates targeted by RING finger E3s. 3': As in 3, but the activated ubiquitin moiety is transferred from E2 to a high-energy thiol intermediate on E3, before its conjugation to the E3-bound substrate or to the previously conjugated ubiquitin moiety. This reaction is catalyzed by HECT domain E3s. 4: Degradation of the ubiquitin- tagged substrate by the 26S proteasome complex with release of short peptides. 5: Ubiquitin is recycled via the activity of deubiquitinating enzymes (DUBs) (Glickman and Ciechanover 2002).

By successively adding activated ubiquitin molecules to lysine residues on the previously conjugated ubiquitin molecule, a polyubiquitin chain is synthesized. At this point the 26S proteasome complex is able to recognize the ubiquitin chain. Thus E3s play a key role in the ubiquitin-mediated proteolytic cascade since they serve as the specific recognition factors of the system. The simplified view of the hierarchical structure of the ubiquitin conjugation machinery is that a single E1 activates ubiquitin for all conjugation reactions. E1 interacts with all E2s. Typically, each E2, interacts with several E3s. Each E3 targets several substrates. However, the interactions of the conjugating enzymes among themselves and with many of the target substrates may differ from this “classical” cascade. (Glickman and Ciechanover 2002).

The proteasome is a large multicatalytic protease (26S) that degrades polyubiquitinated proteins to small peptides. It is composed of two subcomplexes: a 20S core particle (CP) that carries the catalytic activity and a regulatory 19S regulatory particle (RP). The catalytic sites are localized to some of the CP subunits. Each extremity of the 20S barrel can be capped by a 19S RP. One important function of the 19S RP is to recognize ubiquitinated proteins and other potential substrates of the proteasome, moreover because a folded protein would not be able to fit through the narrow proteasomal channel, it is assumed that the 19S particle unfolds substrates and inserts them into the 20S CP. After degradation of the substrate, short peptides derived from the substrate are released, as well as reusable ubiquitin (Bochtler et al. 1999; Glickman 2000; Voges et al. 1999).

Ubiquitin-mediated proteolysis plays an important role in many basic cellular processes: regulation of cell cycle and division, differentiation and development, involvement in the cellular response to stress and extracellular effectors, morphogenesis of neuronal networks, modulation of cell surface receptors, ion channels and the secretory pathway, DNA repair, transcriptional regulation, transcriptional silencing, long-term memory, circadian rhythms, regulation of the immune and inflammatory responses, and biogenesis of organelles (Glickman and Ciechanover 2002). The number of cellular proteins that are targeted by ubiquitin is growing rapidly. Among them are cell cycle regulators such as cyclins, cyclin dependent kinase inhibitors, and proteins involved in sister chromatid separation, tumor suppressors, as well as transcriptional activators and their inhibitors. Cell surface receptors and endoplasmic reticulum proteins are also targeted by the system. Finally, mutated and denatured/misfolded proteins are recognized specifically and are removed efficiently. In this capacity, the system is a key player in the cellular quality control and defense mechanisms.

With the numerous substrate proteins targeted and the multitude of processes involved, it is not surprising that aberrations in the ubiquitin system have been implicated in the pathogenesis of many inherited and acquired human pathologies (Glickman and Ciechanover 2002).

1.5 UbcH10 involvement in cancer

As it was in precedence stated, the progression through the eukaryotic cell cycle is accomplished by the degradation of key cell-cycle regulators by the means of ubiquitin-proteasome pathway (Pickart 2001). The E3 anaphase-promoting complex/cyclosome (APC) (Figure 4) is the central coordinator of cell-cycle progression in mitosis and G1 (Peters 2002). This complex is activated at the onset of mitosis through cyclin B/Cdk1-dependent phosphorylation and the binding of its activator Cdc20.

Moreover, APC becomes active only after that sister chromatid separation is initiated, after all kinetochores have been correctly attached to the mitotic spindle. During anaphase, Cdc20 is replaced by Cdh1, a homologous activator. By promoting the sequential degradation of key regulators, APC-Cdh1 orchestrates exit from mitosis and events in G1.

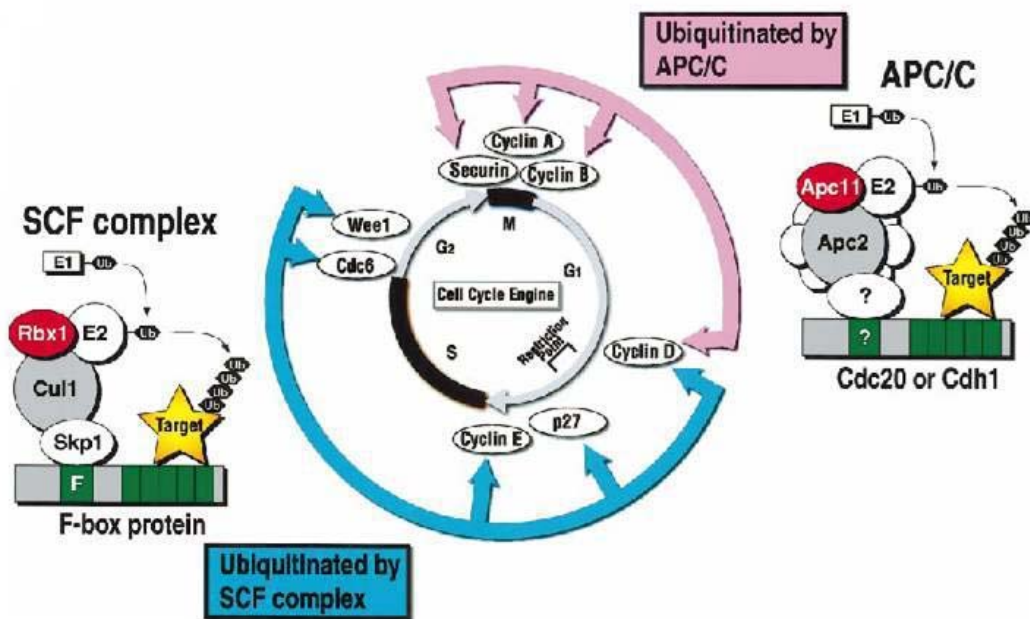


Figure 4 The Anaphase Promoting Complex (APC). The anaphase-promoting complex/cyclosome (APC/C) is a ubiquitin ligase that controls cell-cycle progression by targeting proteins for destruction by the 26S proteasome. The APC/C is active throughout late mitosis and G1 phase but APC/C substrates are degraded in a specific order.

Before entry into S phase the APC is inactivated by degradation of its E2 UbcH10 and by the E2F-dependent expression of the inhibitors cyclin A and Emi1 (Lukas et al. 1999; Hsu et al. 2002; Rape and Kirschner 2004). The correct sequence of APC-mediated ubiquitinations ensures the orderly progression of mitosis and G1. Substrates are mainly recognized by Cdc20 and Cdh1 but in this process also direct interactions between APC and substrates are important (Burton et al. 2005; Kraft et al. 2005; Yamano et al. 2004). The recognition is due to short stretch of aminoacids within substrates, the D-box and the Ken-box (Glutzer et al. 1991; Pflieger and Kirschner 2000). During the recognition process APC-Cdh1 discriminates between substrates and catalyzes their multiubiquitination in a sequential manner: Cdc20 is ubiquitinated shortly after APC-Cdh1 activation in anaphase, Plk1 and Aurora A are ubiquitinated later, after they have functioned in telophase and cytokinesis, and UbcH10 autoubiquitination is promoted in G1 after these substrates have been degraded. Additionally, the degradation of UbcH10 stabilizes cyclin A, while APC-Cdh1 substrates, such as securin or geminin, can still be degraded (Rape et al. 2006). It is clear that APC regulates the cell cycle transition through mitosis, triggering the timely destruction of key regulatory molecules such as cyclins and protein involved in the chromatid separation (Harper et al. 2002; Peters 2002). Securin and cyclin B ubiquitination also appears to require the E3 ligase proteins contained within the APC and the E2 conjugating enzyme UbcH10.

So, it is not surprising to find that mutation of the active site cysteine of UbcH10 confers a dominant-negative phenotype that results in metaphase arrest, demonstrating that this protein is essential for cell cycle progression (Townsend et al.

al. 1997). Although clearly associated with regulation of the cell cycle, the potential role of UbcH10 in cancer development has only recently been explored. Expression of the mouse ortholog of human UbcH10, mEC-2, was reported up-regulated in NIH3T3 cells transformed by EWS/FLI1, activated cdc42, v-ABL or c-myc, but not in a nontransformed NIH3T3 clone expressing EWS/FLI1 (Arvand et al. 1998). Recently, a comparison of expression levels of 17 E2 ubiquitin ligase genes in normal and tumor tissues identified UbcH10 as most specifically associated with cancer and, consistent with this notion, overexpression of UbcH10 in NIH3T3 cells led to an increased proliferative capacity (Okamoto et al. 2003). Moreover, in expression profiling studies, it was reported that the levels of UbcH10 transcript are highly elevated in different types of cancers (Welsh et al. 2001; La Tulippe et al. 2002; Wagner et al. 2004). It was demonstrated that overexpression of UbcH10 in some carcinomas may be due, at least in part, to genomic amplification of the UbcH10 locus (Wagner et al. 2004). It was also reported that the silencing of UbcH10 by RNA interference (RNAi), in combination with TRAIL/DR5 agonistic antibodies, resulted in enhanced cell death in neoplastic but not nonmalignant human cells (Wagner et al. 2004).

1.6 CBX7 and Polycomb group genes

Within the context of this microarray study, we found that the CBX7 (Chromobox homolog 7) gene was down-regulated in the thyroid carcinoma-derived cell lines and also in thyroid fresh tumors. CBX7 encodes a novel protein that is a part of the Polycomb Group protein.

Polycomb Group genes (PcG) are a set of genes linking histone modifications with transcriptional repression: they are structurally diverse but functionally epistatic (Otte and Kwaks 2003; Lund and Van Lohuizen 2004). PcG proteins are part of two complexes with high molecular weight called Polycomb repressive complexes 1 and 2, PRC1 and PRC2, (Figure 5) (Lund and Van Lohuizen 2004; Wang et al. 2004).

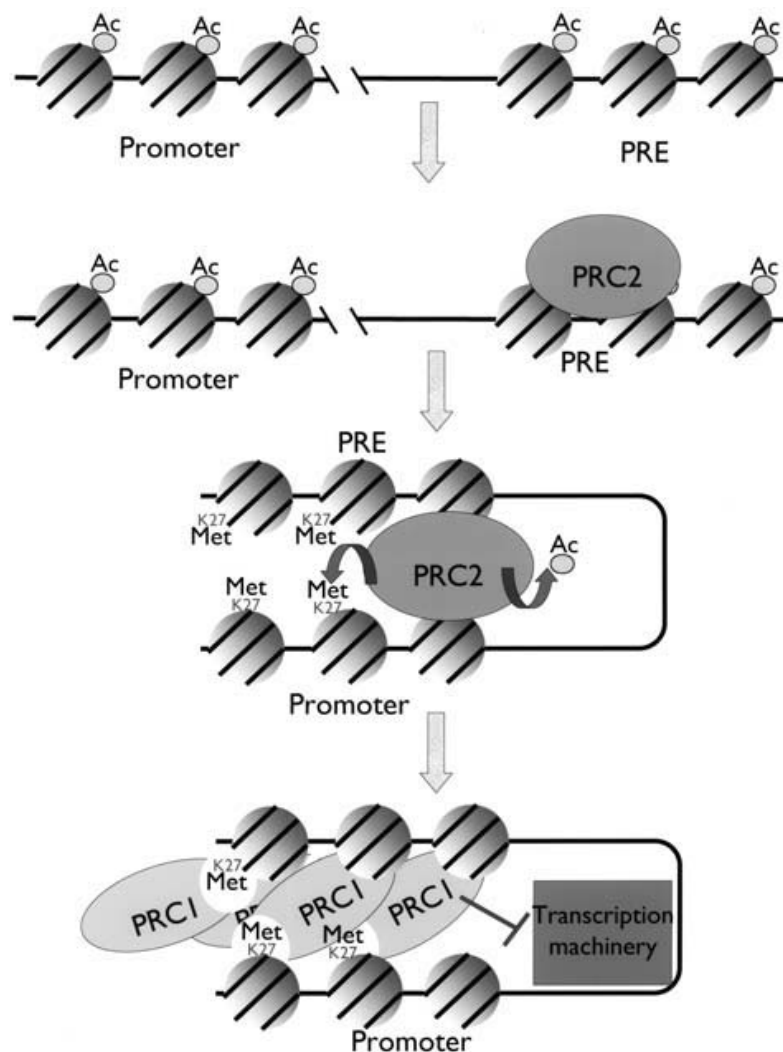


Figure 5 Mechanism of transcriptional repression by Polycomb Group proteins. The binding of Polycomb repressive complex 2 (PRC2) to Polycomb responsive elements (PRE) triggers histone deacetylation, and methylation of lysine 27 in Histone H3, both around the PRE and in the promoter region of the genes silenced. This modification constitute one of the signals

for the recruitment of the Polycomb repressive complex 1 (PRC1), or maintenance complex, which repress gene expression by inhibiting transcription initiation (Gil et al. 2005).

The PRC1 complex can recognize and bind to trimethylated K27 of Histone H3 through Polycomb proteins, and contributes to gene repression by inhibiting transcription initiation (Cao et al. 2002). The components of the core of this complex in mammals are the homologs of *Drosophila* Polycomb (Pc), Posterior sex combs (Psc), Sex combs extra (Sce) and Polyhomeiotic (Ph). The PRC2 complex, instead, has associated histone deacetylase and histone methyl transferase (specific for lysine of Histone H3, K27H3) activities, thus it contributes to establish an histone repressive marks (Kuzmichev et al. 2002; Kirmizis et al. 2004). Between the known mammalian components of this second complex are Enhancer of Zeste (EZH2), Early embryonic deficient (EED), Suppressor of Zeste (SUZ12) and other associated proteins.

It is well known that PcG proteins deregulation is involved in tumorigenesis in fact several studies have demonstrated that, for example, Bmi-1 is amplified in blood malignancies and medulloblastomas (Raaphorst et al. 2000; Bea et al. 2001; Van Kemenade et al. 2001; Lessard and Sauvageau 2003), EZH2 is involved in blood malignancies (Raaphorst et al. 2000; Visser et al. 2001), and its expression is increased during the process of metastasis of prostate and breast tumors (Varambally et al. 2002; Kleer et al. 2003), Me118 has been suggested to act as a tumor suppressor gene (Kanno et al. 1995), Rae28/Ph1 alterations are observed in acute lymphoblastic leukemia (Tokimasa et al. 2001) and SUZ12 is up-regulated in colon tumors (Kirmizis et al. 2003). Evidence is rapidly increasing that PcG genes are a novel class of oncogenes and anti-oncogenes, which may in future years become central to the development of novel cancer therapies based on epigenetic gene silencing (Nakao et al. 2004, Egger et al. 2004). Not only are PcG genes such as BMI-1 and EZH2 capable of cellular transformation, but also they are vital for cell survival. To date, abnormal PcG genes expression has been described in most human cancers. Also, the correlation between PcG expression and biological behavior of clinically defined cancer subtypes suggests that these genes play a central role in oncogenesis, and holds a promise for discovery of novel diagnostic markers (Raaphorst et al. 2004).

CBX7 and the others PcG proteins contain a chromodomain in the N-terminus (CBX7 between amino acids 10 and 46). This domain was originally identified in *Drosophila melanogaster* as a 37-amino-acid region of homology shared by heterochromatin protein 1 (HP1) and Polycomb (Pc) proteins (Paro and Hogness 1991). Phylogenetic and sequence analyses of the chromodomain (Figure 6A and B) revealed that CBX7 has a great similarity to other known or putative Pc proteins like CBX2 (Pc1), CBX4 (Pc2), CBX6 and CBX8 (Pc3). This similarity is less pronounced respect to the HP1 proteins, such as CBX1 (HP1 β), CBX3 (HP1 γ), CBX5 (HP1 α) and, moreover, CBX7 does not contain the “chromo-shadow domain” that, instead, is a hallmark of HP1 proteins. CBX7 protein contains also other specific conserved residues that distinguish Pc and HP1 chromodomains: these residues specific of the Pc proteins are necessary both for Pc dimerization and recognition of tri-methylated Lys 27 on histone H3 (Min et al. 2003).

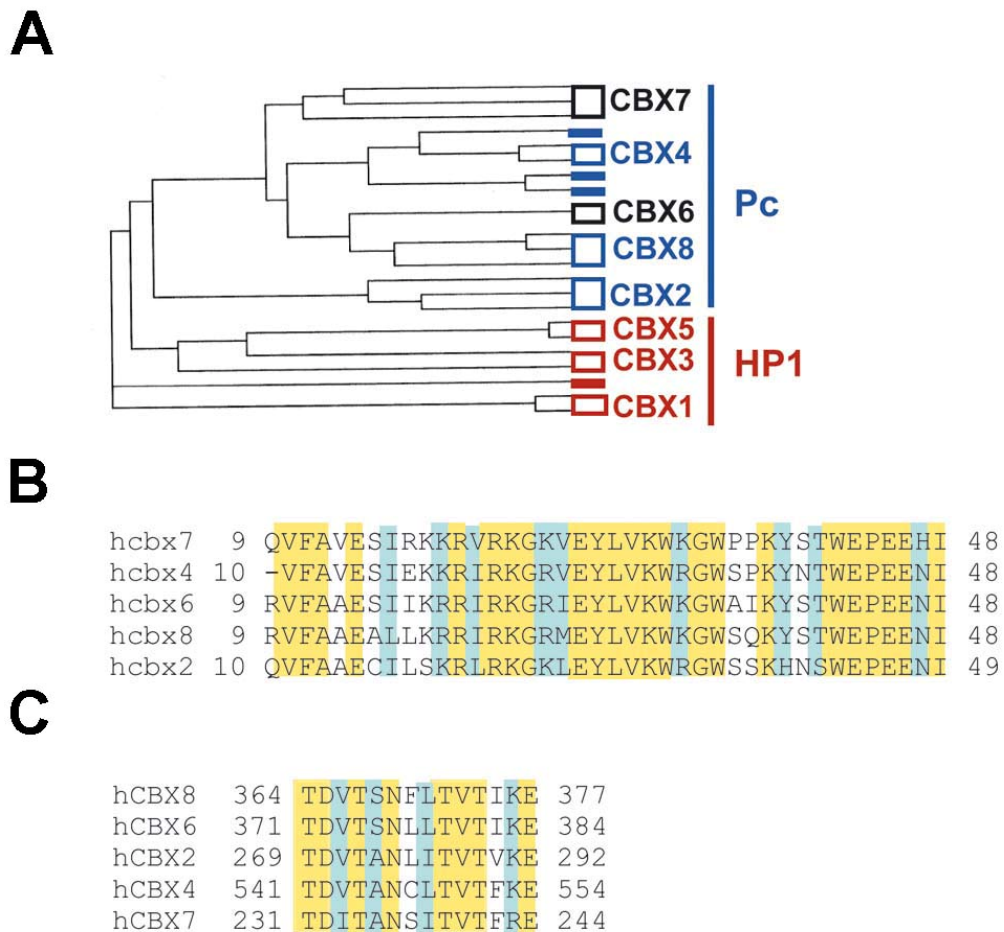


Figure 6 CBX7 and chromodomain. Identification of CBX7 as a Polycomb protein. (A) Phylogenetic analysis of Chromobox (CBX) proteins. Lines grouped by open rectangles denote orthologs of a same CBX protein (name in the right). Full rectangles refer to proteins that cannot be considered purely orthologs of any of the CBX proteins. Pc proteins are shown in blue, and HP1 proteins in red. CBX7 and CBX6 are shown in black. (B) Alignment of CBX7 chromodomain with that of other known and putative human Polycombs. Identical residues are shown in a yellow background, and similar residues are shown in a cyan background. (C) Alignment of CBX7 Polycomb box with that of other known and putative human Polycombs. Background colours are as described in (B) (from Gil et al. 2004).

In addition to the high homology within the chromodomain, CBX7 has also homology to Pc proteins in a carboxy-terminal region (Figure 6C) previously defined as the Pc box or C-box (Jones et al. 2000). It is known that either the Pc box (amino acids 231–243) and the chromodomain (Jones et al. 2000) are both necessary for CBX7 function. It was seen that a fusion protein between CBX7 and the DNA-binding domain of Gal4 is able to repress in a dose dependent manner, the transcription over a 4×Gal4-tk-luc reporter, suggesting that CBX7 functions by repressing transcription (Gil et al. 2004). So, CBX7 seems to act like the others Pc proteins exerting its effect through transcriptional repression.

CBX7 is highly expressed in a number of different normal tissue types, including brain, kidney, heart and skeletal muscle, although it has not previously

been investigated in tumor cells (Gil et al. 2004). A recent study has demonstrated that CBX7 expression is associated with extension of cellular life span in mouse embryonic fibroblasts and human prostate primary epithelial cells by downregulating expression of the Ink4a/Arf locus (Gil et al. 2004. Bernard et al. 2005). However another study on ependymoma (Suarez-Merino et al. 2005) reported a consistent down-regulation of CBX7 in the tumor samples, with the loss of at least one copy of the gene in 55% of cases examined, and proposed other mechanisms than CBX7/p16 pathway, since in ependymoma although gene mutations are rare, hypermethylation of p16Ink4a, Rb and p14ARF has been reported in a subgroup of tumors (4%–32%) (Suarez-Merino et al. 2005). Mouse CBX7 is, moreover, able to associate with facultative heterochromatin and with the inactive X chromosome, which indicates that CBX7 is really involved in the repression of gene transcription (Bernstein et al. 2006). CBX7 is also capable to interact with different Pc group members. In fact, similarly to other Pc proteins, CBX7 is able to inter-functions with itself and with the ring-finger protein Ring1 (Gil et al. 2004), as reported by the mean of Glutathione S-transferase (GST) pull-down experiments (Satijn and Otte 1999; Satijn et al. 1997). In addition, within the nucleus, CBX7 co-localizes with Ring1 to distinct foci-like structures termed Pc-bodies (Saurin et al. 1998), in several cell lines, as demonstrated with immunofluorescence microscopy studies. However there is not association between CBX7 and other PcG proteins, such as Bmi1, EED or EH2 (Gil et al. 2004) so this let think that CBX7 is part of different complexes than Bmi1 and Pc2.

2. AIMS OF THE STUDY

Thyroid tumors are the result of the accumulation of different modifications in critical genes involved in the control of cell proliferation. Although various therapeutic approaches are followed in clinical practice, most of them are not life-saving. Hence, the discovery of ways to diagnose cancer at an early stage and to establish more effective therapies is a critical and urgent issue. To achieve this goal, identification and characterization of key molecules that participate in carcinogenesis are essential steps.

In this context, we studied the modulation of gene expression associated with the progression towards a malignant phenotype of thyroid cancer. To this aim, we used RNA samples extracted from human thyroid carcinoma cell lines to perform a screening with Affymetrix microarrays containing about 10.500 human genes.

The main aim of the study would be the identification and characterization of genes whose expression and function are deregulated in the carcinoma samples of human thyroid origin.

If the deregulated expression/function of these genes results strongly associated with the expression of a highly malignant phenotype, the final objective of this study would be the perspective to use them as new tools for diagnosis and prognosis.

3. MATERIALS AND METHODS

3.1 Cell culture and transfections

We used the following human thyroid carcinoma cell lines in this study: TPC-1, WRO, NPA, ARO, FRO, NIM 1, B-CPAP, FB-1, FB-2, Kat-4 and Kat-18, which are described elsewhere (Pallante et al. 2005). They were grown in DMEM (Gibco Laboratories, Carlsbad, CA) containing 10% fetal calf serum (Gibco Laboratories), glutamine (Gibco Laboratories) and ampicillin/streptomycin (Gibco Laboratories) in a 5% CO₂ atmosphere. Normal human thyroid primary culture cells have been established and grown as already described (Curcio et al. 1994). PC CL 3 (Fusco et al. 1987) and FRTL-5 (Ambesi-Impiombato et al. 1980) cell lines were cultured in modified F12 medium supplemented with 5% calf serum (Gibco Laboratories) and six growth factors (thyrotropic hormone, hydrocortisone, insulin, transferrin, somatostatin and glycyl-histidyl-lysine) (Sigma, St. Louis, MO). PC CL 3 and FRTL-5 infected with several oncogenes PC KiMSV, PC HaMSV, PC v-raf, PC MPSV (Fusco et al. 1987), PC PyMLV (Berlingieri et al. 1988), PC E1A, PC E1A+v-raf (Berlingieri et al. 1993), PC RET/PTC, PC HaMSV+RET/PTC1 (Santoro et al. 1993), PC MPSV-HMGA2 (Berlingieri et al. 1995), FRTL-5 KiMSV (Fusco et al. 1985), FRTL-5 KiMSV-HMGA1 (Berlingieri et al. 2002) cells were cultured in the same medium as PC CL 3 and FRTL-5 cells but without the six growth factors.

Thyroid cells were transfected using Lipofectamine reagent (Invitrogen, Carlsbad, CA) according to the manufacturer's instructions. The transfected cells were selected in a medium containing geneticin (G418) (Life Technologies, Milan, Italy). For each transfection, several G418 resistant clones and the mass cell population were isolated and expanded for further analysis.

3.2 Human thyroid tissue samples

Neoplastic human thyroid tissues and normal adjacent tissue or the controlateral normal thyroid lobe were obtained from surgical specimens and immediately frozen in liquid nitrogen. Thyroid tumors were collected at the Laboratoire d'Histologie et de Cytologie, Centre Hospitalier Lyon Sud, France, and at the Laboratoire d'Anatomie Pathologique, Hopital de L'Antiquaille Lyon, France. The tumor samples were stored frozen until RNA or protein extractions were performed.

3.3 RNA isolation

Total RNA was extracted from tissues and cell cultures using the RNeasy mini kit (Qiagen, Valencia, CA) according to the manufacturer's instructions. The integrity of the RNA was assessed by denaturing agarose gel electrophoresis.

3.4 Microarray analysis

In this study we used commercially available high density Affymetrix (Santa Clara, CA) oligonucleotide microarrays (HG_U95Av2) consisting of 12.625 probe set each representing a transcript. cRNA preparation, hybridization,

scanning and analysis were performed as previously reported (Dyrskjot et al. 2003). Briefly, after cRNA hybridization to microarray, analysis of the readings from the quantitative scanning was performed using the Affymetrix Gene Expression Analysis Software (Affymetrix), according to Affymetrix protocols. Comparisons were made for each carcinoma cell line sample versus normal thyroid primary culture, taking normal thyroid cells as baseline. The fold change values, indicating the relative change in the expression levels between transformed cell line and normal thyroid primary culture samples, were used to identify genes differentially expressed between these conditions.

3.5 Reverse transcriptase and PCR analysis

Reverse transcription

1 µg of total RNA from each sample was reverse-transcribed with QuantiTect® Reverse Transcription Kit (Qiagen) using an optimized blend of oligo-dT and random primers according to the manufacturer's instructions.

Semiquantitative RT-PCR

PCR was carried out on cDNA using the GeneAmp PCR System 9600 (Applied Biosystems, Foster City, CA). The RNA PCR Core Kit (Applied Biosystems) was used to perform amplifications. After a first denaturing step (94°C for 3 min), PCR amplification was performed for 25-30 (variable) cycles (94°C for 30 s, 55-60°C (variable) for 30 s, 72°C for 30 s).

The sequences of primers used are shown in Table 1. To ensure that RNA samples were not contaminated with DNA, negative controls were obtained by carrying out the PCR on samples that were not reverse-transcribed, but otherwise identically processed. The PCR products were separated on a 2% agarose gel, stained with ethidium bromide and scanned with a Typhoon 9200 scanner (GE Healthcare, Piscataway, NJ).

Selection of primers and probes for qRT-PCR

To design a qRT-PCR assay we used the Human ProbeLibrary™ system (Exiqon, Vedbaek, Denmark). Briefly, using locked nucleic acid (LNA™) technology (Obika et al. 1997; Koskhin et al. 1998), Exiqon provides 90 human prevalidated TaqMan probes of only 8-9 nucleotides that recognize 99% of human transcripts in the RefSeq database at NCBI (Mouritzen et al. 2004; Mouritzen et al. 2005). Using the ProbeFinder assay design software (freely accessed on the web site www.probelibrary.com) we chose the best probe and primers pair. To amplify a fragment for Real-Time PCR of CBX7 mRNA, we entered its accession number (NM_175709.2) on the assay design page of the ProbeFinder software and we chose an amplicon of 71 nucleotides that spanned the 3rd and 4th exons. The probe number was "human 63" (according to the numbering of Exiqon's Human ProbeLibrary kit) and the primer sequences are reported in Table 1.

The same procedure was used to choose the probe and primers for the housekeeping gene G6PD (accession number X03674). We opted for an amplicon of 106 nucleotides that spanned the 3rd and 4th exons. The probe number was "human 05" (according to the numbering of Exiqon's Human ProbeLibrary kit)

and the primer sequences are reported in Table 1. All fluorogenic probes were dual-labeled with FAM at 5'-end and with a black quencher at the 3'-end.

qRT-PCR

Real-Time Quantitative TaqMan PCR was carried out with the Chromo4 Detector (MJ Research, Waltham, MA) in 96-well plates using a final volume of 20 μ l. For PCR we used 8 μ l of 2.5x RealMasterMix™ Probe ROX (Eppendorf AG, Hamburg, Germany) 200 nM of each primer, 100 nM probe and cDNA generated from 50 ng of total RNA. The conditions used for PCR were 2 min at 95°C and then 45 cycles of 20 sec at 95°C and 1 min a 60°C. Each reaction was carried out in duplicate. Fold mRNA overexpression was calculated according to the formula $2^{(Rt-Et)}/2^{(Rn-En)}$ as described previously (El-Rifai et al. 2001), where Rt is the threshold cycle number for the reference gene in the tumor, Et for the experimental gene in the tumor, Rn for the reference gene in the normal sample and En for the experimental gene in the normal sample.

We also carried out qRT-PCR reactions with mouse cDNA in a final volume of 20 μ l using 10 μ l of 2x Power SYBR Green PCR Master Mix (Applied Biosystems), 200 nM of each primer and cDNA generated from 50 ng of total RNA. The conditions used for PCR were 10 min at 95°C and then 45 cycles of 30 sec at 95°C and 1 min a 60°C. Each reaction was carried out in duplicate, and at the end of the PCR run, a dissociation curve was constructed using a ramping temperature of 0.2°C per sec from 65°C to 95°C. A single melting point was obtained for CBX7 and β -Actin amplicons (data not shown). The mouse β -Actin gene served as control. The primers used are reported in Table 1.

3.6 Protein extraction, Western blotting, and antibodies

The detailed procedure for protein extraction and Western blotting for UbcH10 has been described in detail in the original article by Pallante et al. (Pallante et al. 2005).

3.7 Immunohistochemistry

Tissue samples

UbcH10 protein cellular distribution was assessed by immunohistochemical analysis and compared to that of the standard cell proliferation marker Ki-67/MIB1. A series of surgical specimens from patients with thyroid diseases comprised of Hashimoto's thyroiditis-HT (6 cases), nodular goiter (12 cases), follicular carcinoma (13 cases), papillary carcinoma (33 cases), poorly differentiated carcinoma (5 cases) and anaplastic carcinoma (15 cases) was chosen to represent a wide range of thyroid pathology. As control, ten areas of normal thyroid parenchyma were selected from the lobe contralateral to the tumor in surgical specimens of papillary carcinoma.

The cell distribution of the CBX7 protein was assessed by immunostaining formalin-fixed, paraffin-embedded thyroid tumor blocks retrieved from the files of the Dipartimento di Scienze Biomorfologiche e Funzionali at the University of Naples Federico II and selected to represent a wide range of thyroid neoplastic diseases. To ensure that we evaluated CBX7 expression only on technically

adequate slides, we discarded slides that lacked a convincing internal control, namely labeling of stromal, endothelial or lymphoid cell, shown to be positive in a preliminary normal tissue micro-array analysis (data not shown). Based on these criteria, we scored paraffin-embedded stained slides from 20 cases of FA, 30 cases of classical PTC, 6 cases of TCV PTC, 32 cases of FTC, 12 cases of poorly differentiated carcinoma, and 12 cases of ATC. As controls, we selected areas of normal thyroid parenchyma from the lobe contralateral to the tumor in 20 surgical specimens of PTC.

Immunostaining: technique, evaluation and statistical analysis

Xylene dewaxed and alcohol rehydrated paraffin sections were placed in Coplin jars filled with a 0.01 M tri-sodium citrate solution, and heated for 3 minutes in a conventional pressure cooker (Troncone et al. 2003). After heating, slides were thoroughly rinsed in cool running water for 5 minutes. They were then washed in Tris-Buffered Saline (TBS) pH 7.4 before incubating overnight with the specific antibody, diluted as it follows: rabbit polyclonal α -UbcH10 (BostonBiochem Inc, Cambridge, MA) 1:1000; α -MIB-1 (Novocastra, Newcastle upon Tyne, UK) 1:50; α -CBX7 1:500 [raised against the C-terminus of the human CBX7 protein (Neosystem, Strasbourg, France)].

After incubation with the primary antibody, tissue sections were stained with biotinylated anti-rabbit or anti-mouse immunoglobulins, followed by peroxidase labelled streptavidine (Dako, Carpinteria, CA, USA); the signal was developed by using diaminobenzidine (DAB) chromogen as substrate. Incubations both omitting the specific antibody, and including unrelated antibodies, were used as negative controls.

Individual cells were scored for expression of UbcH10 and Ki-67 in similar areas of adjacent sections, and CBX7 by quantitative analysis performed with a computerised analyser system (Ibas 2000, Kontron, Zeiss), as already described. (Troncone et al. 2003). In each case the distribution of these proteins was evaluated in at least 500 epithelial follicular cells and expressed as a percentage of the total cell population.

The statistical analysis was performed using SPSS “Ver. 9.0.1 for Windows”. Data in the text and tables are expressed as median value and range. The nonparametric Mann Whitney U-test was used to compare differences in labelling indexes for UbcH10 and Ki-67 in thyroid carcinomas. The Spearman rank order correlation was used to verify the association between UbcH10 and Ki-67. A P-value less than 0.05 was considered statistically significant.

3.8 Thyroid Fine-Needle Aspiration Biopsies (FNAB)

The FNAB were carried out at the Dipartimento di Anatomia Patologica e Citopatologia (University of Naples Federico II) as described elsewhere (Zeppa et al. 1990; Troncone et al. 2000). Samples were obtained from 15 patients with thyroid neoplasias who subsequently underwent surgery because the FNAB cytology indicated a diagnosis of cancer. Normal thyroid cells, used as controls, were obtained from FNAB of thyroids carrying non-neoplastic nodules. FNAB samples were washed twice with 1x PBS and then processed for RNA extraction using the procedure detailed in a previous section.

3.9 Loss-of-heterozygosity (LOH) analysis

We used several SNP markers to evaluate LOH at the CBX7 locus on chromosome 22q13.1. We selected the SNP markers (<http://www.ncbi.nih.gov/SNP/>) that showed high average heterozygosity levels in order to obtain the highest number of informative cases. Briefly, genomic DNA was PCR-amplified in a region spanning about 200 bp around the SNP analyzed, then the purified PCR product was sequenced. We measured the height of the two peaks on the chromatogram and calculated the ratio of the two alleles in the matched tumor/normal samples: LOH was defined if the ratio in the carcinoma sample was less than 50%. SNPs and relative primers used to amplify them are reported in Table 1.

3.10 Methylation analysis using bisulphite genomic sequencing

The promoter region and the entire coding sequence of the human CBX7 gene were analyzed for CG content; CpG islands were determined based on a 200-bp length of DNA with a CG content of >50% and a CpG/GpC ratio of >0.5, using the CpGplot program, available at <http://www.ebi.ac.uk/emboss/cpgplot/>. Bisulphite genomic sequencing was used to analyze the methylation patterns of individual DNA molecules. Sodium bisulphite conversion of genomic DNA (about 200 ng for each conversion) was obtained using the EZ DNA Methylation Kit® (Zymo Research, Orange, CA) following the manufacturer's instructions. The CpG islands identified were then PCR-amplified using the primers reported in Table 1. PCR reactions were carried out using FastStart Taq DNA polymerase (Roche, Basel, Switzerland) under the following conditions: (1) Pre-nested PCRs were normally carried out on 10 ng of bisulphite-treated DNA in a final reaction volume of 50 µl, using standard conditions with 5 min at 95°C, 2 min at 70°C, followed by 5 cycles of 1 min at 95°C, 2 min at 57-60°C, and 1.5 min at 72°C, then 25 cycles of 30 sec at 95°C, 1.5 min at 50-55°C, and 1.5 min at 72°C, then a final elongation of 5 min at 72°C before holding at 4°C; (2) Nested PCRs were carried out under the same conditions using 5 µl of the corresponding pre-nested PCRs in a final reaction volume of 50 µl. The PCR final products were cloned into the pGEM®-T Easy Vector System II (Promega, Madison, WI) following the supplier's procedures. The positive screened colonies contained the sequence of one individual DNA molecule. The plasmid DNA from the selected positive colonies containing vectors with the insert was purified using the Qiagen plasmid Mini Kit. The purified plasmids were sequenced in both directions using T7 and Sp6 primers. Twenty independent clones for each genomic preparation and fragment of interest were sequenced to determine the methylation pattern of individual molecules. Sequencing was carried out at the CEINGE Sequencing Core Facility (Naples, Italy).

3.11 Plasmid constructs and cell colony-forming assay

CBX7 expression plasmid was constructed by cloning the human cDNA sequence in a pCRTMII TA Cloning® vector (Invitrogen). The primers used were: CBX7 forward 5'-ATGGAGCTGTCAGCCATC-3' and CBX7 reverse 5'-TCAGAACTTCCCACTGCG-3'. The inserted cDNA was then subcloned into

the BamHI/XhoI sites of the mammalian expression vector pcDNA 3.1 (Invitrogen). The expression of CBX7 was assessed by Western blotting. Cells, plated at a density of 90% in 100-mm dishes, were transfected with 5 ug pcDNA3.1 or pCBX7 and supplemented with geneticin (G418) 24 h later. Two weeks after the onset of drug selection, the cells were fixed and stained with crystal violet (0.1% crystal violet in 20% methanol).

3.12 Preparation of recombinant adenovirus and infection protocol

The recombinant adenovirus was constructed using AdEasy™ Vector System (Quantum Biotechnologies, Montreal, Quebec). The cDNA fragment was inserted in the sense orientation into the NotI and HindIII sites of the pShuttle-CMV vector to generate the recombinant pShuttle-CBX7-CMV construct. It was linearized and co-transformed through electroporation with pAdEasy-1, which carries the adenovirus genome, in BJ5183 electrocompetent cells. After homologous recombination, a recombinant AdEasy-CMV-CBX7 plasmid was generated (Ad-CBX7), which was then extracted and linearized. QBI-293A cells were transfected with different clones to produce different viral particles, and the infectivity of each clone was tested. Viral stocks were expanded in QBI-293A cells, which were harvested 36-40 h after infection and lysed. The virus titer of the 293 cells was determined. The adenovirus AdCMV-GFP (Quantum Biotechnologies) was used as control. Cells (5×10^4) were seeded in a six-well plate. After 24 h, cells were infected at MOI 100 with Ad-CBX7 or Ad-GFP for 90 min using 500 µl of infection medium (DMEM supplemented with 2% FBS) at 37°C in a 5% CO₂ incubator. Pilot experiments with Ad-GFP were carried out to determine the optimal MOI for each cell line. At MOI 100, the cell lines became GFP-positive without manifesting toxicity. Infected cells were harvested and counted daily in a hemacytometric chamber.

3.13 RNA Interference

The detailed procedure for UbcH10 RNA interference experiments has been described in detail in the original article (Pallante et al. 2005).

3.14 Assay of the transformed state

Tumorigenicity of the cell lines was tested by injecting 2×10^6 cells subcutaneously into athymic mice. Soft agar colony assay was performed as previously described (Macpherson et al. 1964).

Table 1 List of primers

<i>Expression</i>	<i>Fwd 5'-->3'</i>	<i>Rev 5'-->3'</i>
Hs-KIF2C (U63743)	CAGAACAAGGCTCACACC	AGCAGGCTTCCATCTCTT
Hs-CXCL1 (X54489)	CACCTGGATTGTGCCTAA	TGCAGGCTCCTCAGAAAT
Hs-PHLDA2 (AF035444)	GGCACGACATGAAATCC	GTGGTGACGATGGTGAAGT
Hs-CDC20 (U05340)	CCGTTACATTCCTTCCCT	AGTTGCCCTCTTTGATCC
Hs-PIB5PA (U45975)	TGGAGGTGGCAGATGAGT	GGATGCTGTGGTTGTGAC
Hs-TFF3 (L08044)	ATGTCACCCCAAGGA	TGGCAGCAATCACAGC
Hs-BTG2 (U72649)	ACCTCAACCTGGGGAAC	CCAAACGTCTCCACTTC
Hs-RARRES3 (AF060228)	GCTATCGGGTCAACAACA	CCTAATCGAAAAGAGCA
Hs-CBX7	CATGGAGCTGTCAGCCATC	CTGTACTTTGGGGCCATC
Hs-β-actin	TCGTGCGTGACATTAAGGAG	GTCAGGCAGCTCGTAGCTCT
Rn-CBX7	GTCATGGCCTACGAGGAGAA	CTTGGGTTTCGGACCTCTCT
Rn-GAPDH	TGATTCTACCCACGGCAAGTT	TGATGGGTTTCCCATTGATGA
Hs-UbcH10	GCCCGTAAAGGAGCTGAG	GGGAAGGCAGAAAATCCCT
Hs-CBX7 qRT-PCR	CGTCATGGCCTACGAGGA	TGGGTTTCGGACCTCTCTT
Hs-G6PD qRT-PCR	ACAGAGTGAGCCCTTCTTCAA	GGAGGCTGCATCATCGTACT
Mm-CBX7 qRT-PCR	AATGGCATGGCTAAGGATGG	ACATAGGTTTCGTATGGTAGCA
Mm-β-actin qRT-PCR	TCAGAAGGACTCCTATGTGG	CGCAGCTCATTGTAGAAGGT
<i>LOH</i>	<i>Fwd 5'-->3'</i>	<i>Rev 5'-->3'</i>
rs710190 - LOH1	TGAATCCACAGACCCACAGA	GGTTCAGAGGGGACTCTTCC
rs5750753 - LOH2	GACAGCCAAGGAAAGACAGG	GTGTGATGGGCAGGCTTT
rs713841 - LOH3	CCAGACGTCTCAAAGCCTGT	CAGCACAAAAGACCTCACCA
rs2076476 - LOH4	ACAGGGCATCTTTGTGAAGC	GTGAAAATGGTGGGCACTG
rs2281258 - LOH5	AGAACCATTACAAGTGGGG	TCTGGAAAGCACAGCAAATG
rs2235686 - LOH6	TGGCCTCAGCATGTTAAGAA	GTTCTTCCCCACTTTGAT
rs714016 - LOH7	TGGCTGCACTGTAAGGACAC	CTTCTGGGGGTCAGGAATTT
rs139390 - LOH8	CACCTGCCCTGTAGGCTTAG	GCAGGATATTGGAAGCCAGA
rs139393 - LOH9	CCTTACCCCTGTCTGGTAA	TTCATCCTCTCTTGCTGGT
<i>Methylation analysis</i>	<i>5'-->3'</i>	
1F: -440 -407	TTC/GGGTTTTTGGTAGTTATTGGGAGGTTATGAGG	
1Fn: -114 -84	AGGAAAAC/GGTTGC/GGTAGGTTAAAAATGGAA	
1R: +211+178	AAAACG/AAAAAAAACCCCACTAAAATCCTAAAAAC	
1Rn: +186 +155	CCTAAAAACCG/ACCCCG/AAACAACCTCACCTTC	
2F: +155 +186	GAAGGTGAGGTTGTTC/GGGGGGC/GGGTTTTTAGG	
2R: +593 +560	CCG/AAAAAAAACCTTTCCAAAACCTCCACTTACAAC	
2Rn: +535 +503	CCAAAATCCCG/AAATTCAAAACCCCACTTAACC	
3Fn: +7005 +7031	GGTGTGGGAAGGGTGTTTTGGGATTTG	
3R: +7259 +7230	CACCAACATCTTAATTATTTAAACCCAACC	
3Rn: +7196 +7170	CCCTCCG/ACAATACAAAACCCAAAAAC	

Hs: *Homo sapiens*;
Rn: *Rattus norvegicus*;
Mm: *Mus musculus*.

4. RESULTS AND DISCUSSION

4.1 Gene expression profile analysis of six thyroid carcinoma cell lines compared to normal human thyroid primary cells

To search for candidate genes involved in the neoplastic transformation of the thyroid gland, we hybridized the RNAs extracted from normal human thyroid primary cells and six human thyroid carcinoma cell lines of different origin (WRO cell line from a follicular carcinoma, TPC-1 and FB-2 cell lines, both deriving from papillary thyroid carcinoma, NPA cell line, which derives from a poorly differentiated papillary carcinoma, ARO and FRO cell lines originating from anaplastic carcinomas) to an U95Av2 Affymetrix oligonucleotide arrays containing 12.625 sequences.

Among the transcripts represented on the array, 510 have a fold change higher than 10 and 320 lower than -10 in most of the cell lines versus normal thyroid cells (data not shown). To validate the results obtained by the microarray analysis we evaluated the expression of 50 transcripts by semiquantitative RT-PCR in a large number of thyroid carcinoma cell lines. The results essentially overlapped those achieved by microarray analysis, thus validating them. Some representative RT-PCR analyses are shown in Figure 7: in the panel A it's reported the expression of some genes, such as KIF2C, CXCL1, PHLDA2 and CDC20, that are up-regulated in thyroid carcinoma cell lines, while in panel B we show the expression of other genes down-regulated in the neoplastic cell lines, such as PIB5PA, TFF3, BTG2 and RARRES3.

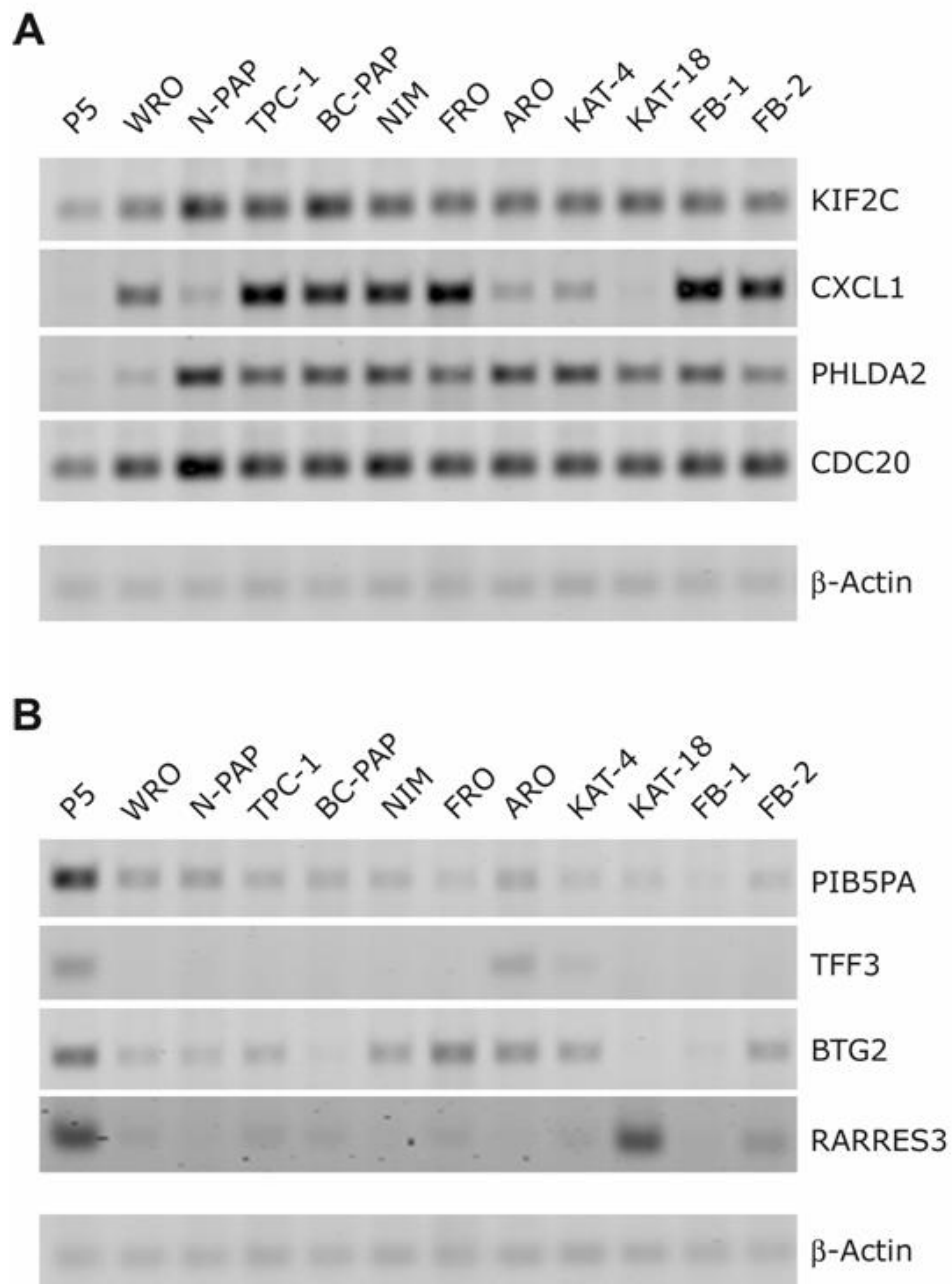


Figure 7 Validation of microarray data by semiquantitative RT-PCR. (A) Semiquantitative RT-PCR of some up-regulated genes in a panel of 11 thyroid carcinoma cell lines versus the normal thyroid cell line and (B) some down-regulated genes resulting by the microarray analysis. In both cases human β -Actin gene expression was evaluated as control to normalize the amount of the used RNAs.

We have assumed that the up- or down-regulation of some genes in all of the thyroid carcinoma cell lines would indicate the presence of a general event linked to thyroid cell transformation, independently from the genetic mechanisms underlying this process. Therefore we focused on the genes up- or down-regulated

in all of the carcinoma cell lines with a higher fold change. Some of them were further analysed by other techniques.

4.2 Expression of UbcH10 gene in normal human thyroid cells and thyroid carcinoma cell lines

Among the genes that were up-regulated more than 10 fold in thyroid carcinoma cell lines compared to the normal thyroid cells, we concentrated our attention on the UbcH10 gene that resulted up-regulated about 150 fold in all of the cell lines tested by the cDNA microarray. We confirmed this result by semiquantitative RT-PCR in a larger panel of thyroid carcinoma cell lines using as control normal thyroid primary culture (Figure 8A). Western blot analysis of UbcH10 expression, shown in Figure 8B, confirmed the RT-PCR data. In fact, the UbcH10 protein was abundantly expressed in all of the carcinoma cell lines, whereas it was barely detectable in normal thyroid cells.

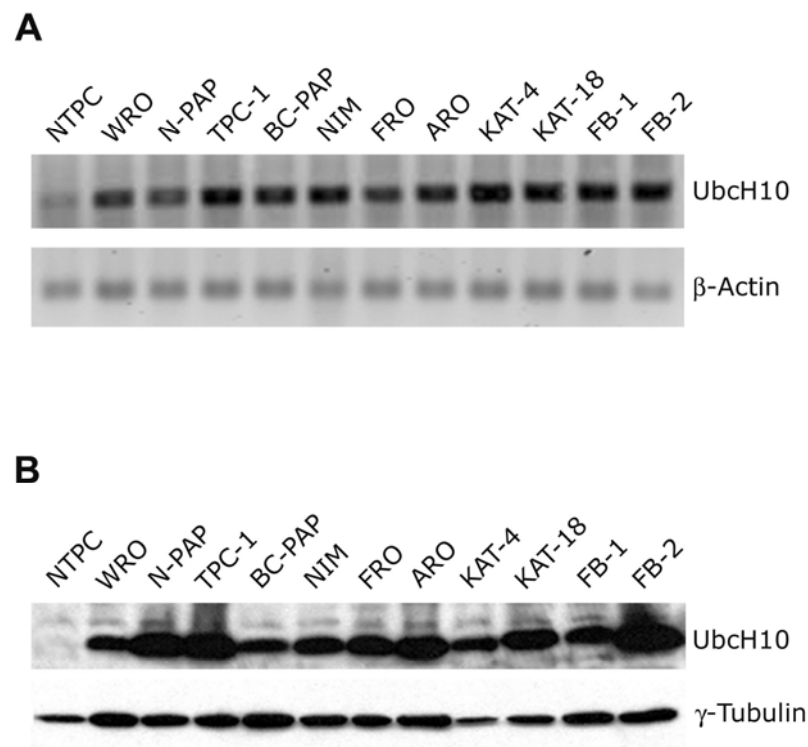


Figure 8 UbcH10 expression in human thyroid carcinoma cell lines. (A) UbcH10 gene expression analysis by RT-PCR in human thyroid carcinoma cell lines vs the normal human thyroid primary culture cells (NTPC). β -Actin gene expression was evaluated as control to normalise the amount of the used RNAs. (B) UbcH10 protein expression analysis by Western blot in human thyroid carcinoma cell lines. Blot against γ -Tubulin has been performed as control for equal protein loading.

4.3 Analysis of UbcH10 expression in normal and neoplastic thyroid tissues by immunohistochemistry, Western blot and RT-PCR

To evaluate whether the overexpression of UbcH10 is not only a feature of cultured thyroid carcinoma cell lines, but also of thyroid tumors, we performed an immunohistochemical analysis using a commercial antibody against UbcH10 protein. This methodology allows a rapid and sensitive screening of thyroid pathological tissues and is amenable to regular use as a routine diagnostic test. To find the best experimental conditions, ARO cell line and tumors, induced by injecting the ARO cell line into athymic mice, were used as positive controls (Cerutti et al, 1996). No staining was observed with normal human thyroid primary cell culture, whereas a positive staining was obtained with ARO cell line and ARO induced tumors (data not shown). By analysing paraffin-embedded tissue sections we found that normal thyroid, nodular goiter and Hashimoto's thyroiditis (HT) were almost always completely negative for UbcH10 expression. Only occasionally, single UbcH10 labelled thyroid epithelial cells showing mitotic figures could be observed by meticulous scrutiny (Figure 9A).

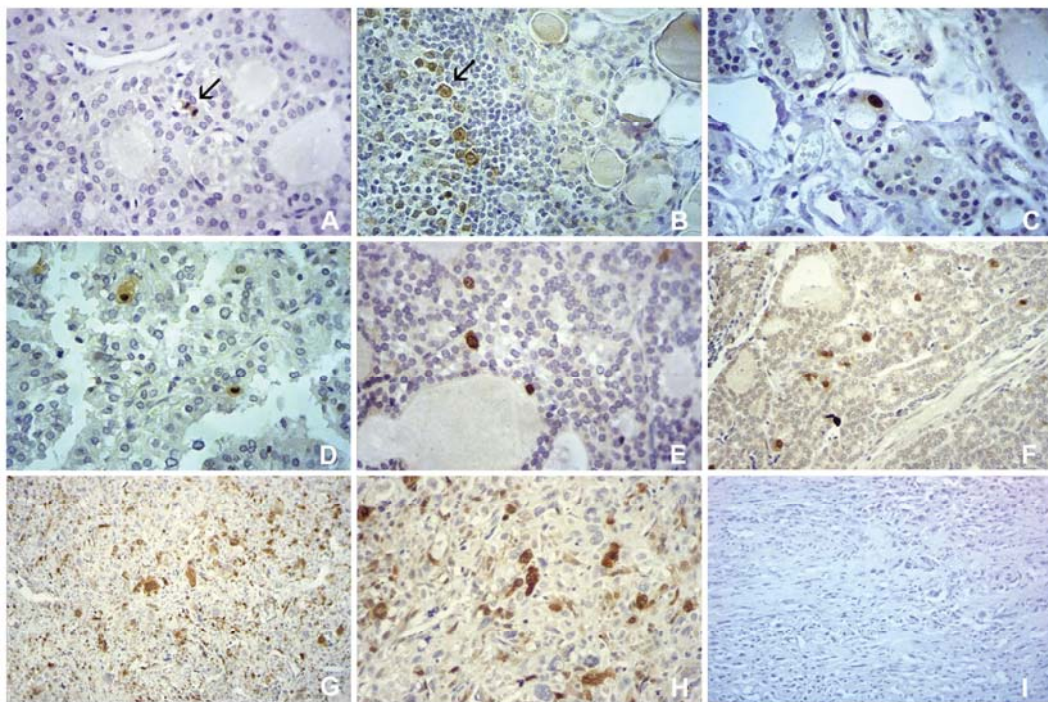


Figure 9 UbcH10 staining pattern in normal, inflammatory and neoplastic thyroid tissues. Follicular epithelial cells of normal thyroid (A) and oxyphilic cells of Hashimoto's thyroiditis (HT) (B) do not stain for UbcH10, with occasional mitotic figures (A, arrow) and lymphoid centробlasts of HT (B, arrow) providing the appropriate internal positive control. In neoplastic thyroid, UbcH10 staining pattern is strongly related to tumour grade, being weak in follicular adenoma (C), slightly more evident in well-differentiated papillary (D) and follicular (E) carcinomas, whereas stronger in poorly differentiated (F) and in anaplastic (G) carcinomas. In the latter, most of neoplastic cells show a very intense labelling, with intense nuclear staining (H), whereas signal disappeared by antigen incubation (I).

In HT sections there was a sharp contrast between the epithelial oxyphilic cells (negative) and the lymphoid germinal centers (positive) (Figure 9B). While a weak staining is detectable in follicular adenomas (Figure 9C), higher levels of UbcH10 were recorded in PTC (median value 2.2% of positive cells, range 0.9-4.1%), FTC (median value 2.8% of positive cells, range 1-6.1%) and PDC (median value 10.4% of positive cells, range 8-14.9%), signal being always easily detectable in the nuclei of scattered neoplastic cells (Figure 9D, E and F). UbcH10 staining pattern was different in ATC, being large the percentage (median value 45.8% of positive cells, range 38.8-56.2%) of stained cells and strong the intensity of the neoplastic cells (Figure 9, G and H). No staining was observed when the same ATC samples were stained with antibodies pre-incubated with UbcH10 recombinant protein (Figure 9I) or in the absence of the primary antibodies (data not shown).

Therefore, as a general rule, UbcH10 expression is negligible in non neoplastic thyroid, noticeable in well-differentiated carcinomas and conspicuous in less differentiated tumors (Figure 10A).

A

Kruskal-Wallis Test: $P < 0.001$

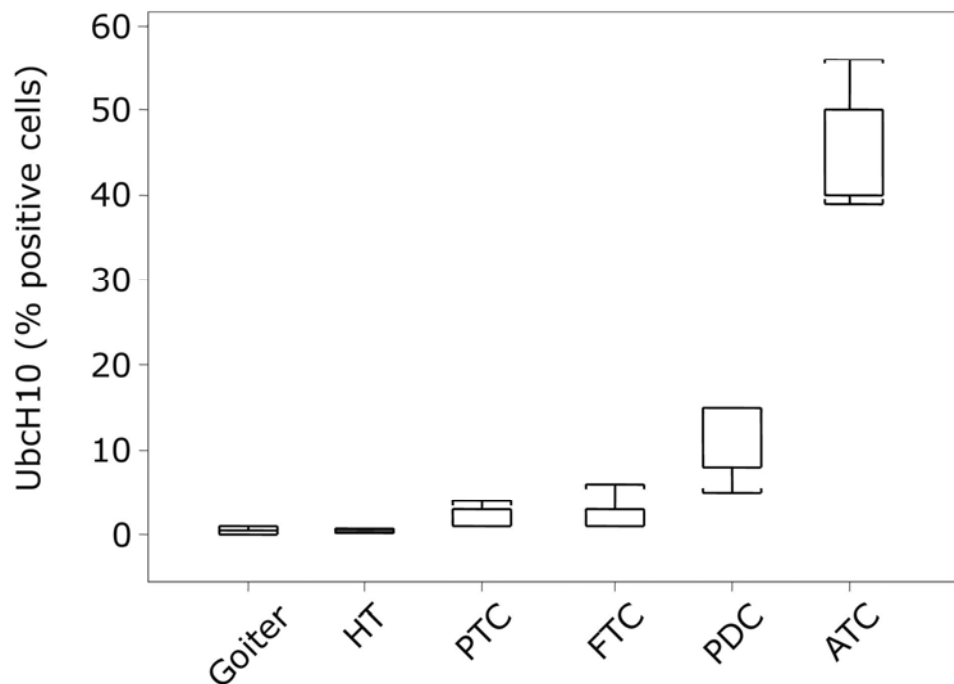


Figure 10A Statistical analysis of the immunohistochemical data. Protein expression of UbcH10 (% positive cells) progressively increases in the several diagnostic categories from thyroid goiter to the thyroid anaplastic carcinomas. The analysis has been carried out using the Kruskal-Wallis test. HT, Hashimoto's thyroiditis; PTC, papillary thyroid carcinoma; FTC, follicular thyroid carcinoma; PDC, poorly differentiated thyroid carcinoma; ATC, anaplastic thyroid carcinoma.

We correlated also the expression of UbcH10 in carcinomas with the proliferation rate of thyrocytes (as measured by Ki-67 staining) to determine the relationship between its expression and tissue proliferation. By the use of Spearman rank order correlation, we determined that the association between UbcH10 and Ki-67 expression in thyroid cancer was statistically significant (the value of the Spearman R was 0.4, $P < 0.001$) (Figure 10B).

B

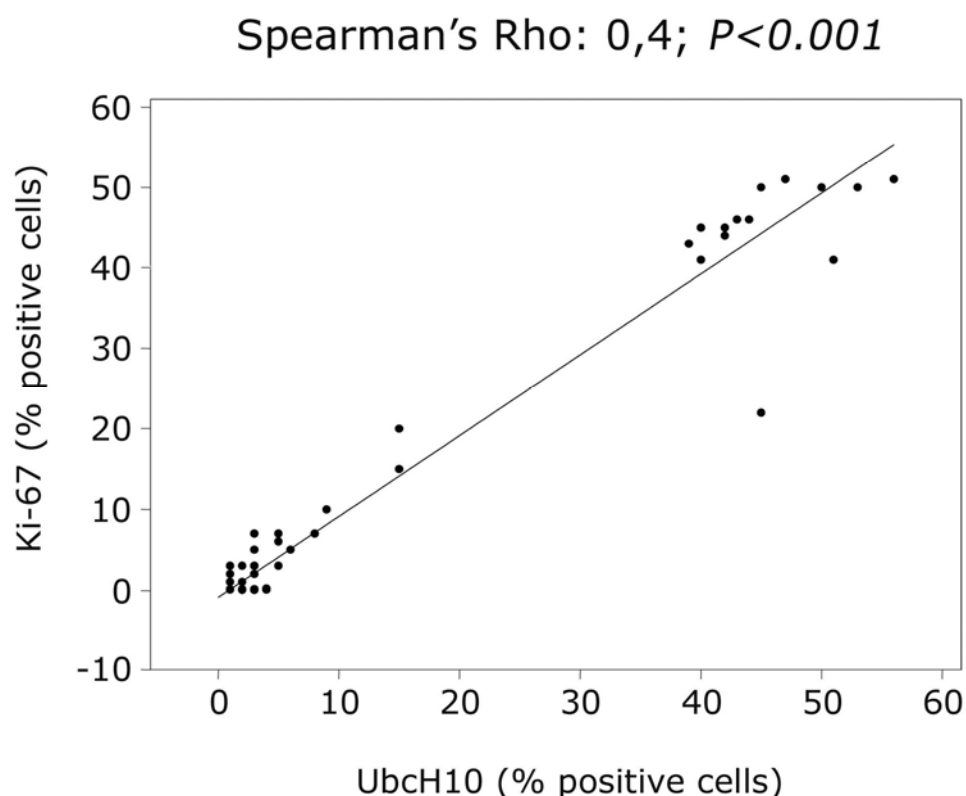


Figure 10B Statistical analysis of the immunohistochemical data. Protein expression of UbcH10 (% positive cells) is correlated to that of Ki-67 (% positive cells) in the several diagnostic categories. The analysis has been carried out calculating the Spearman rank correlation coefficient.

Western blot analysis, performed on 30 surgically removed thyroid tumors, confirmed the immunohistochemical data. A representative Western blot is shown in Figure 11A. A strong band of 19.6 kDa corresponding to the UbcH10 protein was detected in ATC and a weak one in PDC, but not in PTC and normal thyroids.

These data strongly indicate that the expression of UbcH10 is more abundant in highly malignant and aggressive thyroid carcinomas. Equal amounts of total proteins were used for each sample as demonstrated by the same gel analysed with an antibodies against γ -Tubulin.

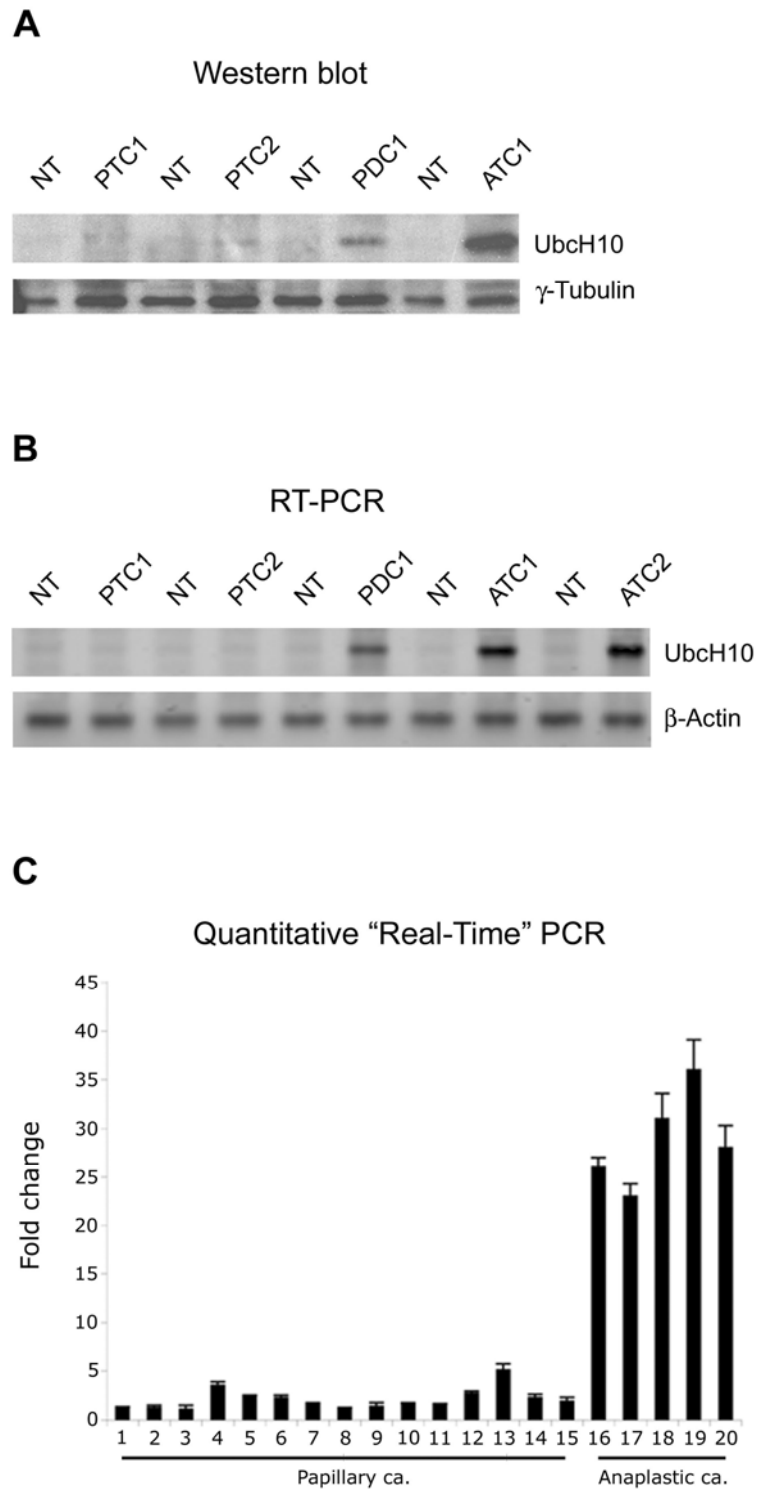


Figure 11 Ubch10 expression in human thyroid fresh tumour samples. (A) Western blot analysis of Ubch10 protein expression in a panel of thyroid neoplasias. The level of γ -Tubulin has been used as loading control. NT, normal thyroid tissue; PTC1 and PTC2, papillary thyroid carcinomas from two different patients; PDC1, poorly differentiated carcinoma; ATC1,

anaplastic thyroid carcinoma. (B) RT-PCR analysis of UbcH10 expression in human thyroid tumour samples vs their normal thyroid counterparts. β -Actin expression shows the same amount of RNAs used. NT, normal thyroid tissue; PTC1 and PTC2, papillary thyroid carcinomas from two different patients; PDC1, poorly differentiated carcinoma; ATC1 and ATC2, anaplastic thyroid carcinomas from two different patients. (C) Quantitative RT-PCR analysis was performed on human thyroid tumour samples of different histotype. The Fold Change values indicate the relative change in the expression levels between tumour samples and normal samples, assuming that the value of each normal sample is equal to 1.

We also evaluated UbcH10 expression on a panel of matched tumor/normal tissues by semiquantitative RT-PCR analysis. This analysis confirmed the protein data. In fact, an amplified band corresponding to UbcH10 was clearly detected in five ATCs, but not in the corresponding normal thyroid tissues (Figure 11B). Finally, quantitative RT-PCR analysis confirmed a great increase of UbcH10 expression in thyroid anaplastic samples, whereas a light increase was observed in papillary carcinoma samples. (Figure 11C).

These data, therefore, strongly indicate that UbcH10 overexpression could be associated with the thyroid tumor progression since there is a good correlation with the late stage of thyroid neoplastic transformation. These findings are consistent with previous published data showing that UbcH10 was expressed at high levels in primary tumors of diverse anatomic origin (lung, stomach, uterus, and bladder) as compared with their corresponding normal tissues, suggesting that UbcH10 is involved in tumorigenesis or cancer progression (Wagner et al. 2004, Okamoto et al. 2003)

The low UbcH10 levels detected in the differentiated thyroid malignancies would appear in contrast with the data showing an abundant UbcH10 expression in the cell lines deriving from differentiated carcinomas. Really we retain that this discrepancy is only apparent since thyroid carcinoma cell lines, even deriving from differentiated tumors, cannot be completely compared to surgically removed tumors. These cell lines, in fact, harbour p53 mutations that are rare in thyroid differentiated neoplasias (Ito et al. 1992; Fagin et al. 1993; Dobashi et al. 1993; Fabien et al. 1994; Fiore et al. 1997; Basolo et al. 2002) and they have a high proliferation rate. However, this consideration does not exclude the validity of the use of the thyroid carcinoma cell lines as experimental model to draw new information that, however, need to be subsequently validated on fresh tumors.

Our results also indicate a correlation between UbcH10 overexpression and the proliferation status since there is a good association with the proliferation marker Ki-67/MIB1.

4.4 UbcH10 expression in experimental models of thyroid carcinogenesis

Subsequently we analysed for UbcH10 expression thyroid neoplasias developing in transgenic animals lines expressing TRK (Tg-TRK) (Russell et al. 2000), RET/PTC3 (Tg-RET/PTC3) (Powell et al. 1998) and large T SV40 (Tg-SV40) (Ledent et al. 1991) oncogenes under the transcriptional control of the thyroglobulin (Tg) promoter. Transgenic mice carrying TRK and RET/PTC3 oncogenes develop thyroid papillary carcinomas (Russell et al. 2000, Powell et al. 1998), thyroid anaplastic carcinomas were, conversely, obtained in the Tg-SV40 mice (Ledent et al. 1991). We observed elevated UbcH10 protein levels in the

ATC derived from large T SV40 transgenic mice (Figure 12). Conversely, UbcH10 protein was absent in normal mouse thyroid tissue and in the PTCs originating from TRK and RET/PTC3 mice.

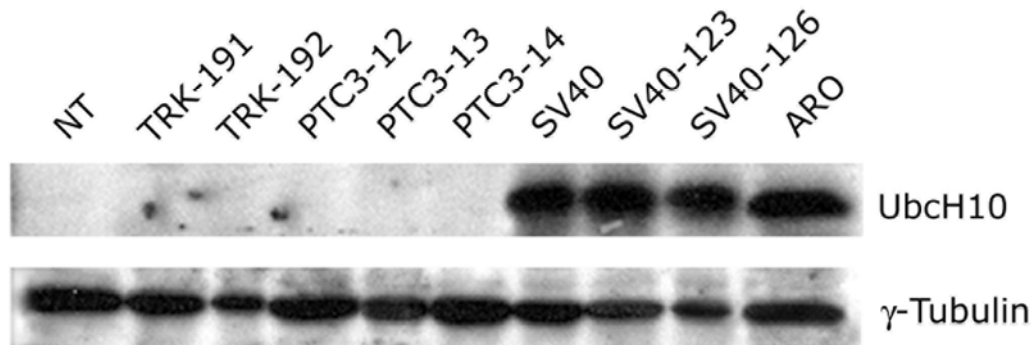


Figure 12 UbcH10 expression in experimental mouse thyroid tumours. Western blot analysis of experimental thyroid carcinomas developed in transgenic mice expressing TRK, RET-PTC-3 and large T SV40 oncogenes. ARO cell line was used as positive control. γ -Tubulin shows the same amount of protein level.

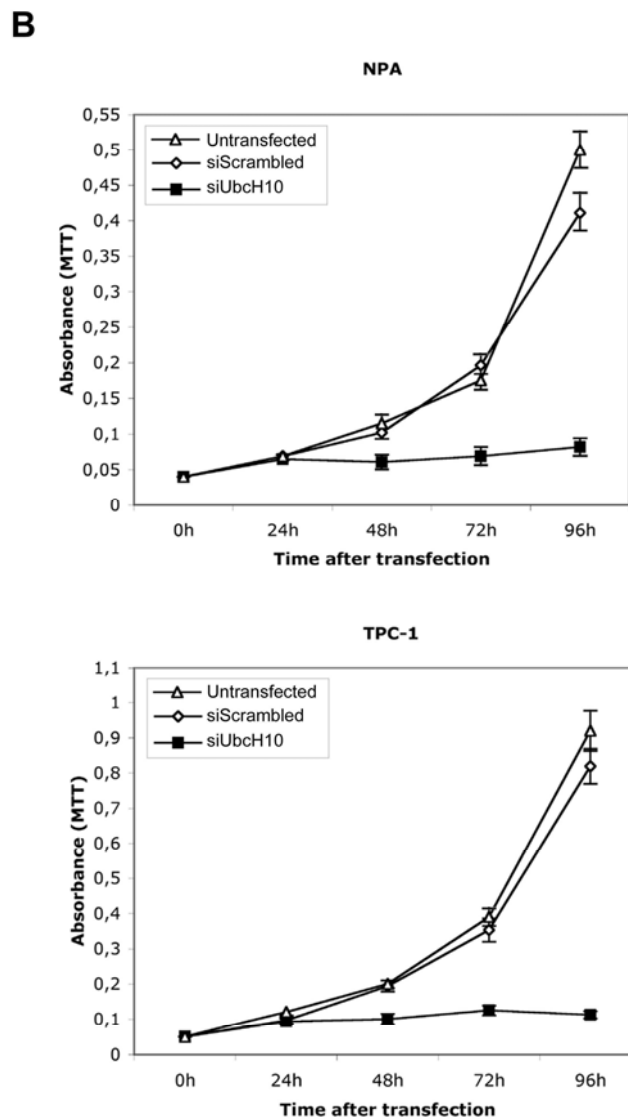
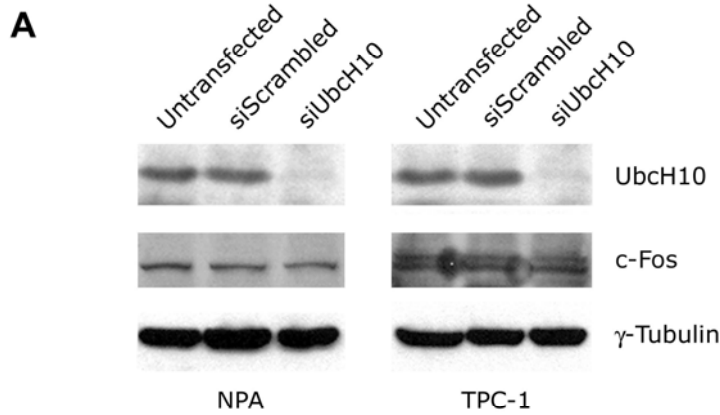
This results are consistent with previous findings showing that UbcH10 is up-regulated in NIH 3T3 cell line transformed by EWS/FLI1, but not in untransformed NIH 3T3 cell clone expressing EWS/FLI1 (Arvand et al. 1998).

Therefore, this analysis seems to confirm that the UbcH10 overexpression is essentially restricted to the undifferentiated histotype.

4.5 Suppression of the UbcH10 synthesis inhibits thyroid carcinoma cell growth

We asked whether UbcH10 overexpression had a role in the process of thyroid carcinogenesis by evaluating the growth rate of two thyroid carcinoma cell lines after the suppression of UbcH10 synthesis by RNA interference. The NPA and TPC-1 cell lines were treated with siRNA duplexes targeting to the UbcH10 mRNA. After transfection we observed an efficient knock-down of the UbcH10 protein levels at 48 h after treatment (Figure 13A).

Figure 13 The block of UbcH10 protein synthesis by RNA interference inhibits the proliferation of thyroid carcinoma cells.



(A) Inhibition of UbcH10 protein expression by RNAi in NPA and TPC-1 cell lines evaluated by Western blot analysis. At 48 h after siRNA transfection, total cell lysates were prepared and normalised for protein concentration. The expression of γ -Tubulin was used to control equal protein loading (30 μ g). In this figure, we also show the expression of a fast turning-over gene like c-Fos to confirm the specific effect of siRNAs against UbcH10. (B) Growth curves of NPA and TPC-1 cell lines after siUbcH10 treatment. NPA and TPC-1 cells were transfected with siUbcH10 duplexes (siUbcH10) and the relative number of viable cells was determined by MTT assay. Cells transfected with a scrambled duplex (siScrambled) and untransfected cells (Untransfected) were used as negative controls. Absorbance was read at 570 nm and the data are the mean of triplicates.

The block of UbcH10 protein synthesis significantly inhibits thyroid carcinoma cell growth. In fact, as shown in Figure 13B, a significant reduction in cell growth rate was observed in NPA and TPC-1 cell lines treated with UbcH10 siRNA in comparison to the untreated cells or those treated with the control scrambled siRNA. Indeed, the block of proteins synthesis significantly inhibited the growth of several thyroid carcinoma cell lines, suggesting an important role of UbcH10 in thyroid cell proliferation, and then in the progression step of thyroid carcinogenesis. In fact, it has been shown that UbcH10 is required for override metaphase, likely degrading growth suppressor, and for destruction of mitotic cyclins, indicating a role of UbcH10 in cell cycle progression (Arvand et al. 1998).

4.6 UbcH10 overexpression is not sufficient to transform rat thyroid cells

We further characterized the role of UbcH10 in thyroid carcinogenesis transfecting normal rat thyroid cells with the UbcH10 gene under the transcriptional control of the cytomegalovirus promoter. The selected clones were shown to express high UbcH10 protein levels (data not shown). By evaluating the growth rate of the UbcH10 transfected PC Cl 3 cells and the same cells transfected with a backbone vector we did not observe any differences. Equally, we evaluated the neoplastic phenotype of the UbcH10-transfected PC Cl 3 cells by a soft agar colony assay and by injection into athymic mice. As reported in Table 2, the PC Cl 3 cells transfected with the UbcH10 expression vector were not able to give rise to colonies in soft agar and induce tumors in athymic mice.

Table 2 Analysis of the neoplastic phenotype of the UbcH10-transfected rat thyroid cell lines

<i>Cell line</i>	<i>Doubling time (h)</i>	<i>Colony-forming^a efficiency (%)</i>	<i>Tumor incidence^b</i>
PC CL 3	24	0	0/4
PC UbcH10 CL1	24	0	0/4
PC UbcH10 CL2	23	0	0/4
PC MPSV	18	70	4/4

^a Colony-forming efficiency was calculated by the formula (number of colonies formed/number of plated cells) x100. ^b Tumorigenicity was assayed by injecting 2x10⁶ cells into athymic mice (4 to 6 week old).

As a positive control we used the PC Cl 3 cells transformed with the Myeloproliferative sarcoma virus (PC MPSV): these cells have a very highly malignant phenotype (Fusco et al. 1987).

These results indicate that UbcH10 overexpression is not able to transform rat thyroid cells in vitro and, more generally, would indicate that UbcH10 overexpression is not sufficient for malignant thyroid cell transformation. This might appear in contrast with other published results showing that NIH3T3 stable

transfectants overexpressing UbcH10 exhibited a malignant phenotype as compared with parental NIH3T3 cells (Okamoto et al. 2003). In our opinion the discrepancy is, just apparent since we have to consider that NIH 3T3 cells are preneoplastic cells, whereas PC Cl 3 cells are much more resistant to express the neoplastic phenotype, since even the expression of several oncogenes (v-ras-Ki, v-ras-Ha, etc) are not able to lead these cells to the fully malignant phenotype that is achieved only when there is a synergy of two different oncogenes (Fusco et al. 1987).

4.7 UbcH10 involvement in ovarian carcinoma

We extended the study of UbcH10 gene also to other neoplasias like ovary carcinoma (Berlingieri et al. 2006). As in thyroid carcinoma, we found that all the ovary carcinoma cell lines showed a high UbcH10 expression, which was barely detectable in the normal tissue. The same analyses, performed on ovarian carcinoma tissues, showed a different expression in the different histotypes analysed: UbcH10 was expressed at low levels in clear cell carcinomas, endometrioid carcinomas and serous cystadenocarcinomas, whereas the undifferentiated carcinomas expressed high level of UbcH10 (Berlingieri et al. 2006).

Immunohistochemistry essentially confirmed the data obtained by RT-PCR and Western blot analyses. Abundant expression of UbcH10 was detected in primary ovarian tumors compared with benign ovarian tissues and significantly correlated to tumor grade ($P=0.0008$) and undifferentiated histotype ($P=0.015$). These results are consistent with our data in thyroid and further support the involvement of UbcH10 in the differentiation process of several human epithelial tissues (Wagner et al., 2004). UbcH10 is also a negative predictor of clinical outcome in our series, further suggesting its ability to confer a more aggressive phenotype to tumor cells. Studies are ongoing to assess this hypothesis on a larger series of patients with a longer follow-up.

Functional studies also demonstrated that the suppression of the UbcH10 expression by RNA interference reduced the growth of one ovarian carcinoma cell line indicating a role of UbcH10 overexpression in ovarian carcinogenesis, in particular, in influencing the hyperproliferative status of the most malignant cells (Berlingieri et al. 2006). These results, therefore, indicate a role of UbcH10 also in neoplastic ovarian cell proliferation, and, for this reason we propose the UbcH10 expression as a possible tool to be used in the diagnosis and prognosis of ovarian carcinomas.

4.8 CBX7 gene expression is down-regulated in human thyroid carcinoma cell lines

Analysing the above mentioned Affymetrix microarray, we also concentrated our attention upon those genes that resulted down-regulated in the thyroid carcinoma cell lines, considering them as potential tumor suppressor genes. Among the down-regulated genes, CBX7 was drastically down-regulated in all the cell lines tested with the cDNA microarray (Figure 14A).

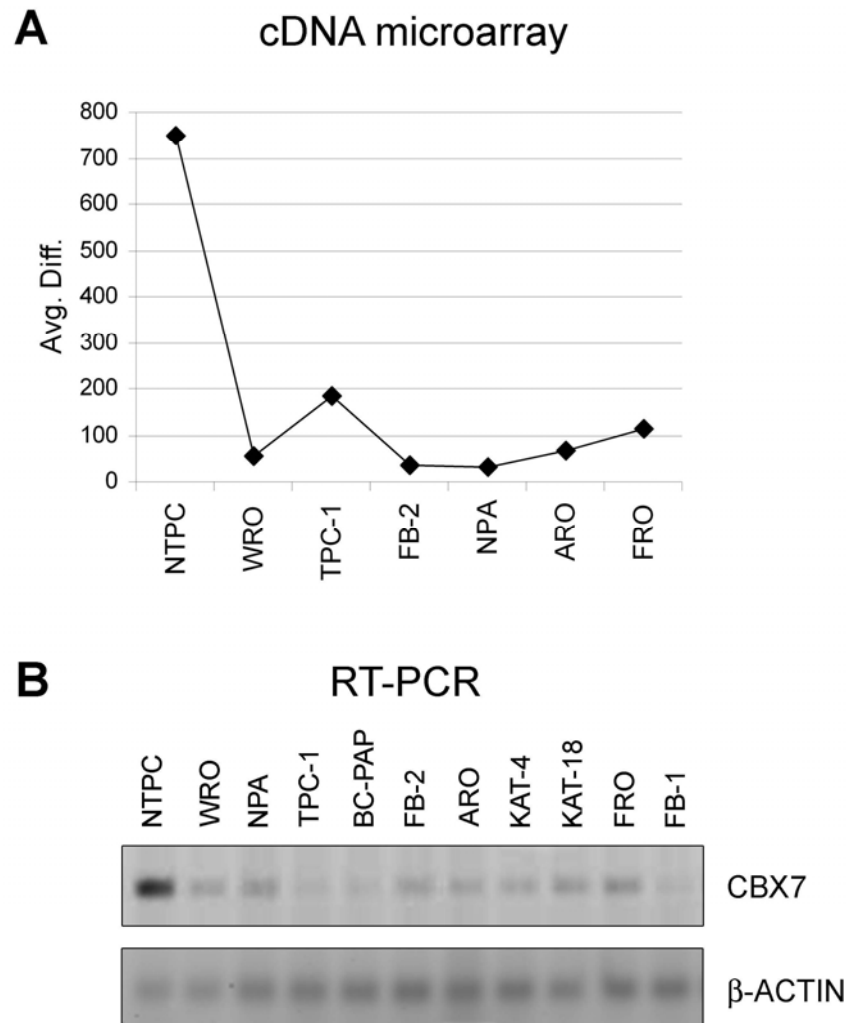


Figure 14 CBX7 expression in human thyroid carcinoma cell lines. (A) CBX7 gene expression by microarray analysis in human thyroid carcinoma cell lines vs normal human thyroid primary culture cells (NTPC). Avg. Diff, average difference: it is a quantitative relative indicator of a transcript expression level ($\sum(\text{PM-MM})/\text{pairs}$ on average). (B) CBX7 gene expression analysis by RT-PCR in human thyroid carcinoma cell lines vs the normal human thyroid primary culture cells (NTPC). β -Actin gene expression served as loading control.

This result was confirmed by RT-PCR analysis in a large panel of thyroid carcinoma cell lines with normal thyroid primary culture cells as control (Figure 14B).

4.9 The loss of CBX7 expression correlates with a more aggressive phenotype of thyroid carcinomas

To determine whether the loss of CBX7 expression is a feature of thyroid tumors and not only of cultured thyroid carcinoma cell lines, we carried out an immunohistochemical analysis of paraffin-embedded tissues using polyclonal antibodies raised against the carboxy-terminal region of human CBX7 protein (see Methods). As shown in Table 3, all 20 samples of normal thyroid parenchyma expressed CBX7 at a very high level, which coincides with the strong CBX7 staining in all follicles (Figure 15A).

Table 3 CBX7 expression in normal and neoplastic thyroid tissues by IHC

<i>Histotype</i>	<i>Cases</i>	<i>CBX7 expression</i> ^a			
		<i>High</i>		<i>Low</i>	
Normal Thyroid Parenchyma	n=20	100%	(20/20)	0%	(0/20)
Follicular Adenomas	n=20	100%	(20/20)	0%	(0/20)
Follicular Carcinomas	n=32	34%	(11/32)	66%	(21/32)
Papillary Carcinomas - Classic Variant	n=30	43%	(13/30)	57%	(17/30)
Papillary Carcinomas - Tall Cell Variant	n=6	17%	(1/6)	83%	(5/6)
Poorly Differentiated Carcinomas	n=12	17%	(2/12)	83%	(10/12)
Anaplastic Carcinomas	n=12	0%	(0/12)	100%	(12/12)

^aHigh: cases with more than 50% of neoplastic cells showing CBX7 staining; Low: cases with less than 50% of neoplastic cells showing CBX7 staining.

The intensity of nuclear labeling of epithelial thyroid cells in follicular adenoma was similar to that of the internal control stromal and endothelial cells (Figure 15B). Conversely, CBX7 expression was reduced in malignant lesions. As shown in Table 3, and in Figure 15C and D, the percent of low expressors was high in well-differentiated tumors, namely FTC (66%; 21/32 samples) and PTC (57%; 17/30 samples). It was even higher in the less differentiated tumors, namely PDC (83%; 10/12) (Table 3, and Figure 15F and G) and “tall cell variant”(TCV)-PTC (83%; 5/6) (Table 3, and Figure 15E). In the latter, neoplastic cells were almost devoid of CBX7 expression, which sharply contrasted with the intense staining of the infiltrating lymphocytes and stromal cells. Similarly, CBX7 expression was completely lost in all cases of ATC (100%; 12/12) (Table 3, Figure 15H). No staining was observed when normal thyroid gland samples were stained with antibodies pre-incubated with CBX7 recombinant protein (Figure 15I) or in the absence of the primary antibodies (data not shown). Therefore, CBX7 was expressed in normal thyroid and in benign neoplastic lesions, decreased in well-differentiated carcinomas and was drastically reduced in aggressive thyroid tumors.

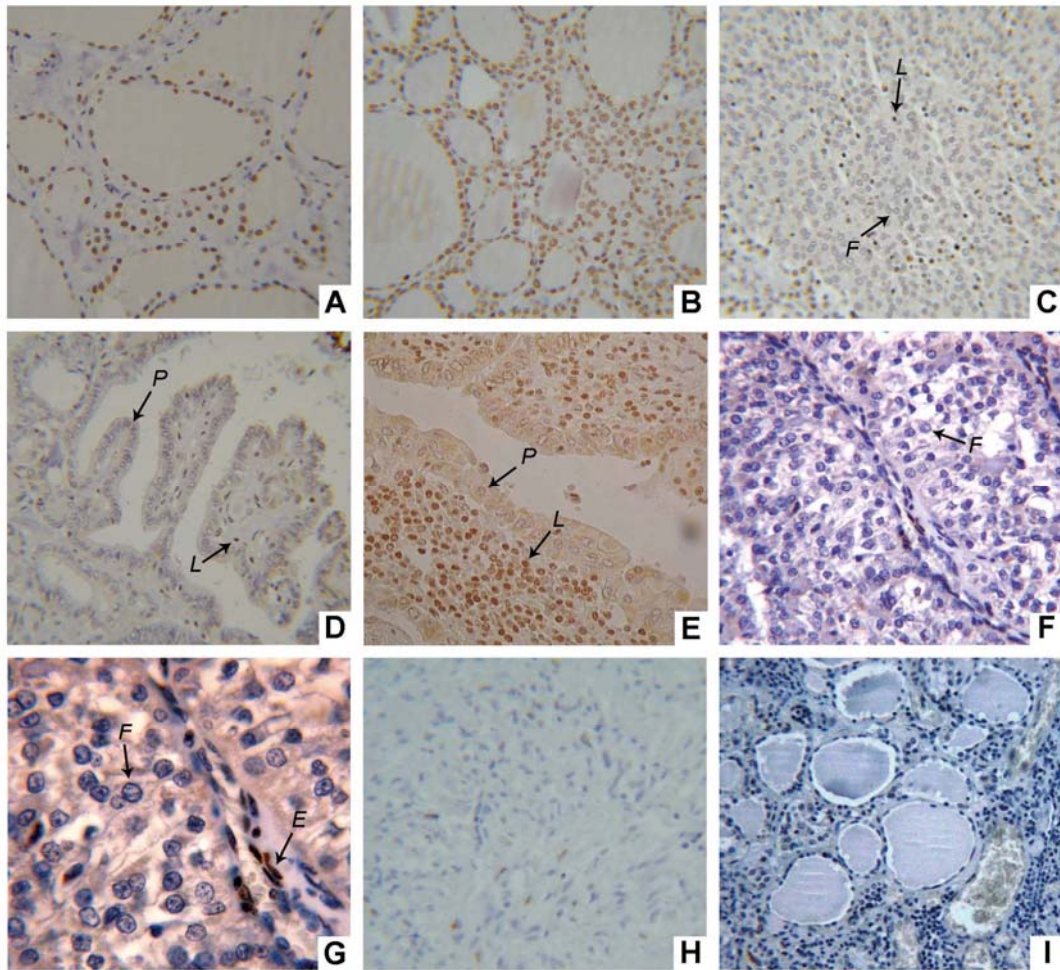


Figure 15 CBX7 staining in normal and neoplastic thyroid tissues. CBX7 nuclear staining was intense in benign follicular epithelial cells of normal thyroid (A) and of follicular adenoma (B), whereas it was weak in follicular carcinoma (C). CBX7 progressively decreased going from well-differentiated “classic variant” papillary (D) carcinomas to the “tall cell variant” of PTC (E), to poorly differentiated (F, G) and anaplastic (H) carcinomas. The signal disappeared after incubation of the sample with antigen (I). Sample showed in the G panel is the same of F, but magnified, to better show cell nuclei. Arrows with letters indicate the following sample features: (*P*→) nuclei showing cytological features of PTC negative for CBX7 expression; (*F*→) FTC nuclei negative for CBX7 expression; (*L*→) lymphocyte showing CBX7 expression and providing positive internal control; (*E*→) endothelial cells showing CBX7 expression and providing positive internal control.

4.10 Analysis of CBX7 expression in normal and neoplastic thyroid tissues by semiquantitative RT-PCR and quantitative Real-Time PCR

We also evaluated CBX7 expression by semiquantitative RT-PCR in a panel of matched normal/tumor tissues. The results confirmed the immunohistochemical data. In fact, there was an amplified band corresponding to CBX7 in normal thyroid tissues (Figure 16A).

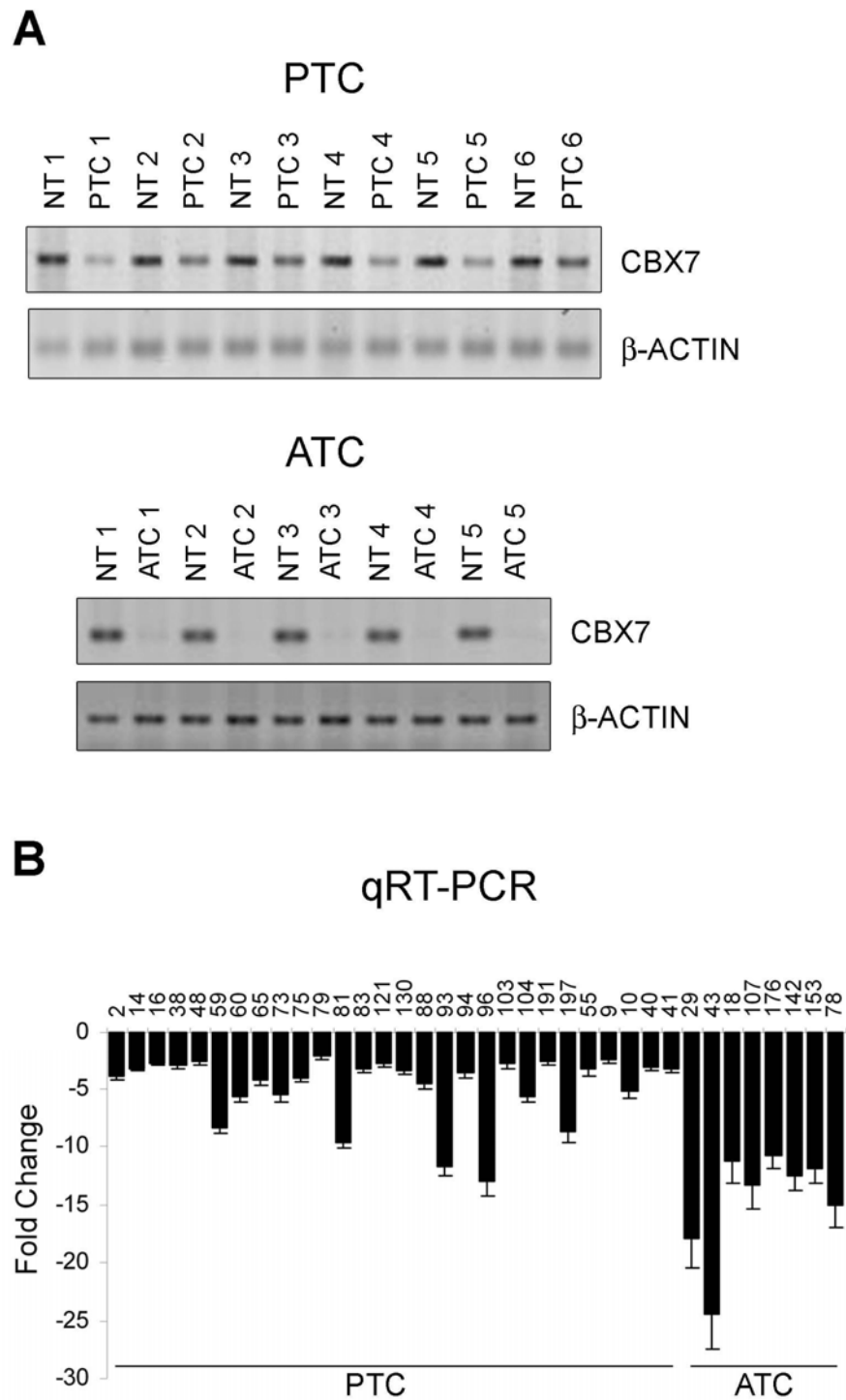


Figure 16 CBX7 expression in fresh thyroid tumor samples from patients. (A) RT-PCR analysis of CBX7 expression in human thyroid tumor samples vs their normal thyroid counterparts. β -Actin expression served as loading control. NT, normal thyroid tissue; PTC1 to PTC6, papillary thyroid carcinomas from different patients; ATC1 to ATC5, anaplastic thyroid carcinomas from different patients. (B) qRT-PCR analysis of human thyroid tumor samples of different histotypes. The fold change indicates the relative change in expression levels between tumor samples and normal samples, assuming that the value of each normal sample is equal to 1.

The amplified band decreased in PTC samples and almost disappeared in ATC. qRT-PCR analysis of a large number of human thyroid carcinoma samples of different histotypes confirmed a correlation between the reduction of CBX7 expression and a more malignant phenotype of thyroid neoplasias. In fact, as reported in Figure 16B, there was a negative fold change in CBX7 expression from -2.1 to -13 (average -4.8) in the PTC samples versus normal counterpart tissue. The reduction was even more pronounced in the anaplastic carcinoma samples, with a fold change ranging from -10.8 to -24.5 (average -14.6). These data are well correlated with the immunohistochemical data and suggest that CBX7 expression is controlled at transcriptional level.

4.11 Analysis of human thyroid fine-needle aspiration biopsy

Fine-needle aspiration biopsy has become an integral part of the pre-operative evaluation of thyroid nodules. To evaluate whether CBX7 gene expression analysis can be applied to FNAB samples, we studied 15 cases of PTC by immunocytochemistry and qRT-PCR.

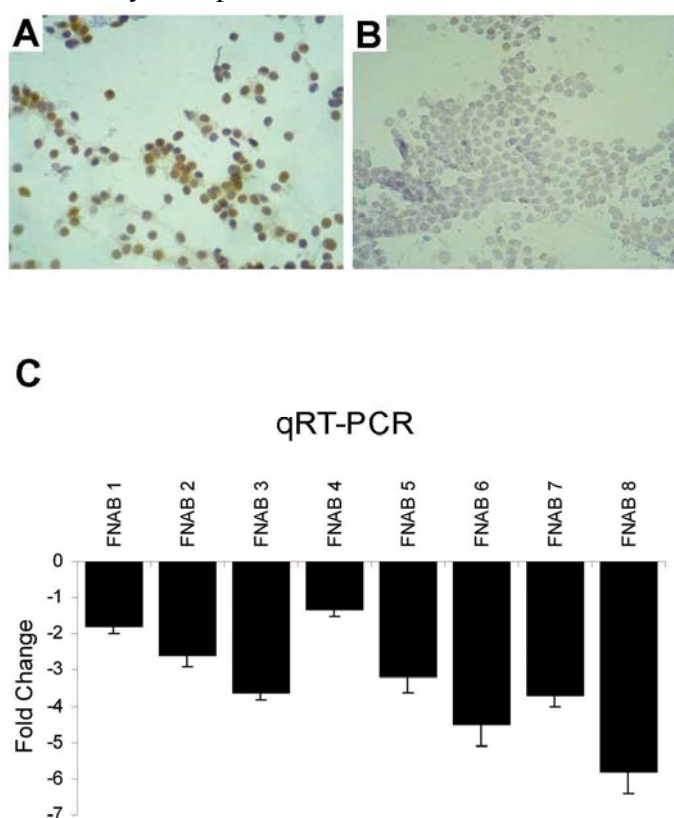


Figure 17 FNAB analysis. Immunocytochemistry (A, B) and qRT-PCR (C) analyses of CBX7 of fine needle aspiration biopsies (FNAB), whose PTC pre-operative cytological diagnosis was histologically proven. FNAB goiter samples were used as controls. The fold change indicates the relative change in expression levels between tumor and goiter samples, assuming that the value of the normal sample was equal to 1. FNAB 1 to 8, from different patients.

In 8 cases out of 15, CBX7 expression was lower in FNABs from patients affected by a carcinoma (Figure 17B) than in FNABs from thyroid goiter (Figure

17A) as evaluated by immunocytochemistry (Figure 17A and B) and qRT-PCR (Figure 17C).

Based on these findings, it is feasible that CBX7 levels could serve to differentiate between benign and malignant thyroid neoplasms. Indeed, in clinical practice, it is difficult to distinguish between FTC and the benign FA (Yeh et al. 2004; Segev et al. 2003). In the perspective of diagnosis/prognosis, CBX7 expression level in FNAB may be used to identify PTC by immunohistochemistry and qRT-PCR. Interestingly, a recent paper concerning the cytogenetics of Chernobyl thyroid tumors identified a correlation between the deletion of the chromosomal region 22q13.1, where the CBX7 gene is located, and a worse prognosis (Richter et al. 2004).

4.12 LOH at CBX7 locus (22q13.1)

In some types of cancers, LOH of tumor suppressor genes at region 22q is believed to be a key step in carcinogenesis (Wild et al. 2002; Iida et al. 1998; Allione et al. 1998). We, therefore, used several SNP markers to evaluate LOH on chromosome 22q13.1 (at the CBX7 locus) in 60 cases of thyroid carcinomas of different histotypes. As shown in Table 4, LOH at CBX7 locus occurred in 36.8% of the informative PTC (7 out of 19 cases), whereas in 68.7% (11/16 cases) of informative ATC. The percentage of LOH was much higher in the TCV variant of PTC (3/4 cases; 75%) than in classical PTC (7/19 cases; 36.8%). Again, LOH of CBX7 was well correlated with tumor phenotype, TCV being more aggressive than classical PTC (Nardone et al. 2003).

Table 4 Loh frequency statistics at CBX7 locus (22q13.1) by SNP sequencing method.

<i>Histotype</i>	<i>Cases</i>	<i>(Inf^a)</i>	<i>LOH^b</i>
Papillary Carcinoma- Classic Variant	n=36	(19)	36.8% (7/19)
Papillary Carcinoma- Tall Cell Variant	n=6	(4)	75% (3/4)
Follicular Carcinomas	n=5	(3)	66.6% (2/3)
Anaplastic Carcinomas	n=20	(16)	68.7% (11/16)

^aInf: informative cases are samples showing SNP heterozygosity corresponding to two peaks (two alleles) on the sequencing chromatogram. ^bThe LOH frequency is equal to the ratio between allelic loss and informative cases.

We next looked for CBX7 gene mutations in human thyroid carcinoma samples. We analyzed 20 PTC samples and 6 ATC samples and found no mutations (data not shown).

4.13 Methylation status of the CBX7 gene

To investigate the mechanisms underlying CBX7 downregulation in thyroid tumors, we evaluated DNA methylation of the CBX7 gene in normal and tumor tissues. An analysis of CBX7, carried out with the CpG plot program (see Methods), revealed two CpG islands. The first extended about 1000 nucleotides

around the transcription initiation site and the second was located at the distal part of intron 2 (Figure 18).

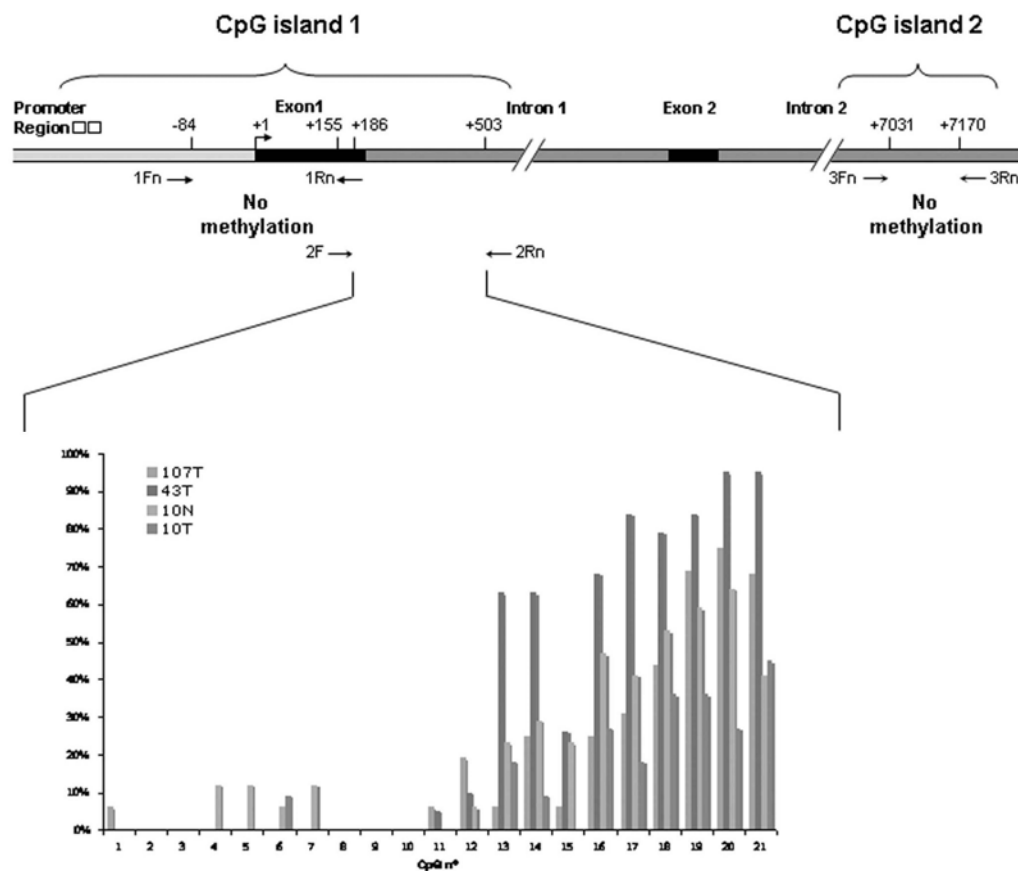


Figure 18 Methylation analysis of the CBX7 gene. The structure of CBX7 is shown in the upper panel. The transcriptional start site is indicated as +1. The positions of the CpG islands and of the primers used for bisulfate analysis are indicated. The first part of the upstream portion of CpG island 1 (-84 to +155) and the CpG island 2 (+7031 to +7170) were unmethylated in normal, tumor tissues and in the tumoral cell line TPC1. Lower panel, methylation of the first intron (21 CpG sites): two anaplastic tumors (43T and 107 T), one papillary tumor (10T) and its corresponding normal tissue (10N) are shown. The degree of methylation is reported as the percentage of m-C obtained for each CpG dimer on a total of 20 independent clones analyzed (see Methods).

We analysed the putative promoter region (between -83 and +154) of genomic DNA extracted from five PTC and corresponding adjacent normal tissues, from 5 ATC, and from the thyroid papillary carcinoma cell line TPC-1 (Figure 18, upper panel). We found no methylation in any of the 42 CpGs present in this region (data not shown). By contrast, methylation of the last part of this CpG island (from +187 to +502, Figure 18, upper panel), which contains 21 CpGs, was much higher in ATC than in PTC and normal tissues (Figure 18, lower panel). No significant methylation was found in the second CpG island.

Indeed, there was a hypermethylation status in ATC, which are practically devoid of CBX7 expression, moreover, in ATC we also found a high percentage of LOH: this suggest that gene methylation, associated in most cases with LOH, might

account for the block of CBX7 expression in ATC, whereas the decreased expression in PTC may be due to an allelic loss plus other epigenetic mechanism.

4.14 CBX7 expression in rat thyroid cells transformed by viral oncogenes

The infection of two rat thyroid differentiated cell lines, PC Cl 3 (Fusco et al. 1987) and FRTL-5 (Ambesi-Impiombato et al. 1980), with several murine retroviruses induces different effects on the differentiated and transformed phenotype (Berlingieri et al. 1988; Berlingieri et al. 1993; Santoro et al. 1993). PC MPSV and PC PyMLV cells are dedifferentiated and tumorigenic, whereas PC v-raf, PC KiMSV and PC E1A cells are dedifferentiated, but not tumorigenic when injected into nude mice. PC E1A cells are transformed to an irrefutable neoplastic phenotype after introducing a second oncogene such as the polyoma middle-T antigen or v-raf genes (Berlingieri et al. 1993). Conversely, FRTL-5 cells become tumorigenic after infection with the Kirsten murina sarcoma virus carrying the v-ras-Ki oncogene (Fusco et al. 1985). We evaluated CBX7 expression in these cell lines (Figure 19).

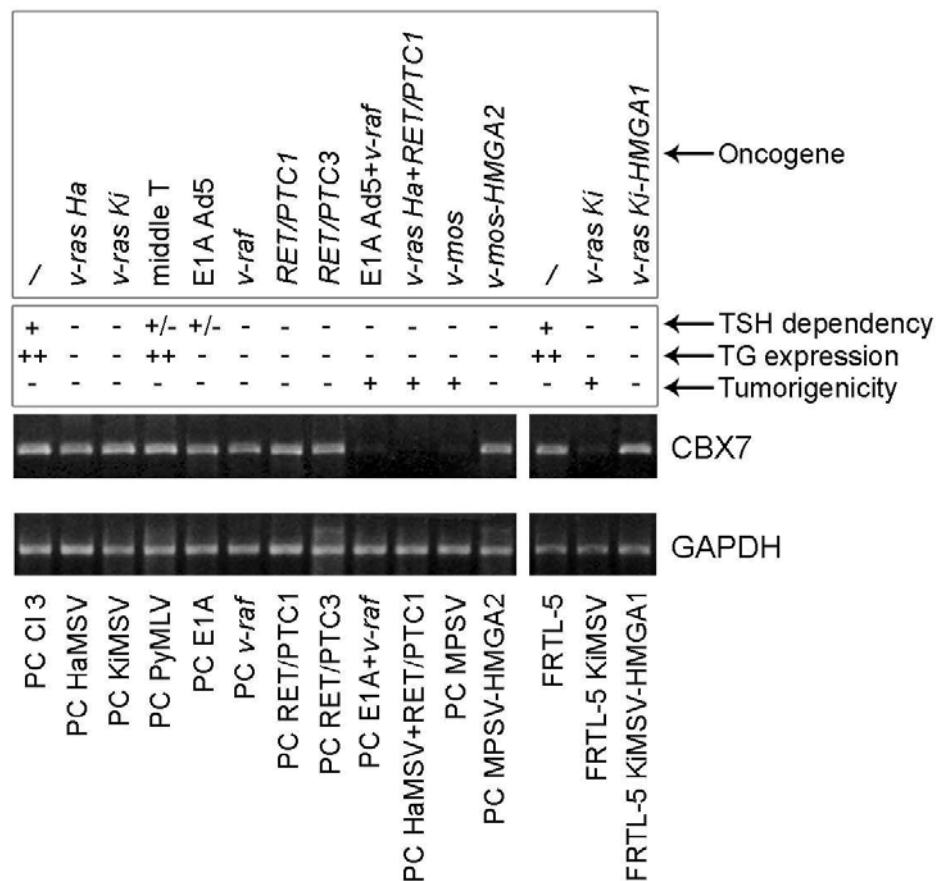


Figure 19 CBX7 expression in rat models of thyroid carcinogenesis. CBX7 expression by RT-PCR in rat thyroid cells transformed by several oncogenes. GAPDH gene expression was evaluated as control to normalize the amount of the used RNAs.

As shown in Figure 19, the gene was abundantly expressed in normal thyroid cells and in all cells that did not show the malignant phenotype, whereas its expression was abolished in the malignantly transformed cells FRTL-5 KiMSV and PC MPSV, and in PC E1A cells infected with a virus carrying the v-raf oncogene. Interestingly, CBX7 expression was retained in FRTL-5 KiMSV-HMGA1 and in PC MPSV-HMGA2, cells carrying respectively the HMGA1 and HMGA2 gene in an antisense orientation, able to prevent the malignant transformation of FRTL-5 and PC Cl 3 cells (Berlingieri et al. 2002; Berlingieri et al. 1995). In fact, although these cells undergo morphological changes and lose the thyroid differentiation markers, they are unable to grow in soft agar and to induce tumors after injection into athymic mice (Berlingieri et al. 2002; Berlingieri et al. 1995).

In conclusion, also the analysis of rat thyroid cells transformed in vitro confirms that the loss of CBX7 expression is associated with the expression of a highly malignant phenotype.

4.15 CBX7 expression in experimental mouse models of thyroid carcinogenesis

We used qRT-PCR analysis to evaluate CBX7 expression in thyroid neoplasias developing in the transgenic animal lines (described in the UbcH10 section) expressing TRK, RET/PTC3, large T SV40 and N-ras (Tg-N-ras) (Vitagliano et al. 2006) oncogenes under the transcriptional control of the thyroglobulin promoter. In this case we also used N-ras mice developing thyroid follicular neoplasms that undergo de-differentiation, predominantly FTC (Vitagliano et al. 2006). As shown in Figure 20, CBX7 expression was much lower in ATC from large T SV40 transgenic mice compared with mouse normal thyroid tissue. CBX7 mRNA expression was significantly, albeit not greatly, reduced in PTC from TRK and RET/PTC3 mice. CBX7 expression was also reduced in the FTC from N-ras mice.

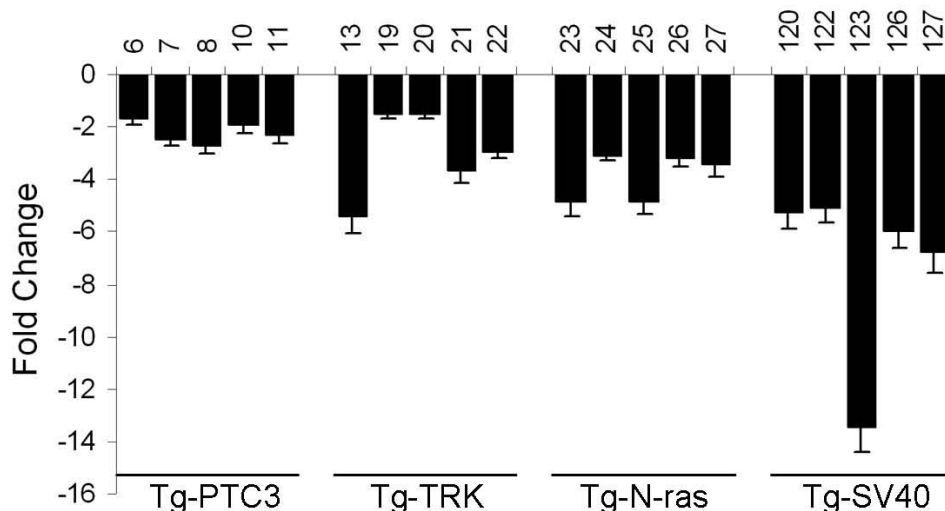


Figure 20 CBX7 expression in mouse models of thyroid carcinogenesis. CBX7 expression by qRT-PCR in thyroid carcinomas developing in transgenic mice expressing RET-PTC-3, TRK, N-ras and large T SV40 oncogenes. The fold change indicates the relative change in

expression levels between tumor samples and normal samples, assuming that the value of each normal sample is equal to 1.

In summary, the analysis of the experimental models of thyroid carcinogenesis confirms that the loss of CBX7 expression is related to the undifferentiated histotype.

Therefore, also considering the results obtained in rat and mouse models of thyroid carcinogenesis, our data indicate that loss of CBX7 expression is well related with a more aggressive phenotype of thyroid carcinomas and perhaps with a worst prognosis. This result is consistent with our preliminary finding of a correlation between low CBX7 expression and reduced survival in colon carcinoma (Pallante and Terracciano, manuscript in preparation). Moreover, the association between lack of CBX7 expression and a more aggressive histotype seems to apply also to breast, ovary and prostate carcinomas (Pallante and Troncone, manuscript in preparation).

4.16 Restoration of CBX7 gene expression inhibits the growth of thyroid carcinoma cell lines

To determine whether loss of CBX7 gene expression affects thyroid carcinogenesis, we evaluated the growth rate of thyroid carcinoma cell lines in which CBX7 expression had been restored. To this aim we carried out a colony forming assay with cell lines obtained from human thyroid carcinomas (NPA, TPC-1 and FB-2) after transfection with the vector carrying the CBX7 gene or the empty backbone vector (Figure 21)

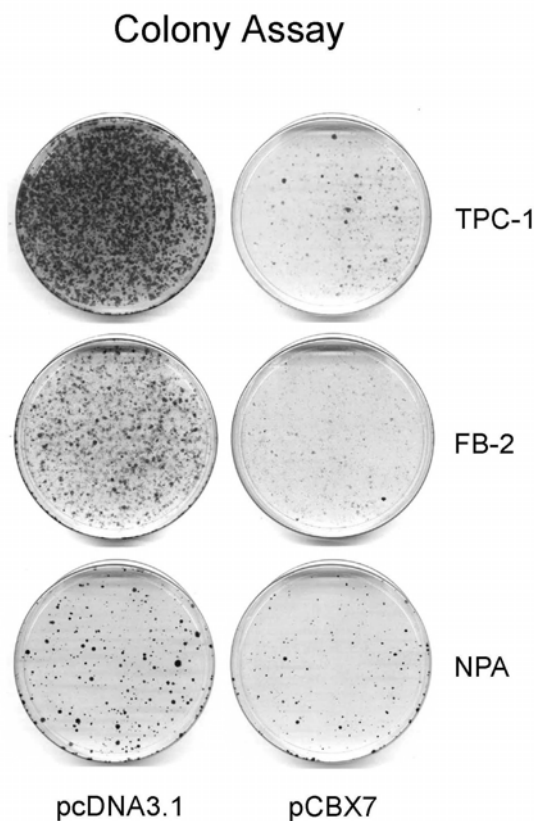


Figure 21 Colony-forming assay with CBX7 transfection in several thyroid carcinoma cell lines.

NPA, FB-2 and TPC-1 cells were transfected with a vector expressing CBX7 cDNA and its corresponding empty vector pcDNA3.1. Cells were selected for resistance to G418 and clones were stained and counted after 14 days.

The colonies were scored after two weeks. As shown in Figure 21, cells transfected with the CBX7 gene generated a lower number of colonies than did cells transfected with the backbone vector: for the NPA cells the inhibition was about 48% (representative experiment: empty vector, 296 colonies; CBX7, 154 colonies) while for FB-2 and TPC-1 cells the inhibition was even much higher.

4.17 Generation of an adenovirus carrying the CBX7 gene

We generated a replication-defective adenovirus carrying the CBX7 gene in the sense (Ad-CBX7) orientation. We then infected thyroid carcinoma cell lines with the Ad-CBX7 virus, and measured protein levels in cell lysates collected at different time points after adenovirus infection. No CBX7 protein was detected in carcinoma cells infected with the control virus (Ad-GFP). We then constructed growth curves of cells infected with Ad-CBX7 and control adenovirus (Ad-GFP). As shown in Figure 22, cell growth rate was significantly lower in ARO and NPA cell lines infected with Ad-CBX7 than in the same cells infected with the control virus.

The percentage of growth inhibition five days after infection was 38.5% in ARO cells and 54% in NPA cells. CBX7 expression clearly reduced cell growth rate, which indicates that the gene plays a critical role in thyroid carcinogenesis. One may speculate that restoration of CBX7 function by adenovirus-mediated delivery could be applied in the most highly aggressive thyroid tumors.

4.18 CBX7 deregulation in other cancers

Since CBX7 expression levels were drastically down-regulated in thyroid carcinomas, the loss of this protein may be related also to the malignant phenotype in other cancers. To evaluate whether loss of CBX7 was a common event in human malignancies, we screened its expression in normal and neoplastic tissues (Pallante and Troncone, Manuscript in preparation). Therefore a multi-tumour tissue microarray (TMA), constructed using 968 samples taken from 484 tumours of 56 (10 benign and 46 malignant) different types and a normal-tissue microarray, constructed using 310 samples from 42 different tissues, were stained for CBX7. The obtained results were further confirmed in selected tumour types (ovary, breast and colon carcinoma). CBX7 expression was always observed in all the different samples of the normal tissue microarray. Benign tumours also maintained CBX7 expression. 89% (41/46) of the malignant tumour types examined showed a variable degree of CBX7 loss of expression. The tumours showing the higher rate of CBX7 loss of expression (>75% of negative neoplastic cells) were Hodgkin lymphoma, germ cell of the testis and lung carcinoma.

Next we evaluated more approfonditely CBX7 expression in colon carcinoma (CRC) (Pallante and Terracciano, Manuscript in preparation). By using immunohistochemistry, we found that CBX7 could really be considered a critical prognostic marker for the survival of the CRC patients. In fact several associations were found among loss of CBX7 expression and clinico-pathological features. In particular, there was an association between the loss of CBX7 expression and an advanced pT. Additionally, even more significant is the relationship observed between CBX7 expression-staining and the survival in the whole series and in pT3N0 groups.

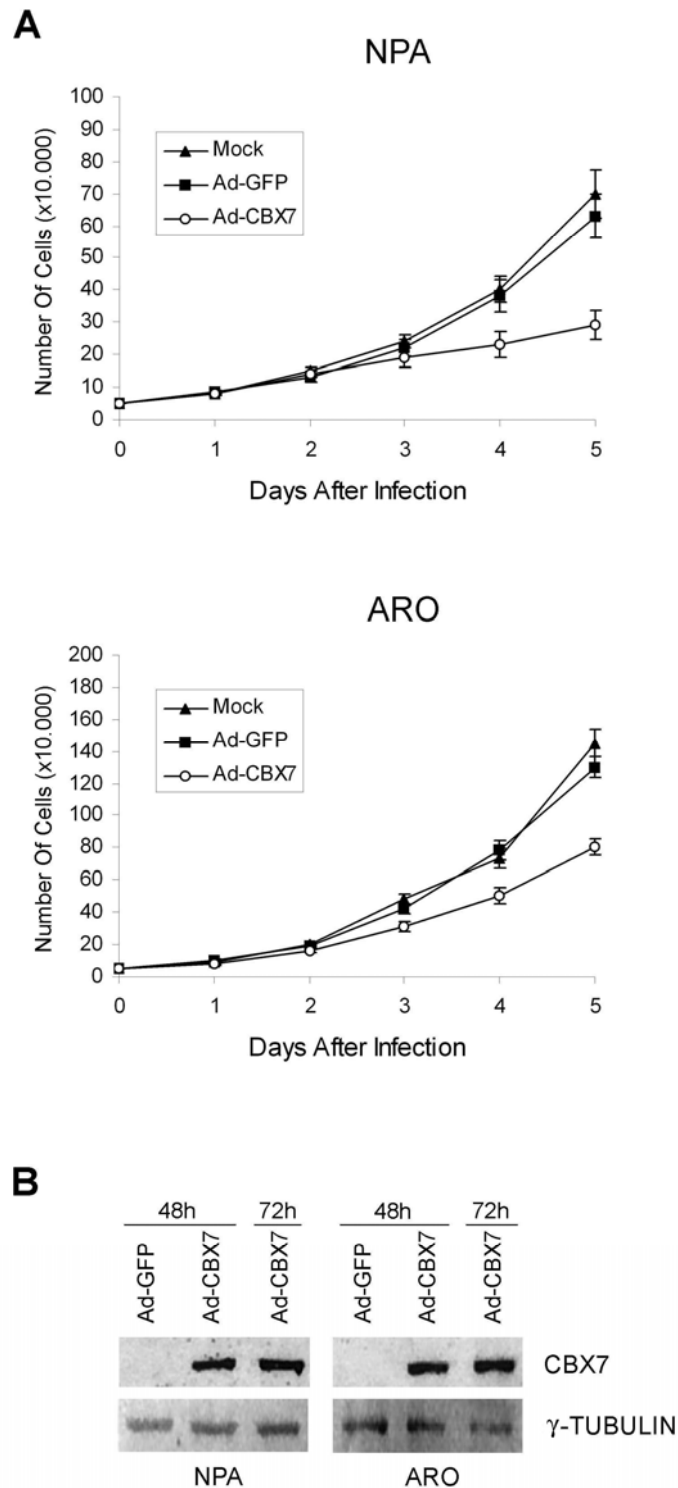


Figure 22 Inhibitory effects of Ad-CBX7 infection on the growth of human thyroid carcinoma cell lines. (A) The cell lines indicated were infected with Ad-CBX7 or Ad-GFP (control adenovirus) at MOI 100 and counted daily. Representative curves of three independent experiments are reported. (B) CBX7 protein expression was assessed 48 h after infection with Ad-CBX7 at MOI 100 by Western blot with an anti CBX7 antibody. Blot against γ -Tubulin is to demonstrate an equal protein loading.

In general the prognosis is poorer when the protein is less expressed therefore it is conceivable that CBX7 might have a role in determining patient survival.

To validate a negative role of CBX7 in cell growth proliferation, colony assay experiments were performed: they showed that CBX7 was able to inhibit the growth of two colon carcinoma cell lines (Pallante and Terracciano, Manuscript in preparation).

In summary, our study in CRC has shown that loss of CBX7 expression is associated with a poorer prognosis in CRC patients and that this gene might be promising in establishing a personalized prognosis and therapeutic approach for patients, in particular in association with other CRC phenotype markers.

5. CONCLUSIONS

Thyroid tumors are the result of the accumulation of different modifications in critical genes involved in the control of cell proliferation. Although various therapeutic approaches are followed in clinical practice, most of them are not life-saving. Hence, the discovery of ways to diagnose cancer at an early stage and to establish more effective therapies is a critical and urgent issue. To achieve this goal, identification and characterization of key molecules that participate in carcinogenesis are essential steps.

In this study we show that by the use of cDNA microarray it is possible to identify genes potentially involved in human cancers. In fact we identified at least two genes, UbcH10 and CBX7, that could be actively involved in the process of thyroid carcinogenesis.

For UbcH10, no significant expression was observed in normal thyroids, goiters and adenomas, whereas a great expression induction was observed in human anaplastic thyroid carcinomas and in mouse experimental undifferentiated thyroid tumors. Just a weak expression of UbcH10 was observed in human follicular and papillary thyroid carcinomas indicating that UbcH10 overexpression could be associated with the thyroid tumor progression since there is a good correlation with the late stage of thyroid neoplastic transformation. Our data propose the UbcH10 overexpression as a feature of the anaplastic carcinoma histotype.

Therefore, even though the mechanisms by which UbcH10 overproduction contributes to the neoplastic phenotype remains unclear, we can assume that it leads to a deregulation of cell growth. The block of UbcH10 expression significantly reduced the growth of thyroid carcinoma cell lines indicating an involvement of UbcH10 in the increased proliferation of these carcinoma cell lines.

In conclusion, these results open the perspective of a therapy of the anaplastic thyroid carcinoma, one of the most aggressive tumors in mankind, based on the suppression of the UbcH10 synthesis and/or function.

CBX7, instead, is abundantly expressed in normal thyroid gland, but its expression decreased with malignancy grade and neoplasia stage. In fact, CBX7 expression was comparable to normal thyroid tissue in benign follicular adenomas, slightly reduced in papillary thyroid carcinomas displaying the classical histotype, and drastically reduced, and in most cases absent, in follicular thyroid carcinomas, in the tall cell variant of papillary thyroid carcinomas, in poorly differentiated and in anaplastic thyroid carcinomas. Based on these findings, it is feasible that CBX7 levels could serve to differentiate between benign and malignant thyroid neoplasms. In the perspective of diagnosis/prognosis, CBX7 expression level in FNAB may be used to identify PTC by immunocytochemistry qRT-PCR.

Our finding of a decrease in CBX7 levels in relation to malignancy was supported by our model of rat thyroid cells transformed by several oncogenes and in transgenic mice carrying thyroglobulin promoter-driven oncogenes. Therefore,

our data indicate that the loss of CBX7 expression is related with a more aggressive phenotype of thyroid carcinomas and perhaps with a worst prognosis.

In an attempt to unravel the mechanism underlying the loss of CBX7 gene expression in malignant thyroid neoplasias, we analysed LOH at the CBX7 locus (22q13.1) and methylation status of its promoter: we suggest that gene methylation, associated in most cases with LOH, might account for the block of CBX7 expression at least in anaplastic carcinoma, whereas in papillary one the reduced CBX7 expression may be due to an allelic loss plus other epigenetic mechanism.

To determine whether CBX7 plays an important role in thyroid carcinogenesis, we restored its function in human thyroid cancer cell lines and examined cell growth rate: CBX7 expression clearly reduced cell growth rate, which indicates that the gene plays a critical role in thyroid carcinogenesis. One may speculate that restoration of CBX7 function by adenovirus-mediated delivery could be applied in the most highly aggressive thyroid tumors.

In conclusion, for CBX7 our data suggest that its low expression is associated with a malignant phenotype of thyroid neoplasias, and that its loss could play a critical role in thyroid cancer progression.

6. ACKNOWLEDGEMENTS

I would like to acknowledge Prof. Giancarlo Vecchio who directed this Doctorate Program.

A special thank goes to Prof. Giancarlo Troncone and his group at the Dipartimento di Scienze Biomorfologiche e Funzionali – University of Naples Federico II.

I wish to thank Prof. Luigi Terracciano and his group at the Institute of Pathology – University of Basel. Switzerland.

I am particularly indebted to Prof Carlo Croce for his kind hospitality during my two visits at Kimmel Cancer Center – Thomas Jefferson University, Philadelphia, Pennsylvania, and at the Comprehensive Cancer Center – Ohio State University, Columbus, Ohio, USA. I profited a lot from discussion with the members of his group.

I wish also to thank all the friends and colleagues at the Dipartimento di Biologia e Patologia Cellulare e Molecolare which made these years a great experience.

I would like to thank all the members of my laboratory for the support, the friendship and the enlightening scientific discussions. I am very grateful to Dr. Maria Teresa Berlingieri. I really appreciated her constant support and her precious advices.

I wish to thank Prof. Alfredo Fusco, who supervised my work. His extraordinary knowledge of oncology, his great enthusiasm and his kindness are really uniques. It has been a pleasure for me to work in his laboratory at DBPCM.

7. REFERENCES

Agrawal D, Chen T, Irby R, Quackenbush J, Chambers AF, Szabo M, Cantor A, Coppola D, Yeatman TJ. Osteopontin identified as lead marker of colon cancer progression, using pooled sample expression profiling. *J Natl Cancer Inst* 2002;94:513-21.

Alizadeh AA, Eisen MB, Davis RE, Ma C, Lossos IS, Rosenwald A, Boldrick JC, Sabet H, Tran T, Yu X, Powell JJ, Yang L, Marti GE, Moore T, Hudson J Jr, Lu L, Lewis DB, Tibshirani R, Sherlock G, Chan WC, Greiner TC, Weisenburger DD, Armitage JO, Warnke R, Levy R, Wilson W, Grever MR, Byrd JC, Botstein D, Brown PO, Staudt LM. Distinct types of diffuse large B-cell lymphoma identified by gene expression profiling. *Nature* 2000;403:503-11.

Allione F, Eisinger F, Parc P, Noguchi T, Sobol H, Birnbaum D. Loss of heterozygosity at loci from chromosome arm 22Q in human sporadic breast carcinomas. *Int J Cancer* 1998;75:181-6.

Alon U, Barkai N, Notterman DA, Gish K, Ybarra S, Mack D, Levine AJ. Broad patterns of gene expression revealed by clustering analysis of tumor and normal colon tissues probed by oligonucleotide arrays. *Proc Natl Acad Sci U S A* 1999;96:6745-50.

Ambesi-Impiombato FS, Parks LA, Coon HG. Culture of hormone dependent functional epithelial cells from rat thyroids. *Proc Natl Acad Sci U S A* 1980;77:3455-9.

Arvand A, Bastians H, Welford SM, Thompson AD, Ruderman JV, Denny CT. EWS/FLI1 up regulates mE2-C, a cyclin-selective ubiquitin conjugating enzyme involved in cyclin B destruction. *Oncogene* 1998;17:2039-45.

Basolo F, Giannini R, Toniolo A, Casalone R, Nikiforova M, Pacini F, Elisei R, Miccoli P, Berti P, Faviana P, Fiore L, Monaco C, Pierantoni GM, Fedele M, Nikiforov YE, Santoro M, Fusco A. Establishment of a non-tumorigenic papillary thyroid cell line (FB-2) carrying the RET/PTC1 rearrangement. *Int J Cancer* 2002;97:608-14.

Bea S, Tort F, Pinyol M, Puig X, Hernandez L, Hernandez S, Fernandez PL, Van Lohuizen M, Colomer D, Campo E. *Cancer Res* 2001;61:2409-12.

Beer DG, Kardia SL, Huang CC, Giordano TJ, Levin AM, Misek DE, Lin L, Chen G, Gharib TG, Thomas DG, Lizyness ML, Kuick R, Hayasaka S, Taylor JM, Iannettoni MD, Orringer MB, Hanash S. Gene-expression profiles predict survival of patients with lung adenocarcinoma. *Nat Med* 2002;8:816-24.

Berlingieri MT, Portella G, Greco M, Santoro M, Fusco A. Cooperation between the polyomavirus middle-T-antigen gene and the human c-myc oncogene in a rat thyroid epithelial differentiated cell line: model of in vitro progression. *Mol Cell Biol* 1988;8:2261-6.

Berlingieri MT, Santoro M, Battaglia C, Greco M, and Fusco A. The Adenovirus E1A gene blocks the differentiation of a thyroid epithelial cell line, however the neoplastic phenotype is achieved only after cooperation with other oncogenes. *Oncogene* 1993;8:249-55.

Berlingieri MT, Manfioletti G, Santoro M, Bandiera A, Visconti R, Giancotti V, Fusco A. Inhibition of HMGI-C protein synthesis suppresses retrovirally induced neoplastic transformation of rat thyroid cells. *Mol Cell Biol* 1995;15:1545-53.

Berlingieri MT, Pierantoni GM, Giancotti V, Santoro M, and Fusco A. Thyroid cell transformation requires the expression of the HMGA1 proteins. *Oncogene* 2002;21:2971-80.

Berlingieri MT, Pallante P, Guida M, Nappi C, Masciullo V, Scambia G, Ferraro A, Leone V, Sboner A, Barbareschi M, Ferro A, Troncone G, Fusco A. UbcH10 expression may be a useful tool in the prognosis of ovarian carcinomas. *Oncogene*. 2006 Oct 2; [Epub ahead of print].

Bernard D, Martinez-Leal JF, Rizzo S, Martinez D, Hudson D, Visakorpi T, Peters G, Carnero A, Beach D, Gil J. CBX7 controls the growth of normal and tumor-derived prostate cells by repressing the Ink4a/Arf locus. *Oncogene* 2005;24:5543-51.

Bernstein E, Duncan EM, Masui O, Gil J, Heard E, Allis CD. Mouse Polycomb Proteins Bind Differentially to Methylated Histone H3 and RNA and Are Enriched in Facultative Heterochromatin. *Mol Cell Biol* 2006;26:2560-9.

Bloom G, Yang IV, Boulware D, Kwong KY, Coppola D, Eschrich S, Quackenbush J, Yeatman TJ. Multi-platform, multi-site, microarraybased human tumor classification. *Am J Pathol* 2004;164:9-16.

Bochtler M, Ditzel M, Groll M, Hartmann C, Huber R. The proteasome. *Annu Rev Biophys Biomol Struct* 1999;28:295-317.

Bullinger L, Dohner K, Bair E, Frohling S, Schlenk RF, Tibshirani R, Dohner H, Pollack JR. Use of gene-expression profiling to identify prognostic subclasses in adult acute myeloid leukemia. *N Engl J Med* 2004;350:1605-16.

Burton JL, Tsakraklides V, Solomon MJ. Assembly of an APC-Cdh1-substrate complex is stimulated by engagement of a destruction box. *Mol Cell* 2005;18:533-42.

Cao R, Wang L, Wang H, Xia L, Erdjument-Bromage H, Tempst P, Jones RS, Zhang Y. Role of histone H3 lysine 27 methylation in Polycomb-group silencing. *Science* 2002;298:1039–43.

Carcangiu ML, Zampi G, Rosai J. Poorly differentiated ('insular') thyroid carcinoma. A reinterpretation of Langhans' 'wuchernde Struma'. *Am J Surg Pathol* 1984;8:655–68.

Cerutti J, Trapasso F, Battaglia C, Zhang L, Martelli ML, Visconti R, Berlingieri MT, Fagin JA, Santoro M, Fusco A. Block of c-myc expression by antisense oligonucleotides inhibits proliferation of human thyroid carcinoma cell lines. *Clin Cancer Res* 1996;2:119-26.

Chin KV, Seifer DB, Feng B, Lin Y, Shih WC. DNA microarray analysis of the expression profiles of luteinized granulosa cells as a function of ovarian reserve. *Fertil Steril* 2002;77:1214-8.

Curcio F, Ambesi-Impimbato FS, Perrella G, Coon HG. Long-term culture and functional characterization of follicular cells from adult normal human thyroids. *Proc Natl Acad Sci U S A* 1994;91:9004-8.

Dave SS, Wright G, Tan B, Rosenwald A, Gascoyne RD, Chan WC, Fisher RI, Braziel RM, Rimsza LM, Grogan TM, Miller TP, LeBlanc M, Greiner TC, Weisenburger DD, Lynch JC, Vose J, Armitage JO, Smeland EB, Kvaloy S, Holte H, Delabie J, Connors JM, Lansdorp PM, Ouyang Q, Lister TA, Davies AJ, Norton AJ, Muller-Hermelink HK, Ott G, Campo E, Montserrat E, Wilson WH, Jaffe ES, Simon R, Yang L, Powell J, Zhao H, Goldschmidt N, Chiorazzi M, Staudt LM. Prediction of survival in follicular lymphoma based on molecular features of tumor-infiltrating immune cells. *N Engl J Med* 2004;351:2159–69.

De Felice M, Di Lauro R. Thyroid Development and Its Disorders: Genetics and Molecular Mechanisms. *Endocrine Reviews* 2004;25:722–46.

DeRisi J, Penland L, Brown PO, Bittner ML, Meltzer PS, Ray M, Chen Y, Su YA, Trent JM. Use of a cDNA microarray to analyse gene expression patterns in human cancer. *Nat Genet* 1996;14:457-60.

Deshaies RJ. SCF and Cullin/RING H2-based ubiquitin ligases. *Annu Rev Cell Dev Biol* 1999;15:435–67.

Di Renzo MF, Olivero M, Ferro S, Prat M, Bongarzone I, Pilotti S, Belfiore A, Costantino A, Vigneti R, Pierotti MA. Overexpression of the c-MET/HGF receptor gene in human thyroid carcinomas. *Oncogene* 1992;7:2549-53.

Dobashi Y, Sakamoto A, Sugimura H, Mernyei M, Mori M, Oyama T, Machinami R. Overexpression of p53 as a possible prognostic factor in human thyroid carcinoma. *Am J Surg Pathol* 1993;17:375-81.

Donghi R, Longoni A, Pilotti S, Michieli P, Della Porta G, and Pierotti MA. Gene p53 mutations are restricted to poorly differentiated and undifferentiated carcinomas of the thyroid gland. *J Clin Invest* 1993;91:1753-60.

Dyrskjot L, Thykjaer T, Kruhoffer M, Jensen JL, Marcussen N, Hamilton-Dutoit S, Wolf H, Orntoft TF. Identifying distinct classes of bladder carcinoma using microarrays. *Nature Genetics* 2003;33:90-6.

Egger G, Liang G, Aparicio A, Jones PA. Epigenetics in human disease and prospects for epigenetic therapy. *Nature* 2004;429:457-63.

El-Rifai W, Frierson HF Jr, Moskaluk CA, Harper JC, Petroni GR, Bissonette EA, Jones DR, Knuutila S, Powell SM. Genetic differences between adenocarcinomas arising in Barrett's esophagus and gastric mucosa. *Gastroenterology* 2001;121:592-8.

Erle DJ, Yang YH. Asthma investigators begin to reap the fruits of genomics. *Genome Biol* 2003;4:232.

Eschrich S, Yang I, Bloom G, Kwong KY, Boulware D, Cantor A, Coppola D, Kruhoffer M, Aaltonen L, Orntoft TF, Quackenbush J, Yeatman TJ. Molecular staging for survival prediction of colorectal cancer patients. *J Clin Oncol* 2005;23:3526-35.

Evans SJ, Choudary PV, Vawter MP, Li J, Meador-Woodruff JH, Lopez JF, Burke SM, Thompson RC, Myers RM, Jones EG, Bunney WE, Watson SJ, Akil H. DNA microarray analysis of functionally discrete human brain regions reveals divergent transcriptional profiles. *Neurobiol Dis* 2003;14:240-50.

Fabien N, Fusco A, Santoro M, Barbier Y, Dubois PM, Paulin C. Description of a human papillary thyroid carcinoma cell line. Morphologic study and expression of tumoral markers. *Cancer* 1994;73:2206-12.

Fagin JA, Matsuo K, Karmakar A, Chen DL, Tang SH, Koeffler HP. High prevalence of mutations of p53 gene in poorly differentiated human thyroid carcinomas. *J Clin Invest* 1993;91:179-84.

Fiore L, Pollina LE, Fontanini G, Casalone R, Berlingieri MT, Giannini R, Pacini F, Miccoli P, Toniolo A, Fusco A, Basolo F. Cytokine production by a new undifferentiated human thyroid carcinoma cell line, FB-1. *J Clin Endocrinol Metab* 1997;82:4094-100.

Fontaine J. Multistep migration of calcitonine cell precursors during ontogeny of the mouse pharynx. *Gen Comp Endocrinol* 1979;37:81-92.

Fusco A, Portella G, Di Fiore PP, Berlingieri MT, Di Lauro R, Schneider AB, Vecchio G. A mos oncogene-containing retrovirus, myeloproliferative sarcoma virus, transforms rat thyroid epithelial cells and irreversibly blocks their differentiation pattern. *J Virol* 1985;56:284-92.

Fusco A, Berlingieri MT, Di Fiore PP, Portella G, Grieco M, Vecchio G. One- and two-step transformation of rat thyroid epithelial cells by retroviral oncogenes. *Mol Cell Biol* 1987;7:3365-70.

Gil J, Bernard D, Martínez D, Beach D. Polycomb CBX7 has a unifying role in cellular lifespan. *Nat Cell Biol* 2004;6:67-72.

Glickman MH. Getting in and out of the proteasome. *Semin Cell Dev Biol* 2000;11:149–58.

Glickman MH, Ciechanover A. The ubiquitin-proteasome proteolytic pathway: destruction for the sake of construction. *Physiol Rev* 2002;82:373–428.

Glotzer M, Murray AW, Kirschner MW. Cyclin is degraded by the ubiquitin pathway. *Nature* 1991;349:132–38.

Golub TR, Slonim DK, Tamayo P, Huard C, Gaasenbeek M, Mesirov JP, Coller H, Loh ML, Downing JR, Caligiuri MA, Bloomfield CD, Lander ES. Molecular classification of cancer: class discovery and class prediction by gene expression monitoring. *Science* 1999;286:531-7.

Gorbman A. Comparative anatomy and physiology. In: Ingbar SI, Braverman LE, eds. *The thyroid*. Philadelphia: JB Lippincott Company;1986:p. 43–52.

Harper JW, Burton JL, Solomon MJ. The anaphase-promoting complex: it's not just for mitosis any more. *Genes Dev* 2002;16:2179–206.

Hedinger C, Williams D, Sobin LH. The WHO Histological classification of thyroid tumours: a commentary on the second edition. *Cancer* 1989;63:908–11.

Hershko A, Ciechanover A. The ubiquitin system. *Annu Rev Biochem* 1998;67:425–79.

Heymans S, Schroen B, Vermeersch P, Milting H, Gao F, Kassner A, Gillijns H, Herijgers P, Flameng W, Carmeliet P, Van de Werf F, Pinto YM, Janssens S. Increased cardiac expression of tissue inhibitor of metalloproteinase-1 and tissue inhibitor of metalloproteinase-2 is related to cardiac fibrosis and dysfunction in the chronic pressure-overloaded human heart. *Circulation* 2005;112:1136–44.

Hilt W, Wolfe DH (Editors). *Proteasomes: The World of Regulatory Proteolysis*. Georgetown, TX: Landes Bioscience, 2000.

Hsu JY, Reimann JD, Sorensen CS, Lukas J, Jackson PK. E2F-dependent accumulation of hEml1 regulates S phase entry by inhibiting APC(Cdh1). *Nat Cell Biol* 2002;4:358–66.

Iida A, Kurose K, Isobe R, Akiyama F, Sakamoto G, Yoshimoto M, Kasumi F, Nakamura Y, Emi M. Mapping of a new target region of allelic loss to a 2-cM interval at 22q13.1 in primary breast cancer. *Genes Chromosomes Cancer* 1998;21:108–12.

Ito T, Seyama T, Mizuno T, Tsuyama N, Hayashi T, Hayashi Y, Dohi K, Nakamura N, Akiyama M. Unique association of p53 mutations with undifferentiated but not differentiated carcinomas of the thyroid gland. *Cancer Res* 1992;52:1369–71.

Jackson PK, Eldridge AG, Freed E, Frustenthal L, Hsu JY, Kaiser BK Reinmann JDR. The lore of the RINGs: substrate recognition and catalysis by ubiquitin ligases. *Trends Cell Biol* 2000;10:429–39.

Joazeiro CA, Weissman AM. RING finger proteins: mediators of ubiquitin ligase activity. *Cell* 2000;102:549–52.

Jones DO, Cowell IG, Singh PB. Mammalian chromodomain proteins: their role in genome organisation and expression. *Bioessays* 2000;22:124–37.

Kanno M, Hasegawa M, Ishida A, Isono K, Taniguchi M. mel-18, a Polycomb group-related mammalian gene, encodes a transcriptional negative regulator with tumor suppressive activity. *EMBO J* 1995;14:5672–8.

Kebebew E, Greenspan FS, Clark OH, Woeber KA, McMillan A. Anaplastic thyroid carcinoma. Treatment outcome and prognostic factors. *Cancer* 2005;103:1330–5.

Khan J, Simon R, Bittner M, Chen Y, Leighton SB, Pohida T, Smith PD, Jiang Y, Gooden GC, Trent JM, Meltzer PS. Gene expression profiling of alveolar rhabdomyosarcoma with cDNA microarrays. *Cancer Res* 1998;58:5009–13.

Kihara C, Tsunoda T, Tanaka T, Yamana H, Furukawa Y, Ono K, Kitahara O, Zembutsu H, Yanagawa R, Hirata K, Takagi T, Nakamura Y. Prediction of sensitivity of esophageal tumors to adjuvant chemotherapy by cDNA microarray analysis of gene-expression profiles. *Cancer Res* 2001;61:6474–9.

Kirmizis A, Bartley SM, Farnham PJ. Identification of the polycomb group protein SU(Z)12 as a potential molecular target for human cancer therapy. *Mol Cancer Ther* 2003;2:113–21.

Kirmizis A, Bartley SM, Kuzmichev A, Margueron R, Reinberg D, Green R, Farnham PJ. *Genes Dev* 2004;18:1592–605.

Kleer CG, Cao Q, Varambally S, Shen R, Ota I, Tomlins SA, Ghosh D, Sewalt RGAB, Otte AP, Hayes DF, Sabel MS, Livant D, Weiss SJ, Rubin MA, Chinnaiyan AM. EZH2 is a marker of aggressive breast cancer and promotes neoplastic transformation of breast epithelial cells. *Proc Natl Acad Sci U S A* 2003;100:11606–11.

Kondo T, Ezzat S, Asa SL. Pathogenetic mechanisms in thyroid follicular-cell neoplasia. *Nat Rev Cancer* 2006;6:292–306.

Kraft C, Herzog F, Gieffers C, Mechtler K, Hagting A, Pines J, Peters JM. Mitotic regulation of the human anaphase-promoting complex by phosphorylation. *EMBO J* 2003;22:6598–609.

Kroll TG, Sarraf P, Pecciarini L, Chen CJ, Mueller E, Spiegelman BM, and Fletcher JA. PAX-8-PPAR γ fusion oncogene in human thyroid carcinoma. *Science* 2000;289:1357–60.

Koshkin AA, Singh SK, Nielsen P, Rajwanshi VK, Kumar R, Meldgaard M, Olsen CE, Wengel J. LNA (Locked nucleic acids): synthesis of the adenine, cytosine, guanine, 5-methylcytosine, thymine and uracil biocyclonucleoside monomers, oligomerisation and unprecedented nucleic acid recognition. *Tetrahedron* 1998;54:3607–30.

Kuzmichev A, Nishioka K, Erdjument-Bromage H, Tempst P, Reinberg D. *Genes Dev* 2002;16:2893–905.

Lapointe J, Li C, Higgins JP, van de Rijn M, Bair E, Montgomery K, Ferrari M, Egevad L, Rayford W, Bergerheim U, Ekman P, DeMarzo AM, Tibshirani R, Botstein D, Brown PO, Brooks JD, Pollack JR. Gene expression profiling identifies clinically relevant subtypes of prostate cancer. *Proc Natl Acad Sci U S A* 2004;101:811–6.

La Tulippe E, Satagopan J, Smith A, Scher H, Scardino P, Reuter V, Gerald WL. Comprehensive gene expression analysis of prostate cancer reveals distinct transcriptional programs associated with metastatic disease. *Cancer Res* 2002;62:4499–506.

Ledent C, Dumont J, Vassart G, Parmentier M. Thyroid adenocarcinomas secondary to tissue-specific expression of simian virus-40 large T-antigen in transgenic mice. *Endocrinology* 1991;129:1391–401.

Le Douarin N, Fontaine J, LeLievre C. New studies on the neural crest origin of the avian ultimobranchial glandular cells. Interspecific combinations and cytochemical characterization of Ccells based on the uptake of biogenic amine precursors. *Histochemie* 1974;38:297–305.

- Lee JS, Chu IS, Heo J, Calvisi DF, Sun Z, Roskams T, Durnez A, Demetris AJ, Thorgeirsson SS. Classification and prediction of survival in hepatocellular carcinoma by gene expression profiling. *Hepatology* 2004;40:667–76.
- Lee JS, Thorgeirsson SS. Comparative and integrative functional genomics of HCC. *Oncogene* 2006;25:3801–9.
- Lessard J, Sauvageau G. Bmi-1 determines the proliferative capacity of normal and leukaemic stem cells. *Nature* 2003;423:255–60.
- Li T, Chen YH, Liu TJ, Jia J, Hampson S, Shan YX, Kibler D, Wang PH. Using DNA microarray to identify Sp1 as a transcriptional regulatory element of insulinlike growth factor 1 in cardiac muscle cells. *Circ Res* 2003;93:1202–9.
- Lin HY, Harris TL, Flannery MS, Aruffo A, Kaji EH, Gorn A, Kolakowski LF Jr, Lodish HF, Goldring SR. Expression cloning of an adenylate cyclase-coupled calcitonin receptor. *Science* 1991;254:1022–4.
- Lipshutz RJ, Morris D, Chee M, Hubbell E, Kozal MJ, Shah N, Shen N, Yang R, Fodor SP. Using oligonucleotide probe arrays to access genetic diversity. *Biotechniques* 1995;19:442–7.
- LiVolsi VA, Asa SL. The demise of follicular carcinoma of the thyroid gland. *Thyroid* 1994;4:233–6.
- Lossos IS, Czerwinski DK, Alizadeh AA, Wechser MA, Tibshirani R, Botstein D, Levy R. Prediction of survival in diffuse large-B-cell lymphoma based on the expression of six genes. *N Engl J Med* 2004;350:1828–37.
- Lukas C, Sorensen CS, Kramer E, Santoni-Rugiu E, Lindeneg C, Peters JM, Bertek J, and Lukas J. Accumulation of cyclin B1 requires E2F and cyclin A-dependent rearrangement of the anaphasepromoting complex. *Nature* 1999;401:815–8.
- Lund AH, van Lohuizen M. Polycomb complexes and silencing mechanisms. *Curr Opin Cell Biol* 2004;16:239–46.
- Macpherson I, Montagnier I. Agar suspension culture for the selective assay of cells transformed by polyoma virus. *Virology* 1964;23:291–4.
- Mauchamp J, Mirrione A, Alquier C, Andre` F. Follicle-like structure and polarized monolayer: role of the extracellular matrix on thyroid cell organization in primary culture. *Biol Cell* 1998;90:369–80.
- Mick R, Ziober BL. c-Met expression in tall cell variant papillary carcinoma of the thyroid. *Cancer* 2003;98:1386–93.

- Min J, Zhang Y, Xu R-M. Structural basis for specific binding of Polycomb chromodomain to histone H3 methylated at Lys 27. *Genes Dev* 2003;17:1823–8.
- Mouritzen P, Nielsen PS, Jacobsen N, Noerholm M, Lomholt C, Pfundheller HM, Ramsing NB, Kauppinen S, Tolstrup N. The ProbeLibrary™ - Expression profiling 99% of all human genes using only 90 dual-labeled real-time PCR Probes. *Biotechniques* 2004;37:492–5.
- Mouritzen P, Noerholm M, Nielsen PS, Jacobsen N, Lomholt C, Pfundheller HM, Tolstrup N. ProbeLibrary™ - Expression profiling 99% of all human genes using only 90 dual-labeled 2005. *ProbeLibrary: A new method for faster design and execution of quantitative real-time PCR. Nat Methods* 2005;2:313–7.
- Moch H, Schraml P, Bubendorf L, Mirlacher M, Kononen J, Gasser T, Mihatsch MJ, Kallioniemi OP, Sauter G. Identification of prognostic parameters for renal cell carcinoma by cDNA arrays and cell chips. *Verh Dtsch Ges Pathol* 1999;83:225–32.
- Nakao M, Minami T, Ueda Y, Sakamoto Y, Ichimura T. Epigenetic system: a pathway to malignancies and a therapeutic target. *Int J Hematol* 2004;80:103–107.
- Nardone HC, Ziober AF, LiVolsi VA, Mandel SJ, Baloch ZW, Weber RS, Mick R, Ziober BL. c-Met expression in tall cell variant papillary carcinoma of the thyroid. *Cancer* 2003;98:1386–93.
- Nicholson GC, Moseley JM, Sexton PM, Mendelsohn FA, Martin TJ. Abundant calcitonin receptors in isolated rat osteoclasts. Biochemical and autoradiographic characterization. *J Clin Invest* 1986;78:355–60.
- Obika S, Nanbu D, Hari Y, Morio K, In Y, Ishii JK, Imanishi T. Synthesis of 2'-O,4'-C methyleneuridine and cytidine. Novel bicyclic Nucleosides Having a Fixed C3-endo Sugar Puckering. *Tetrahedron Lett* 1997;38:8735–8.
- Ohki R, Yamamoto K, Ueno S, Mano H, Misawa Y, Fuse K, Ikeda U, Shimada K. Gene expression profiling of human atrial myocardium with atrial fibrillation by DNA microarray analysis. *Int J Cardiol* 2005;102:233–8.
- Okamoto Y, Ozaki T, Miyazaki K, Aoyama M, Miyazaki M, Nakagawara A. UbcH10 is the cancer-related E2 ubiquitin-conjugating enzyme. *Cancer Res* 2003;63:4167–73.
- Otte AP, Kwaks TH. Gene repression by Polycomb group protein complexes: a distinct complex for every occasion? *Curr Opin Genet Dev* 2003;13:448–54.
- Pallante P, Berlingieri MT, Troncone G, Kruhoffer M, Orntoft TF, Viglietto G, Caleo A, Migliaccio I, Decaussin-Petrucci M, Santoro M, Palombini L, Fusco A.

UbcH10 overexpression may represent a marker of anaplastic thyroid carcinomas. *Br J Cancer* 2005;93:464–71.

Paro R, Hogness DS. The Polycomb protein shares a homologous domain with a heterochromatin-associated protein of *Drosophila*. *Proc Natl Acad Sci U S A* 1991;88:263–7.

Perou CM, Jeffrey SS, van de Rijn M, Rees CA, Eisen MB, Ross DT, Pergamenschikov A, Williams CF, Zhu SX, Lee JC, Lashkari D, Shalon D, Brown PO, Botstein D. Distinctive gene expression patterns in human mammary epithelial cells and breast cancers. *Proc Natl Acad Sci U S A* 1999;96:9212–7.

Peters J-M, Harris JR, Finley D. *Ubiquitin and the Biology of the Cell*. New York: Plenum 1998, 472 p.

Peters JM. The anaphase-promoting complex: proteolysis in mitosis and beyond. *Mol Cell* 2002;9:931–43.

Pfleger CM, Kirschner MW. The KEN box: an APC recognition signal distinct from the D box targeted by Cdh1. *Genes Dev* 2000;14:655–65.

Pickart CM. Mechanisms underlying ubiquitination. *Annu Rev Biochem* 2001;70:503–33.

Pierce A, Small SA. Combining brain imaging with microarray: isolating molecules underlying the physiologic disorders of the brain. *Neurochem Res* 2004;29:1145–52.

Pierotti MA, Greco A. Oncogenic rearrangements of the NTRK1/NGF receptor. *Cancer Lett* 2006;232:90–8.

Powell DJ Jr, Russell J, Nibu K, Li G, Rhee E, Liao M, Goldstein M, Keane WM, Santoro M, Fusco A, Rothstein JL. The RET/PTC3 oncogene: metastatic solid-type papillary carcinomas in murine thyroids. *Cancer Res* 1998;58:5523–8.

Raaphorst FM, Van Kemenade FJ, Blokzijl T, Fieret E, Hamer KM, Satijn DP, Otte AP, Meijer CJ. *Am J Pathol* 2000;157:709–15.

Raaphorst FM, Vermeer M, Fieret E, Blokzijl T, Dukers D, Sewalt RG, Otte AP, Willemze R, Meijer CJ. Site-specific expression of Polycomb-group genes encoding the HPC-HPH/PRC1 complex in clinically defined primary nodal and cutaneous large B-cell lymphomas. *Am J Pathol* 2004;164:533–42.

Rape M, Kirschner MW. Autonomous regulation of the anaphase-promoting complex couples mitosis to S-phase entry. *Nature* 2004;432, 588–95.

Rape M, Reddy SK, Kirschner MW. The Processivity of Multiubiquitination by the APC Determines the Order of Substrate Degradation. *Cell* 2006;124:89–103.

Richter H, Braselmann H, Hieber L, Thomas G, Bogdanova T, Tronko N, Zitzelsberger H. Chromosomal imbalances in post-chernobyl thyroid tumors. *Thyroid* 2004;14:1061–4.

Rodriguez JM, Parrilla P, Moreno A, Sola J, Pinero A, Ortiz S, Soria T. Insular carcinoma: an infrequent subtype of thyroid cancer. *J Am Coll Surg* 1998;187:503–8.

Roepman P, Wessels LF, Kettelarij N, Kemmeren P, Miles AJ, Lijnzaad P, Tilanus MG, Koole R, Hordijk GJ, van der Vliet PC, Reinders MJ, Slootweg PJ, Holstege FC. An expression profile for diagnosis of lymph node metastases from primary head and neck squamous cell carcinomas. *Nat Genet* 2005;37:182–6.

Rolph MS, Sisavanh M, Liu SM, Mackay CR. Clues to asthma pathogenesis from microarray expression studies. *Pharmacol Ther* 2006;109:284–94.

Russell JP, Powell DJ, Cunnane M, Greco A, Portella G, Santoro M, Fusco A, Rothstein JL. The TRK-T1 fusion protein induces neoplastic transformation of thyroid epithelium. *Oncogene* 2000;19:5729–35.

Santoro M, Melillo RM, Greco M, Berlingieri MT, Vecchio G, Fusco A. The TRK and RET tyrosine kinase oncogenes cooperate with ras in the neoplastic transformation of a rat thyroid epithelial cell line. *Cell Growth Differ* 1993;4:77–84.

Satijn DP, Gunster MJ, van der Vlag J, Hamer KM, Schul W, Alkema MJ, Saurin AJ, Freemont PS, van Driel R, Otte AP. RING1 is associated with the polycomb group protein complex and acts as a transcriptional repressor. *Mol Cell Biol* 1997;17:4105–13.

Satijn DP, Otte AP. Polycomb group protein complexes: do different complexes regulate distinct target genes? *Biochim Biophys Acta* 1999;1447:1–16.

Saurin AJ, Shiels C, Williamson J, Satijn DP, Otte AP, Sheer D, Freemont PS. The human polycomb group complex associates with pericentromeric heterochromatin to form a novel nuclear domain. *J Cell Biol* 1998;142:887–98.

Schena M, Shalon D, Davis RW, Brown PO. Quantitative monitoring of gene expression patterns with a complementary DNA microarray. *Science* 1995;270:467–70.

Segev DL, Clark DP, Zeiger MA, Umbricht C. Beyond the suspicious thyroid fine needle aspirate. A review. *Acta Cytol* 2003;47:709–22.

Sorlie T, Perou CM, Tibshirani R, Aas T, Geisler S, Johnsen H, Hastie T, Eisen MB, van de Rijn M, Jeffrey SS, Thorsen T, Quist H, Matese JC, Brown PO, Botstein D, Eystein Lonning P, Borresen-Dale AL. Gene expression patterns of breast carcinomas distinguish tumor subclasses with clinical implications. *Proc Natl Acad Sci U S A* 2001;98:10869–74.

Suarez HG, Du Villard JA, Severino M, Caillou B, Schlumberger M, Tubiana M, Parmentier C, and Monier R. Presence of mutations in all three ras genes in human thyroid tumors. *Oncogene* 1990;5:565–70.

Suarez-Merino B, Hubank M, Revesz T, Harkness W, Hayward R, Thompson D, Darling JL, Thomas DG, Warr TJ. Microarray analysis of pediatric ependymoma identifies a cluster of 112 candidate genes including four transcripts at 22q12.1-q13.3. *Neuro-oncol* 2005;7:20–31.

Syed F, Panettieri RA Jr, Tliba O, Huang C, Li K, Bracht M, Amegadzie B, Griswold D, Li L, Amrani Y. The effect of IL-13 and IL-13R130Q, a naturally occurring IL-13 polymorphism, on the gene expression of human airway smooth muscle cells. *Respir Res* 2005;6:9.

Tokimasa S, Ohta H, Sawada A, Matsuda Y, Kim JY, Nishiguchi S, Hara J, Takihara Y. Lack of the Polycomb-group gene *rae28* causes maturation arrest at the early B-cell developmental stage. *Exp Hematol* 2001;29:93–103.

Townsley FM, Aristarkhov A, Beck S, Herskho A, Ruderman JV. Dominant-negative cyclin-selective ubiquitin carrier protein E2-C/UbcH10 blocks cells in metaphase. *Proc Natl Acad Sci U S A* 1997;94:2362–7.

Troncone G, Fulciniti F, Zeppa P, Vetrani A, Caleo A, Palombini L. Cyclin-dependent kinase inhibitor p27(Kip1) expression in thyroid cells obtained by fine needle aspiration biopsy: a preliminary report. *Diagn Cytopathol* 2000;23:77–81.

Troncone G, Iaccarino A, Caleo A, Bifano D, Pettinato G, Palombini L. p27 Kip1 protein expression in Hashimoto's thyroiditis. *J Clin Pathol* 2003;56:587–91.

Valk PJ, Verhaak RG, Beijnen MA, Erpelinck CA, Barjesteh Van Waalwijk Van Doorn-Khosrovani S, Boer JM, Beverloo HB, Moorhouse MJ, Van Der Spek PJ, Lowenberg B, Delwel R. Prognostically useful gene-expression profiles in acute myeloid leukemia. *N Engl J Med* 2004;350:1617–28.

Van De Vijver MJ, He YD, Van't Veer LJ, Dai H, Hart AA, Voskuil DW, Schreiber GJ, Peterse JL, Roberts C, Marton MJ, Parrish M, Atsma D, Witteveen A, Glas A, Delahaye L, van der Velde T, Bartelink H, Rodenhuis S, Rutgers ET, Friend SH, Bernards R. A gene-expression signature as a predictor of survival in breast cancer. *N Engl J Med* 2002;347:1999–2009.

Van Kemenade FJ, Raaphorst FM, Blokzijl T, Fieret E, Hamer KM, Satijn DP, Otte AP, Meijer CJ. Coexpression of BMI-1 and EZH2 polycomb-group proteins is associated with cycling cells and degree of malignancy in B-cell non-Hodgkin lymphoma. *Blood* 2001;97:3896–901.

Van 't Veer LJ, Dai H, van de Vijver MJ, He YD, Hart AA, Mao M, Peterse HL, van der Kooy K, Marton MJ, Witteveen AT, Schreiber GJ, Kerkhoven RM, Roberts C, Linsley PS, Bernards R, Friend SH. Gene expression profiling predicts clinical outcome of breast cancer. *Nature* 2002;415:530–6.

Varambally S, Dhanasekaran SM, Zhou M, Barrette TR, Kumar-Sinha C, Sanda MG, Ghosh D, Pienta KJ, Sewalt RGAB, Otte AP, Rubin MA, Chinnaiyan AM. The polycomb group protein EZH2 is involved in progression of prostate cancer. *Nature* 2002;419:624–9.

Visconti R, Federico A, Coppola V, Pentimalli F, Berlingieri MT, Pallante P, Kruhoffer M, Orntoft TF, Fusco A. Transcriptional profile of Ki-Ras-induced transformation of thyroid cells. *Cancer Invest.* 2006 Accepted.

Visser HP, Gunster MJ, Kluin-Nelemans HC, Manders EM, Raaphorst FM, Meijer CJ, Willemze R, Otte AP. The Polycomb group protein EZH2 is upregulated in proliferating, cultured human mantle cell lymphoma. *Br J Haematol* 2001;112:950–8.

Vitagliano D, Portella G, Troncone G, Francione A, Rossi C, Bruno A, Giorgini A, Coluzzi S, Nappi TC, Rothstein JL, Pasquinelli R, Chiappetta G, Terracciano D, Macchia V, Melillo RM, Fusco A, Santoro M. Thyroid targeting of the N-ras(Gln61Lys)oncogene in transgenic mice results in follicular tumors that progress to poorly differentiated carcinomas. *Oncogene.* 2006;25:5467–74.

Voges D, Zwickl P, Baumeister W. The 26S proteasome: a molecular machine designed for controlled proteolysis. *Annu Rev Biochem* 1999;68:1015–68.

Wagner KW, Sapinoso LM, El-Rifai W, Frierson HF, Butz N, Mestan J, Hofmann F, Deveraux QL, Hampton GM. Overexpression, genomic amplification and therapeutic potential of inhibiting the UbcH10 ubiquitin conjugase in human carcinomas of diverse anatomic origin. *Oncogene* 2004;23:6621–9.

Wang L, Brown JL, Cao R, Zhang Y, Kassis JA, Jones RS. Hierarchical recruitment of polycomb group silencing complexes. *Mol Cell* 2004;14:637–46.

Welford SM, Gregg J, Chen E, Garrison D, Sorensen PH, Denny CT, Nelson SF. Detection of differentially expressed genes in primary tumor tissues using representational differences analysis coupled to microarray hybridization. *Nucleic Acids Res* 1998;26:3059–65.

Welsh JB, Zarrinkar PP, Sapinoso LM, Kern SG, Behling CA, Monk BJ, Lockhart DJ, Burger RA, Hampton GM. Analysis of gene expression profiles in normal and neoplastic ovarian tissue samples identifies candidate molecular markers of epithelial ovarian cancer. *Proc Natl Acad Sci U S A* 2001;98:1176–81.

Wild A, Langer P, Celik I, Chaloupka B, Bartsch DK. Chromosome 22q in pancreatic endocrine tumors: identification of a homozygous deletion and potential prognostic associations of allelic deletions. *Eur J Endocrinol* 2002;147:507–13.

World Health Organization Classification of Tumours. Pathology and Genetics of Tumours of Endocrine Organs (eds DeLellis RA, Lloyd RV, Heitz PU, Eng C) (IARC Press, Lyon, 2004).

Wynford-Thomas D. Origin and progression of thyroid epithelial tumours. Cellular and molecular mechanisms. *Horm Res* 1997;47:145–57.

Xing M. BRAF mutation in thyroid cancer. *Endocr Relat Cancer* 2005;12:245–62.

Yamano H, Gannon J, Mahbubani H, Hunt T. Cell-cycle regulated recognition of the destruction box of cyclin B by the APC/C in *Xenopus* egg extracts. *Mol Cell* 2004;13:137–47.

Yeh MW, Demircan O, Ituarte P, Clark OH. False-negative fine-needle aspiration cytology results delay treatment and adversely affect outcome in patients with thyroid carcinoma. *Thyroid* 2004;14:207–15.

Zeppa P, Vetrani A, Marino M, Fulciniti F, Boschi R, De Rosa G, Palombini L. Fine needle aspiration of medullary thyroid carcinoma: a review of 18 cases. *Cytopathology* 1990;1:35–44.

Zhang X, Jafari N, Barnes RB, Confino E, Milad M, Kazer RR. Studies of gene expression in human cumulus cells indicate pentraxin 3 as a possible marker for oocyte quality. *Fertil Steril* 2005;83:1169–79.

Zvara A, Szekeres G, Janka Z, Kelemen JZ, Cimmer C, Santha M, Puskas LG. Over-expression of dopamine D2 receptor and inwardly rectifying potassium channel genes in drug-naive schizophrenic peripheral blood lymphocytes as potential diagnostic markers. *Dis Markers* 2005;21:61–9.

UbcH10 overexpression may represent a marker of anaplastic thyroid carcinomas

P Pallante¹, MT Berlingieri¹, G Troncione², M Kruhoffer³, TF Orntoft³, G Viglietto¹, A Caleo², I Migliaccio², M Decaussin-Petrucci⁴, M Santoro¹, L Palombini² and A Fusco^{*,1,5}

¹Dipartimento di Biologia e Patologia Cellulare e Molecolare c/o Istituto di Endocrinologia ed Oncologia Sperimentale del CNR, Facoltà di Medicina e Chirurgia di Napoli, Università degli Studi di Napoli 'Federico II', via Pansini, 5, 80131 Naples, Italy; ²Dipartimento di Anatomia Patologica e Citopatologia, Facoltà di Medicina e Chirurgia di Napoli, Università di Napoli 'Federico II', via Pansini, 5, 80131 Naples, Italy; ³Department of Clinical Biochemistry, Aarhus University Hospital, Skejby DK 8200 Aarhus N, Denmark; ⁴Service d'Anatomo-Pathologie, Centre Hospitalier Lyon Sud, Pierre Bénite, France; ⁵NOGEC (Naples Oncogenomic Center)-CEINGE, Biotecnologie Avanzate, via Comunale Margherita, 80131 Naples, Italy

The hybridisation of an Affymetrix HG_U95Av2 oligonucleotide array with RNAs extracted from six human thyroid carcinoma cell lines and a normal human thyroid primary cell culture led us to the identification of the UbcH10 gene that was upregulated by 150-fold in all of the carcinoma cell lines in comparison to the primary culture cells of human normal thyroid origin. Immunohistochemical studies performed on paraffin-embedded tissue sections showed abundant UbcH10 levels in thyroid anaplastic carcinoma samples, whereas no detectable UbcH10 expression was observed in normal thyroid tissues, in adenomas and goiters. Papillary and follicular carcinomas were only weakly positive. These results were further confirmed by RT-PCR and Western blot analyses. The block of UbcH10 protein synthesis induced by RNA interference significantly reduced the growth rate of thyroid carcinoma cell lines. Taken together, these results would indicate that UbcH10 overexpression is involved in thyroid cell proliferation, and may represent a marker of thyroid anaplastic carcinomas.

British Journal of Cancer (2005) **93**, 464–471. doi:10.1038/sj.bjc.6602721 www.bjcancer.com

Published online 2 August 2005

© 2005 Cancer Research UK

Keywords: UbcH10; thyroid; carcinomas; immunohistochemistry

Tumours are the result of the accumulation of different modifications in critical genes involved in the control of cell proliferation. In a large number of carcinomas with worst prognosis, lesions are not diagnosed until the disease is at an advanced stage. Although various therapeutic approaches are followed in clinical practice, most of them are not life saving. Hence, the discovery of ways to diagnose cancer at an early stage and to establish more effective therapies is a critical and urgent issue. To achieve this goal, identification and characterisation of key molecules that participate in carcinogenesis are essential steps. Thyroid neoplasms represent a good model for studying the events involved in epithelial cell multistep carcinogenesis, because they comprise a broad spectrum of lesions with different degrees of malignancy from benign adenomas, which are not invasive and very well differentiated, to the undifferentiated anaplastic thyroid carcinomas, which are very aggressive and always fatal; papillary and follicular carcinomas, the most common forms of thyroid cancer, represent intermediate forms of neoplasia being differentiated and

having a good prognosis (Hedinger *et al*, 1989; Wynford-Thomas, 1997).

The involvement of several oncogenes has been demonstrated in papillary thyroid carcinomas. Activation of the RET/PTC oncogene, caused by rearrangements of the RET protooncogene, is detectable in about 30% of the cases (Grieco *et al*, 1990; Tallini *et al*, 1998). Mutations of the B-RAF gene have been demonstrated in almost 40% of papillary carcinomas (Fukushima *et al*, 2003). TRK gene rearrangements (Pierotti *et al*, 1995) and MET gene overexpression are often found in papillary carcinomas (Di Renzo *et al*, 1992). RAS gene mutations (Suarez *et al*, 1990) and PAX8-PPAR- γ rearrangements (Kroll *et al*, 2000) are frequently detected in tumours of the follicular type. Impairment of the p53 tumour suppressor gene function represents a typical feature of the anaplastic carcinomas (Ito *et al*, 1992; Dobashi *et al*, 1993; Donghi *et al*, 1993; Fagin *et al*, 1993; Matias-Guiu *et al*, 1994). Even though critical molecular mechanisms of thyroid carcinogenesis have been clarified, other molecular steps of neoplastic progression need to be investigated.

Therefore, to identify the genes regulated in the process of thyroid carcinogenesis, we analysed a microarray with RNAs extracted from normal human thyroid primary cell culture (NTPC), and six human thyroid carcinoma cell lines of different histotype (one from a follicular carcinoma, three derived from papillary carcinomas and two from anaplastic carcinomas). Our attention was focused on the UbcH10 gene that was upregulated

*Correspondence: Dr A Fusco, Dipartimento di Biologia e Patologia Cellulare e Molecolare, Facoltà di Medicina e Chirurgia di Napoli and, NOGEC (Naples Oncogenomic Center)-CEINGE, Biotecnologie Avanzate, via Pansini 5, 80131 Naples, Italy; E-mail: afusco@napoli.com
Received 2 March 2005; revised 16 June 2005; accepted 22 June 2005; published online 2 August 2005

about 150-fold in all of the cell lines tested by the cDNA microarray. The UbcH10 gene belongs to the E2 gene family and codes for a protein of 19.6 kDa that is involved in the ubiquitin-dependent proteolysis. In this pathway, ubiquitin-conjugating enzyme (E2), together with ubiquitin ligase (E3), transfers ubiquitin to specific substrate proteins (Hershko and Ciechanover, 1998; Joazeiro and Weissman, 2000).

The expression level of UbcH10 was extremely low in the normal thyroid primary culture cells, but strong in all the cancerous cell lines. Immunohistochemical and RT-PCR analyses on a large panel of thyroid neoplasms of different histotypes revealed an increased UbcH10 expression in anaplastic thyroid carcinomas, whereas follicular and papillary carcinomas were just weakly positive. The block of UbcH10 protein synthesis by RNA interference inhibited the growth of two thyroid carcinoma cell lines.

MATERIALS AND METHODS

Cell culture and transfections

The human thyroid carcinoma cell lines used in this study are: TPC-1 (Tanaka *et al*, 1987), WRO (Estour *et al*, 1989), NPA and ARO (Pang *et al*, 1989), FRO (Fagin *et al*, 1993), NIM 1 (Zeki *et al*, 1993), B-CPAP (Fabien *et al*, 1994), FB-1 (Fiore *et al*, 1997), FB-2 (Basolo *et al*, 2002), Kat-4 and Kat-18 (Ain *et al*, 1997). They were grown in DMEM (Gibco Laboratories, Carlsbad, CA, USA) containing 10% fetal calf serum (Gibco Laboratories), glutamine (Gibco Laboratories) and ampicillin/streptomycin (Gibco Laboratories) in a 5% CO₂ atmosphere. Normal human thyroid primary culture cells have been established and grown as already described (Curcio *et al*, 1994). PC Cl 3 cell line derived from Fischer rat thyroid (Fusco *et al*, 1987) was cultured in modified F12 medium supplemented with 5% calf serum (Gibco Laboratories) and six growth factors (thyrotropic hormone, hydrocortisone, insulin, transferrin, somatostatin and glycyl-histidyl-lysine; Sigma, St Louis, MO, USA). Thyroid cells were transfected using Lipofectamine reagent (Invitrogen, Carlsbad, CA, USA) according to the manufacturer's instructions. The transfected cells were selected in a medium containing geneticin (G418) (Life Technologies, Italy). For each transfection, several G418-resistant clones and the mass cell population were isolated and expanded for further analysis.

Human thyroid tissue samples

Neoplastic human thyroid tissues and normal adjacent tissue or the controlateral normal thyroid lobe were obtained from surgical specimens and immediately frozen in liquid nitrogen. Thyroid tumours were collected at the Service d'Anatomo-Pathologie, Centre Hospitalier Lyon Sud, Pierre Bénite, France. The tumour samples were stored frozen until RNA or protein extractions were performed.

RNA isolation

Total RNA was extracted from tissues and cell cultures using the RNAsy mini kit (Qiagen, Valencia, CA, USA) according to the manufacturer's instructions. The integrity of the RNA was assessed by denaturing agarose gel electrophoresis.

Reverse transcriptase-PCR analysis

In total, 5 µg of total RNA from each sample, digested with DNaseI (Invitrogen), were reverse transcribed using random hexanucleotides and MuLV reverse transcriptase (Applied Biosystems, Foster City, CA, USA). PCR was carried out on cDNA using the GeneAmp PCR System 9600 (Applied Biosystems). RNA PCR Core Kit (Applied Biosystems) was used to perform RT-PCR reactions.

For the UbcH10 gene, after a first denaturing step (94°C for 3 min), PCR amplification was performed for 25 cycles (94°C for 30 s, 57°C for 30 s, 72°C for 30 s). The sequences of forward and reverse primers, amplifying a fragment of 115 bp in the UbcH10 cDNA, were: forward 5'-GCCCGTAAAGGAGCTGAG-3' and reverse 5'-GGGAAGGCAGAAATCCCT-3'. The human β-actin gene primers, amplifying a 109 bp cDNA fragment, were used as control; amplification was performed for 25 cycles (94°C for 30 s, 55°C for 30 s, 72°C for 30 s). β-Actin-forward, 5'-TCGTGCGTGACATTAAGGAG-3'; β-actin-reverse, 5'-GTCAGGCAGCTCGTAGCTCT-3'. To ensure that RNA samples were not contaminated with DNA, negative controls were obtained by performing the PCR on samples that were not reverse-transcribed, but otherwise identically processed. The PCR products were separated on a 2% agarose gel, stained with ethidium bromide and scanned using a Typhoon 9200 scanner. Quantitative PCR was performed in triplicate using iCycler (Bio-Rad, Hercules, CA, USA) with SYBR[®] Green PCR Master Mix (Applied Biosystems) as follows: 95°C 10 min and 40 cycles (95°C 15 s and 60°C 1 min). Fold mRNA overexpression was calculated according to the formula $2^{(Rt-Et)}/2^{(Rn-En)}$ as described previously (El-Rifai *et al*, 2001), where Rt is the threshold cycle number for the reference gene in the tumour, Et for the experimental gene in the tumor, Rn for the reference gene in the normal sample and En for the experimental gene in the normal sample.

Protein extraction, Western blotting and antibodies

Cells were washed once in cold PBS and lysed in a lysis buffer containing 50 mM HEPES, 150 mM NaCl, 1 mM EDTA, 1 mM EGTA, 10% glycerol, 1% Triton-X-100, 1 mM phenylmethylsulphonyl fluoride, 1 µg aprotinin, 0.5 mM sodium orthovanadate, 20 mM sodium pyrophosphate. The lysates were clarified by centrifugation at 14 000 r.p.m. × 10 min. Protein concentrations were estimated by a Bio-Rad assay (Bio-Rad), and boiled in Laemmli buffer (Tris-HCl pH 6.8, 0.125 M, SDS 4%, glycerol 20%, 2-mercaptoethanol 10%, bromophenol blue 0.002%) for 5 min before electrophoresis. Proteins were subjected to SDS-PAGE (15% polyacrylamide) under reducing condition. After electrophoresis, proteins were transferred to nitrocellulose membranes (Immobilon-P Millipore Corp., Bedford, MA, USA); complete transfer was assessed using prestained protein standards (Bio-Rad). After blocking with TBS-BSA (25 mM Tris, pH 7.4, 200 mM NaCl, 5% bovine serum albumin), the membrane was incubated with the primary antibody against UbcH10 (Boston Biochem Inc., Cambridge, MA, USA) for 60 min (at room temperature). Primary antibody against c-Fos protein (Santa Cruz Biotechnology Inc., Santa Cruz, CA, USA) was used to confirm the specificity of siRNAs against UbcH10 protein. To ascertain that equal amounts of protein were loaded, the Western blots were incubated with antibodies against the γ-tubulin protein (Sigma). Membranes were then incubated with the horseradish peroxidase-conjugated secondary antibody (1:3000) for 60 min (at room temperature) and the reaction was detected with a Western blotting detection system (ECL; Amersham Biosciences, UK).

Immunohistochemistry: tissue samples

UbcH10 protein cellular distribution was assessed by immunohistochemical analysis and compared to that of the standard cell proliferation marker Ki-67/MIB1. A series of surgical specimens from patients with thyroid diseases comprised of Hashimoto's thyroiditis-HT (six cases), nodular goiter (12 cases), follicular carcinoma (13 cases), papillary carcinoma (33 cases), poorly differentiated carcinoma (five cases) and anaplastic carcinoma (15 cases) was chosen to represent a wide range of thyroid pathology. As control, 10 areas of normal thyroid parenchyma were selected from the lobe controlateral to the tumour in surgical specimens of papillary carcinoma.

Immunostaining: technique, evaluation and statistical analysis

Xylene dewaxed and alcohol-rehydrated paraffin sections were placed in Coplin jars filled with a 0.01 M tri-sodium citrate solution, and heated for 3 min in a conventional pressure cooker (Troncone *et al*, 2003). After heating, slides were thoroughly rinsed in cold running water for 5 min. They were then washed in Tris-Buffered Saline (TBS) pH 7.4 before incubating overnight with the specific antibody, diluted as follows: rabbit polyclonal α -UbcH10 (Boston Biochem) 1:1000; α -MIB-1 (Novocastra, Newcastle upon Tyne, UK) 1:50. After incubation with the primary antibody, tissue sections were stained with biotinylated anti-rabbit or anti-mouse immunoglobulins, followed by peroxidase-labelled streptavidine (Dako, Carpinteria, CA, USA); the signal was developed by using diaminobenzidine (DAB) chromogen as substrate. Incubations both omitting the specific antibody, and including unrelated antibodies, were used as negative controls.

Individual cells were scored for expression of UbcH10 and Ki-67 in similar areas of adjacent sections by quantitative analysis performed with a computerised analyser system (Ibas 2000, Kontron, Zeiss), as already described (Troncone *et al*, 2003). In each case, the distribution of these proteins was evaluated in at least 500 epithelial follicular cells and expressed as a percentage of the total cell population. The statistical analysis was performed using SPSS Ver. 9.0.1 for Windows. Data are expressed as median value and range. The nonparametric Mann-Whitney *U*-test was used to compare differences in labelling indexes for UbcH10 and Ki-67 in thyroid carcinomas. The Spearman rank order correlation was used to verify the association between UbcH10 and Ki-67. A *P*-value less than 0.05 was considered statistically significant.

RNA interference

For small interfering RNA (siRNA) experiments, the following double-strand RNA oligo specific for UbcH10 coding region was used: 5'-AACCTGCAAGAAACCTACTCA-3' as previously described (Wagner *et al*, 2004). As negative control, we used a corresponding scrambled sequence as follows: 5'-AACTAACAC TAGCTCAAGACC-3'. All of the siRNA duplexes were purchased from Qiagen and were transfected using Oligofectamine (Invitrogen) according to the manufacturer's recommendations. Small interfering RNAs were used at a final concentration of 100 nM and 12×10^5 cells well⁻¹ were plated in a six-well format plates. Proteins were extracted 48 h after siRNA treatment and the levels of the UbcH10 protein were evaluated by Western blot.

Assay of the transformed state

Tumorigenicity of the cell lines was tested by injecting 2×10^6 cells subcutaneously into athymic mice. Soft agar colony assay was performed as previously described (Macpherson and Montagnier, 1964).

RESULTS

Expression of UbcH10 gene in normal human thyroid cells and thyroid carcinoma cell lines

To search for candidate genes involved in the neoplastic transformation of thyroid gland, RNAs extracted from normal human thyroid primary cells and six human thyroid carcinoma cell lines of different origin (WRO cell line from a follicular carcinoma, TPC-1 and FB-2 cell lines, both deriving from papillary thyroid cancers, NPA cell line, which derives from a poorly differentiated papillary carcinoma, ARO and FRO cell lines originating from anaplastic carcinomas) were hybridised to U95Av2 Affymetrix oligonucleotide arrays (data not shown). We

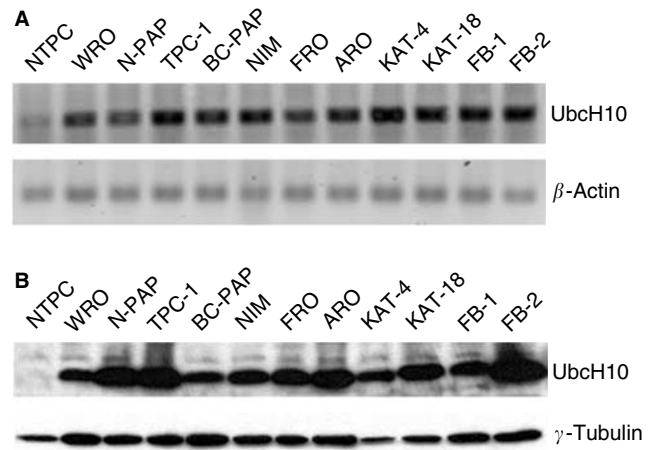


Figure 1 UbcH10 expression in human thyroid carcinoma cell lines. **(A)** UbcH10 gene expression analysis by RT-PCR in human thyroid carcinoma cell lines vs the normal human thyroid primary culture cells (NTPC). β -Actin gene expression was evaluated as control to normalise the amount of the used RNAs. **(B)** UbcH10 protein expression analysis by Western Blot in human thyroid carcinoma cell lines. Blot against γ -tubulin has been performed as control for equal protein loading.

concentrated our attention on the UbcH10 gene that was upregulated about 150-fold in all of the cell lines tested by the cDNA microarray. This result was confirmed by RT-PCR in a larger panel of thyroid carcinoma cell lines using as control normal thyroid primary culture (Figure 1A). Western blot analysis of UbcH10 expression, shown in Figure 1B, confirmed the RT-PCR data. In fact, the UbcH10 protein was abundantly expressed in all of the carcinoma cell lines, whereas it was barely detectable in normal thyroid cells.

Analysis of UbcH10 expression in normal and neoplastic thyroid tissues by immunohistochemistry, Western blot and RT-PCR

In order to evaluate whether the overexpression of UbcH10 is a feature of the thyroid tumours and not only of cultured thyroid carcinoma cell lines, we performed immunohistochemical analysis using a commercial antibody against UbcH10 protein. This methodology allows a rapid and sensitive screening of thyroid pathological tissues and is amenable to regular use as a routine diagnostic test. To find the best experimental conditions, ARO cell line and tumours, induced by injecting the ARO cell line into athymic mice, were used as positive controls (Cerutti *et al*, 1996). No staining was observed with normal human thyroid primary cell culture, whereas a positive staining was obtained with ARO cell line and ARO-induced tumours (data not shown). We found that normal thyroid, nodular goiter and Hashimoto's thyroiditis (HT) were almost always completely negative for UbcH10 expression. Only occasionally, single UbcH10-labelled thyroid epithelial cells showing mitotic figures could be observed by meticulous scrutiny (Figure 2A). In HT, there was a sharp contrast between the negative epithelial oxyphilic cells and the positive lymphoid germinal centers (Figure 2B). While a weak staining is detectable in follicular adenomas (Figure 2C), higher levels of UbcH10 were recorded in papillary (median value 2.2% of positive cells; range 0.9–4.1%), follicular (median value 2.8% of positive cells; range 1–6.1%) and poorly differentiated (median value 10.4% of positive cells; range 8–14.9%) carcinomas, signal being always easily detectable in the nuclei of scattered neoplastic cells (Figure 2D, E and F). UbcH10 staining pattern was somewhat different in

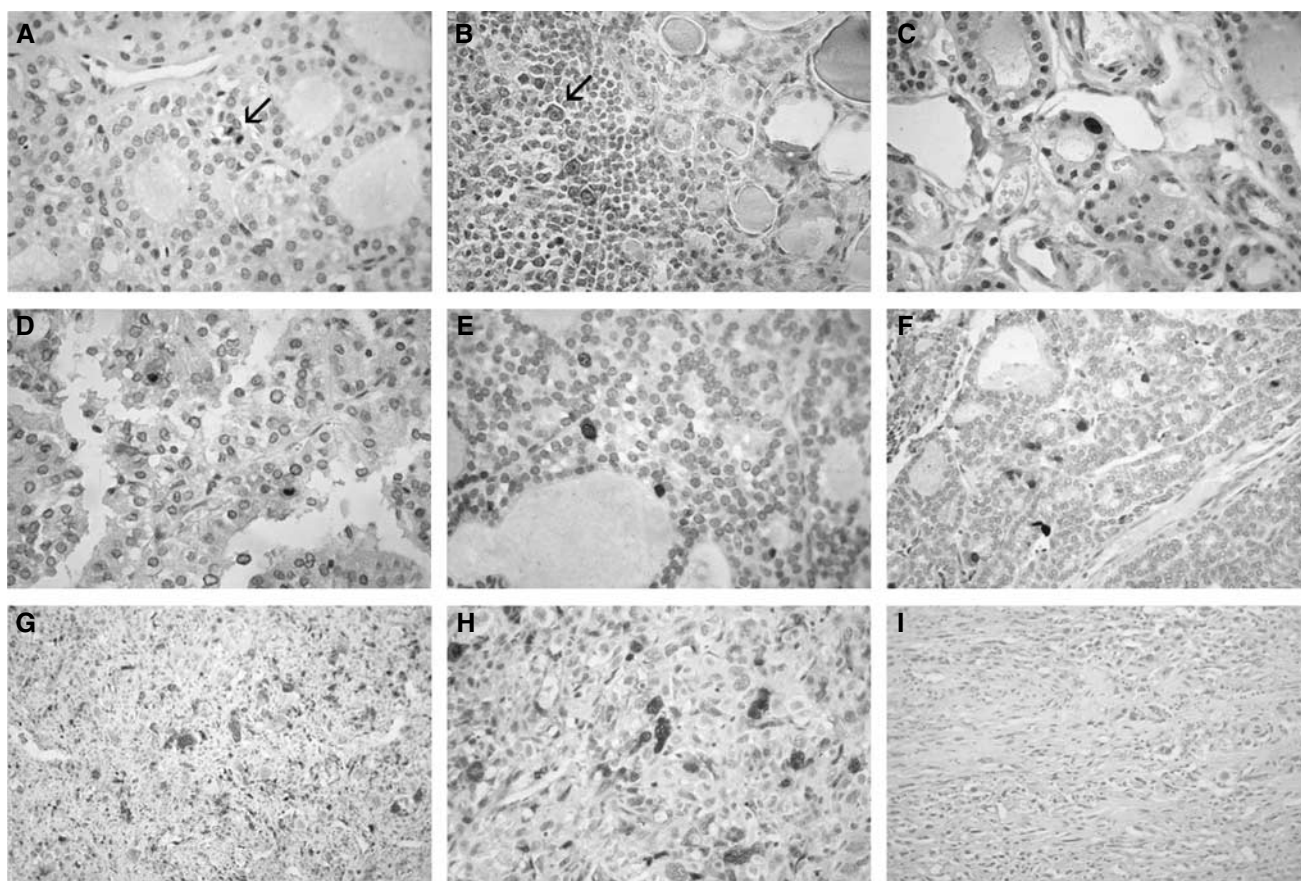


Figure 2 UbcH10 staining pattern in normal, inflammatory and neoplastic thyroid tissues. Follicular epithelial cells of normal thyroid (**A**) and oxyphilic cells of Hashimoto's thyroiditis (HT) (**B**) do not stain for UbcH10, with occasional mitotic figures (**A**, arrow) and lymphoid centroblasts of HT (**B**, arrow) providing the appropriate internal positive control. In neoplastic thyroid, UbcH10 staining pattern is strongly related to tumour grade, being weak in follicular adenoma (**C**), slightly more evident in well-differentiated papillary (**D**) and follicular (**E**) carcinomas, whereas stronger in poorly differentiated (**F**) and in anaplastic (**G**) carcinomas. In the latter, most of neoplastic cells show a very intense labelling, with intense nuclear staining (**H**), whereas signal disappeared by antigen incubation (**I**).

anaplastic carcinomas, the percentage (median value 45.8% of positive cells; range 38.8–56.2%) of stained cells being large and the intensity of the neoplastic cells being strong (Figure 2G and H).

No staining was observed when the same anaplastic carcinoma samples were stained with antibodies preincubated with UbcH10 recombinant protein (Figure 2I) or in the absence of the primary antibodies (data not shown). Therefore, as a general rule, UbcH10 expression is negligible in non-neoplastic thyroid, noticeable in well-differentiated carcinomas and conspicuous in less-differentiated tumours (Figure 3A).

To determine the relationship between UbcH10 expression and tissue proliferation, we correlated its expression in carcinomas with the proliferation rate of thyrocytes, as measured by Ki-67 staining; this latter showed the same tissue distribution of UbcH10, which was evident when adjacent (mirror) sections were stained. By using the Spearman rank order correlation, we determined that the association between UbcH10 and Ki-67 expression in thyroid cancer was statistically significant. In fact, the value of the Spearman R was 0.4 ($P < 0.001$) (Figure 3B).

Western blot analysis, performed on 30 surgically removed thyroid tumours, confirmed the immunohistochemical data. A representative Western blot is shown in Figure 4A. A strong band of 19.6 kDa corresponding to the UbcH10 protein was detected in anaplastic thyroid carcinomas and a weak one in poorly differentiated carcinomas, but not in papillary carcinomas and normal thyroids. These data strongly indicate that the expression

of UbcH10 is more abundant in thyroid carcinomas characterised by a highly malignant and aggressive phenotype. Equal amounts of total proteins were used for each sample as demonstrated by the same gel analysed with an antibody against γ -tubulin.

UbcH10 expression was also evaluated by RT-PCR analysis on a panel of matched tumour/normal tissues. This analysis confirmed the protein data. In fact, as shown in Figure 4B, an amplified band of 115 bp was clearly detected in the anaplastic and poorly differentiated carcinoma samples, but not in the papillary ones and in all the corresponding normal thyroid tissues. Finally, quantitative RT-PCR analysis confirmed a great increase of UbcH10 expression in thyroid anaplastic samples, whereas a light increase was observed in papillary carcinoma samples (Figure 4C).

UbcH10 expression in experimental models of thyroid carcinogenesis

Thyroid neoplasias developing in transgenic animal lines expressing TRK (Tg-TRK) (Russell *et al*, 2000), RET/PTC3 (Tg-RET/PTC3) (Powell *et al*, 1998) and large T SV40 (Tg-SV40) (Ledent *et al*, 1991) oncogenes under the transcriptional control of the thyroglobulin promoter have been analysed for UbcH10 expression by Western blot analysis. Transgenic mice carrying TRK and RET/PTC3 oncogenes develop thyroid papillary carcinomas (Powell *et al*, 1998; Russell *et al*, 2000); thyroid anaplastic carcinomas were, conversely, obtained in the Tg-SV40 mice

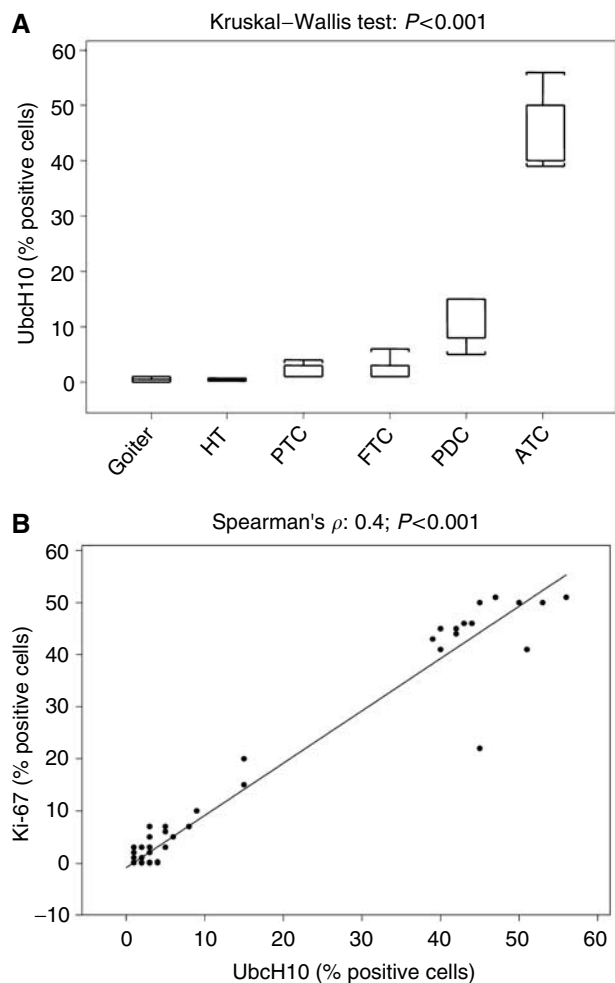


Figure 3 Statistical analysis of the immunohistochemical data. **(A)** Protein expression of UbcH10 (% positive cells) progressively increases in the several diagnostic categories from thyroid goiter to the thyroid anaplastic carcinomas. The analysis has been carried out using the Kruskal–Wallis test. HT, Hashimoto's thyroiditis; PTC, papillary thyroid carcinoma; FTC, follicular thyroid carcinoma; PDC, poorly differentiated thyroid carcinoma; ATC, anaplastic thyroid carcinoma. **(B)** Protein expression of UbcH10 (% positive cells) is correlated to that of Ki-67 (% positive cells) in the several diagnostic categories. The analysis has been carried out calculating the Spearman rank correlation coefficient.

(Ledent *et al*, 1991). As shown in Figure 5, elevated UbcH10 protein levels were observed in the thyroid anaplastic carcinomas derived from large TSV40 transgenic mice. Conversely, UbcH10 protein was absent in normal mouse thyroid tissue and in the papillary carcinomas originating from TRK and RET/PTC3 mice.

Therefore, the analysis of the experimental models of thyroid carcinogenesis seems to confirm that the UbcH10 overexpression is essentially restricted to the undifferentiated histotype.

Suppression of the UbcH10 synthesis inhibits thyroid carcinoma cell growth

We asked whether UbcH10 overexpression had a role in the process of thyroid carcinogenesis by evaluating the growth rate of two thyroid carcinoma cell lines, in which UbcH10 protein was suppressed by RNA interference. The NPA and TPC-1 cell lines were treated with siRNA duplexes targeting to the UbcH10 mRNA. After transfection, we observed an efficient knockdown of the UbcH10 protein levels at 48 h after treatment (Figure 6A). The

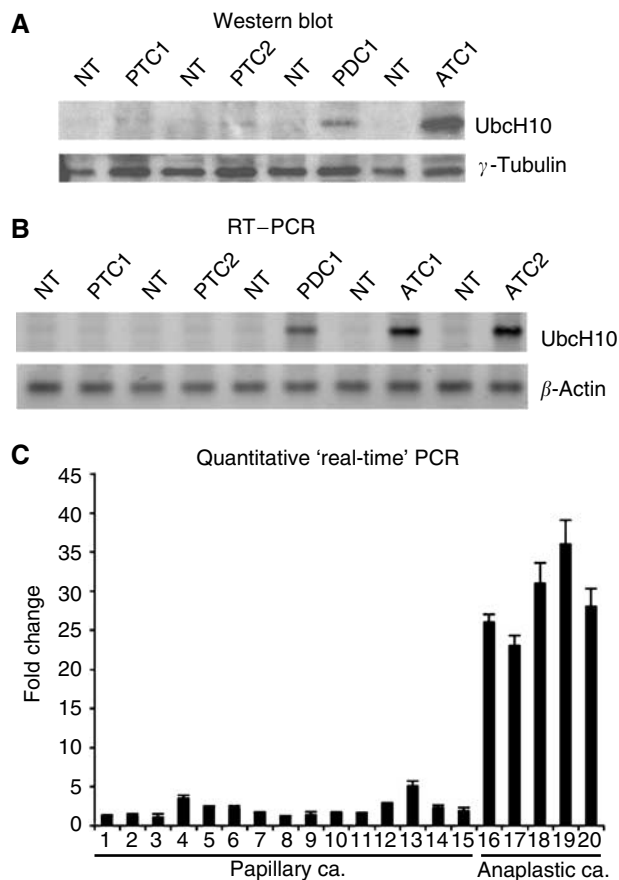


Figure 4 UbcH10 expression in human thyroid fresh tumour samples. **(A)** Western blot analysis of UbcH10 protein expression in a panel of thyroid neoplasias. The level of γ -tubulin has been used as loading control. NT, normal thyroid tissue; PTC1 and PTC2, papillary thyroid carcinomas from two different patients; PDC1, poorly differentiated carcinoma; ATC1, anaplastic thyroid carcinoma. **(B)** RT–PCR analysis of UbcH10 expression in human thyroid tumour samples vs their normal thyroid counterparts. β -Actin expression shows the same amount of RNAs used. NT, normal thyroid tissue; PTC1 and PTC2, papillary thyroid carcinomas from two different patients; PDC1, poorly differentiated carcinoma; ATC1 and ATC2, anaplastic thyroid carcinomas from two different patients. **(C)** Quantitative RT–PCR analysis was performed on human thyroid tumour samples of different histotype. The Fold Change values indicate the relative change in the expression levels between tumour samples and normal samples, assuming that the value of each normal sample is equal to 1.

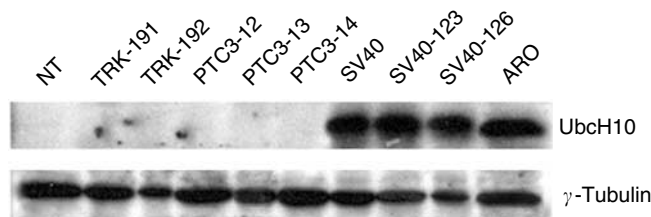


Figure 5 UbcH10 expression in experimental mouse thyroid tumours. Western blot analysis of experimental thyroid carcinomas developed in transgenic mice expressing TRK, RET-PTC-3 and large T SV40 oncogenes. ARO cell line was used as positive control. γ -Tubulin shows the same amount of protein level.

analysis of cell growth of these cell lines in the presence or absence of the UbcH10 siRNA duplexes revealed that the block of the UbcH10 protein synthesis significantly inhibits thyroid carcinoma

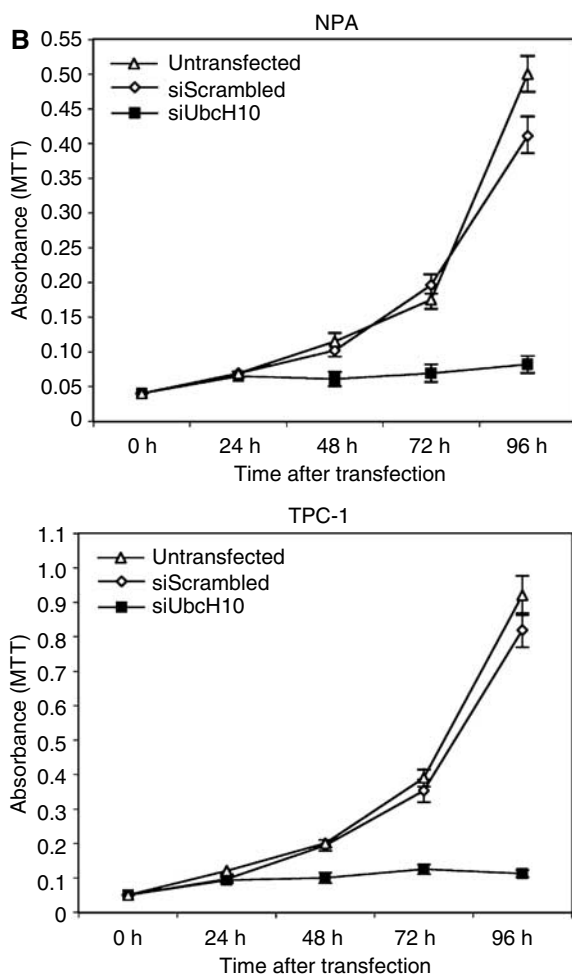
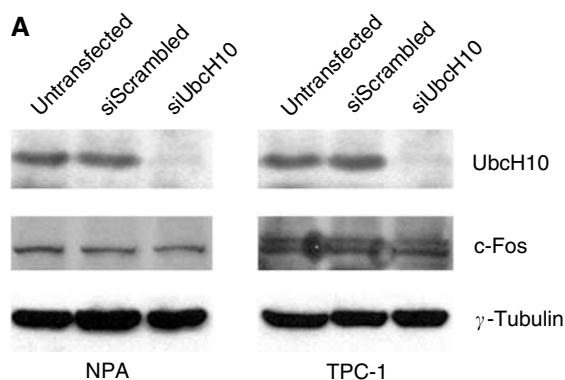


Figure 6 The block of UbcH10 protein synthesis by RNA interference inhibits the proliferation of thyroid carcinoma cells. **(A)** Inhibition of UbcH10 protein expression by RNAi in NPA and TPC-1 cell lines evaluated by Western blot analysis. At 48 h after siRNA transfection, total cell lysates were prepared and normalised for protein concentration. The expression of γ -tubulin was used to control equal protein loading (30 μ g). In this figure, we also show the expression of a fast turning-over gene like c-Fos to confirm the specific effect of siRNAs against UbcH10. **(B)** Growth curves of NPA and TPC-1 cell lines after siUbcH10 treatment. NPA and TPC-1 cells were transfected with siUbcH10 duplexes (siUbcH10) and the relative number of viable cells was determined by MTT assay. Cells transfected with a scrambled duplex (siScrambled) and untransfected cells (Untransfected) were used as negative controls. Absorbance was read at 570 nm and the data are the mean of triplicates.

Table 1 Analysis of the neoplastic phenotype of the UbcH10-transfected rat thyroid cell lines

Cell line	Doubling time (h)	Colony-forming efficiency ^a (%)	Tumour ^b incidence
PC CL 3	24	0	0/4
PC UbcH10 CL1	24	0	0/4
PC UbcH10 CL2	23	0	0/4
PC MPSV	18	70	4/4

^aColony-forming efficiency was calculated by the formula (number of colonies formed/number of plated cells) \times 100. ^bTumorigenicity was assayed by injecting 2×10^6 cells into athymic mice (4–6 weeks old).

cell growth. In fact, as shown in Figure 6B, a significant reduction in cell growth rate was observed in NPA and TPC-1 cell lines treated with UbcH10 siRNA in comparison to the untreated cells or those treated with the control scrambled siRNA.

These results indicate a role of UbcH10 in neoplastic thyroid cell proliferation.

UbcH10 overexpression is not sufficient to transform rat thyroid cells

To further characterise the role of UbcH10 in thyroid carcinogenesis, we transfected normal rat thyroid cells with an expression vector carrying the UbcH10 gene under the transcriptional control of the cytomegalovirus promoter. The selected clones were shown to express high UbcH10 protein levels (data not shown). We evaluated the growth rate of the UbcH10-transfected PC Cl 3 cells and the same cells transfected with a backbone vector: no differences were observed. Equally, the neoplastic phenotype of the UbcH10-transfected PC Cl 3 cells was evaluated by a soft agar colony assay and by injection into athymic mice. As reported in Table 1, the PC Cl 3 cells transfected with the UbcH10 expression vector were not able to give rise to colonies in soft agar and induce tumours in athymic mice. As a positive control, we used the PC Cl 3 cells transformed with the Myeloproliferative sarcoma virus (PC MPSV): these cells have a very highly malignant phenotype (Fusco *et al*, 1987).

These results indicate that UbcH10 overexpression is not able to transform rat thyroid cells *in vitro*.

DISCUSSION

Thyroid neoplasms represent an excellent model for studying the process of cell transformation since they include a broad spectrum of histotypes showing different degree of malignancy (Hedinger *et al*, 1989; Wynford-Thomas, 1997). From the Affymetrix microarray analysis, we found the UbcH10 gene that appeared greatly increased in all of the thyroid carcinoma cell lines. UbcH10 was previously identified as a human homologue of the cyclin-selective E2 (E2-c), which is required for the destruction of mitotic cyclins by the ubiquitination pathway. The UbcH10 gene belongs to the E2 gene family and codes for a protein of 19.6 kDa that is involved in the ubiquitin-dependent proteolysis. In this system, three distinct enzymes cooperate to process target proteins for degradation. More precisely, the ubiquitin-conjugating enzyme (E2) transfers activated ubiquitin by ubiquitin-activating enzyme (E1) to a lysine residue of the target proteins in cooperation with the ubiquitin-ligase (E3). Polyubiquitinated proteins are then recognised by the 26S proteasome and rapidly degraded (Hershko and Ciechanover, 1998; Joazeiro and Weissman, 2000).

In our study, we have evaluated the expression of UbcH10 in human thyroid neoplasias and in mouse experimental tumours. No

significant UbcH10 expression was observed in normal thyroids, goiters and adenomas, whereas a great induction of UbcH10 expression was observed in anaplastic human thyroid carcinomas and in experimental undifferentiated thyroid tumours. Just a weak expression of UbcH10 was observed in follicular and papillary human thyroid carcinomas. Therefore, these data strongly indicate that UbcH10 overexpression could be associated with the thyroid tumour progression since there is a good correlation with the late stage of thyroid neoplastic transformation. The low UbcH10 levels detected in the differentiated thyroid malignancies would appear in contrast with the data showing an abundant UbcH10 expression in the cell lines deriving from differentiated carcinomas. We retain this discrepancy only apparent since thyroid carcinoma cell lines, even deriving from differentiated tumours, cannot be completely compared to surgically removed tumours. In fact, these cell lines harbour p53 mutations that are rare in thyroid differentiated neoplasias (Tanaka *et al*, 1987; Estour *et al*, 1989; Pang *et al*, 1989; Ito *et al*, 1992; Dobashi *et al*, 1993; Donghi *et al*, 1993; Fagin *et al*, 1993; Zeki *et al*, 1993; Fabien *et al*, 1994; Matias-Guiu *et al*, 1994; Ain *et al*, 1997; Fiore *et al*, 1997; Basolo *et al*, 2002) and they have a high proliferation rate. However, this consideration does not exclude the validity of the use of the thyroid carcinoma cell lines as experimental model to draw new information that, however, need to be subsequently validated on fresh tumours.

Our results also indicate a correlation between UbcH10 overexpression and the proliferation status since there is a good association with the proliferation marker Ki-67/MIB1.

An aim of our work was to evaluate the possible causal role of UbcH10 overexpression in thyroid carcinogenesis. Indeed, the block of protein synthesis significantly inhibited the growth of several thyroid carcinoma cell lines, suggesting an important role of UbcH10 in thyroid cell proliferation, and then in the progression step of thyroid carcinogenesis.

Therefore, even though the mechanisms by which UbcH10 overproduction contributes to the neoplastic phenotype remains unclear, we can assume that it leads to a deregulation of cell growth. These results are quite consistent with previous published data showing that UbcH10 was expressed at high levels in primary tumours derived from the lung, stomach, uterus, and bladder as compared with their corresponding normal tissues, suggesting that UbcH10 is involved in tumorigenesis or cancer progression (Okamoto *et al*, 2003; Wagner *et al*, 2004). It has also been shown that UbcH10 is upregulated in NIH3T3 cell line transformed by

EWS/FLI1, but not in untransformed NIH3T3 cell clone expressing EWS/FLI1 (Arvand *et al*, 1998). Moreover, it has been shown that UbcH10 is required for override metaphase, likely degrading growth suppressor, and for destruction of mitotic cyclins, indicating a role of UbcH10 in cell cycle progression (Arvand *et al*, 1998).

However, overexpression of UbcH10 in normal rat thyroid cells did not affect cell growth neither induced a malignant phenotype, indicating that UbcH10 overexpression is not sufficient for malignant thyroid cell transformation. This result might appear in contrast with those showing that NIH3T3 stable transfectants overexpressing UbcH10 exhibited a malignant phenotype as compared with parental NIH3T3 cells (Okamoto *et al*, 2003). This discrepancy is, in our opinion, just apparent since we have to consider that NIH 3T3 cells are preneoplastic cells, whereas PC Cl 3 cells are much more resistant to express the neoplastic phenotype, since even the expression of several oncogenes (v-ras-Ki, v-ras-Ha, etc.) are not able to lead these cells to the fully malignant phenotype that is achieved only when there is a synergy of two different oncogenes (Fusco *et al*, 1987). In conclusion, our data propose the UbcH10 overexpression as a feature of the anaplastic carcinoma histotype. The block of UbcH10 expression significantly reduced the growth of thyroid carcinoma cell lines indicating an involvement of UbcH10 in the increased proliferation of these carcinoma cell lines. Therefore, these results open the perspective of a therapy of the anaplastic thyroid carcinoma, one of the most aggressive tumours in mankind, based on the suppression of the UbcH10 synthesis and/or function.

ACKNOWLEDGEMENTS

This work was supported by grants from the Associazione Italiana Ricerca sul Cancro (AIRC), Progetto Strategico Oncologia Consiglio Nazionale delle Ricerche, the Ministero dell'Università e della Ricerca Scientifica e Tecnologica (MIUR), and 'Piani di Potenziamento della Rete Scientifica e Tecnologica' CLUSTER C-04, the Programma Italia-USA sulla Terapia dei Tumori coordinated by Professor Cesare Peschle, and 'Ministero della Salute'. This work was supported from NOGEC-Naples Oncogenomic Center. We thank the Associazione Partenopea per le Ricerche Oncologiche (APRO) for its support. We are grateful to Jean Ann Gilder (Scientific Communication) for editing the text.

REFERENCES

- Ain KB, Taylor KD, Tofiq S, Venkataraman G (1997) Somatostatin receptor subtype expression in human thyroid and thyroid carcinoma cell lines. *J Clin Endocrinol Metab* **82**: 1857–1862
- Arvand A, Bastians H, Welford SM, Thompson AD, Ruderman JV, Denny CT (1998) EWS/FLI1 up regulates mE2-C, a cyclin-selective ubiquitin conjugating enzyme involved in cyclin B destruction. *Oncogene* **17**: 2039–2045
- Basolo F, Giannini R, Toniolo A, Casalone R, Nikiforova M, Pacini F, Elisei R, Miccoli P, Berti P, Faviana P, Fiore L, Monaco C, Pierantoni GM, Fedele M, Nikiforov YE, Santoro M, Fusco A (2002) Establishment of a non-tumorigenic papillary thyroid cell line (FB-2) carrying the RET/PTC1 rearrangement. *Int J Cancer* **97**: 608–614
- Cerutti J, Trapasso F, Battaglia C, Zhang L, Martelli ML, Visconti R, Berlingieri MT, Fagin JA, Santoro M, Fusco A (1996) Block of c-myc expression by antisense oligonucleotides inhibits proliferation of human thyroid carcinoma cell lines. *Clin Cancer Res* **2**: 119–126
- Curcio F, Ambesi-Impombato FS, Perrella G, Coon HG (1994) Long-term culture and functional characterization of follicular cells from adult normal human thyroids. *Proc Natl Acad Sci USA* **91**: 9004–9008
- Di Renzo MF, Olivero M, Ferro S, Prat M, Bongarzone I, Pilotti S, Belfiore A, Costantino A, Vigneri R, Pierotti MA (1992) Overexpression of the c-MET/HGF receptor gene in human thyroid carcinomas. *Oncogene* **7**: 2549–2553
- Dobashi Y, Sakamoto A, Sugimura H, Mernyei M, Mori M, Oyama T, Machinami R (1993) Overexpression of p53 as a possible prognostic factor in human thyroid carcinoma. *Am J Surg Pathol* **17**: 375–381
- Donghi R, Longoni A, Pilotti S, Michieli P, Della Porta G, Pierotti MA (1993) Gene p53 mutations are restricted to poorly differentiated and undifferentiated carcinomas of the thyroid gland. *J Clin Invest* **91**: 1753–1760
- El-Rifai W, Frierson Jr HF, Moskaluk CA, Harper JC, Petroni GR, Bissonette EA, Jones DR, Knuutila S, Powell SM (2001) Genetic differences between adenocarcinomas arising in Barrett's esophagus and gastric mucosa. *Gastroenterology* **121**: 592–598
- Estour B, Van Herle AJ, Juillard GJ, Totanes TL, Sparkes RS, Giuliano AE, Klandorf H (1989) Characterization of a human follicular thyroid carcinoma cell line (UCLA RO 82 W-1). *Virchows Arch B Cell Pathol Incl Mol Pathol* **57**: 167–174
- Fabien R, Fusco A, Santoro M, Barbier Y, Dubois PM, Paulin C (1994) Description of a human papillary thyroid carcinoma cell line. Morphologic study and expression of tumoral markers. *Cancer* **73**: 2206–2212
- Fagin JA, Matsuo K, Karmakar A, Chen DL, Tang SH, Koeffler HP (1993) High prevalence of mutations of p53 gene in poorly differentiated human thyroid carcinomas. *J Clin Invest* **91**: 179–184

- Fiore L, Pollina LE, Fontanini G, Casalone R, Berlingieri MT, Giannini R, Pacini F, Miccoli P, Toniolo A, Fusco A, Basolo F (1997) Cytokine production by a new undifferentiated human thyroid carcinoma cell line, FB-1. *J Clin Endocrinol Metab* **82**: 4094–4100
- Fukushima T, Suzuki S, Mashiko M, Ohtake T, Endo Y, Takebayashi Y, Sekikawa K, Hagiwara K, Takenoshita S (2003) BRAF mutations in papillary carcinomas of the thyroid. *Oncogene* **22**: 6455–6457
- Fusco A, Berlingieri MT, Di Fiore PP, Portella G, Grieco M, Vecchio G (1987) One- and two-step transformation of rat thyroid epithelial cells by retroviral oncogenes. *Mol Cell Biol* **7**: 3365–3370
- Grieco M, Santoro M, Berlingieri MT, Melillo RM, Donghi R, Bongarzone I, Pierotti MA, Della Porta G, Fusco A, Vecchio G (1990) PTC is a novel rearranged form of the RET proto-oncogene and is frequently detected *in vivo* in human thyroid papillary carcinomas. *Cell* **60**: 557–563
- Hedinger C, Williams D, Sobin LH (1989) The WHO histological classification of thyroid tumours: a commentary on the second edition. *Cancer* **63**: 908–911
- Hershko A, Ciechanover A (1998) The ubiquitin system. *Annu Rev Biochem* **67**: 425–479
- Ito T, Seyama T, Mizuno T, Tsuyama N, Hayashi T, Hayashi Y, Dohi K, Nakamura N, Akiyama M (1992) Unique association of p53 mutations with undifferentiated but not differentiated carcinomas of the thyroid gland. *Cancer Res* **52**: 1369–1371
- Joazeiro CA, Weissman AM (2000) RING finger proteins: mediators of ubiquitin ligase activity. *Cell* **102**: 549–552
- Kroll TG, Sarraf P, Pecciarini L, Chen CJ, Mueller E, Spiegelman BM, Fletcher JA (2000) PAX-8-PPARGamma1 fusion oncogene in human thyroid carcinoma. *Science* **289**: 1357–1360
- Ledent C, Dumont J, Vassart G, Parmentier M (1991) Thyroid adenocarcinomas secondary to tissue-specific expression of simian virus-40 large T-antigen in transgenic mice. *Endocrinology* **129**: 1391–1401
- Macpherson I, Montagnier I (1964) Agar suspension culture for the selective assay of cells transformed by polyoma virus. *Virology* **23**: 291–294
- Matias-Guiu X, Cuatrecasas M, Musulen E, Prat J (1994) p53 expression in anaplastic carcinomas arising from thyroid papillary carcinomas. *J Clin Pathol* **47**: 337–339
- Okamoto Y, Ozaki T, Miyazaki K, Aoyama M, Miyazaki M, Nakagawara A (2003) UbcH10 is the cancer-related E2 ubiquitin-conjugating enzyme. *Cancer Res* **63**: 4167–4173
- Pang XP, Hershman JM, Chung M, Pekary AE (1989) Characterization of tumor necrosis factor-alpha receptors in human and rat thyroid cells and regulation of the receptors by thyrotropin. *Endocrinology* **125**: 1783–1788
- Pierotti MA, Bongarzone I, Borrello MG, Mariani C, Miranda C, Sozzi G, Greco A (1995) Rearrangements of TRK proto-oncogene in papillary thyroid carcinomas. *J Endocrinol Invest* **18**: 130–133
- Powell Jr DJ, Russell J, Nibu K, Li G, Rhee E, Liao M, Goldstein M, Keane WM, Santoro M, Fusco A, Rothstein JL (1998) The RET/PTC3 oncogene: metastatic solid-type papillary carcinomas in murine thyroids. *Cancer Res* **58**: 5523–5528
- Russell JP, Powell DJ, Cunnane M, Greco A, Portella G, Santoro M, Fusco A, Rothstein JL (2000) The TRK-T1 fusion protein induces neoplastic transformation of thyroid epithelium. *Oncogene* **19**: 5729–5735
- Suarez HG, du Villard JA, Severino M, Caillou B, Schlumberger M, Tubiana M, Parmentier C, Monier R (1990) Presence of mutations in all three ras genes in human thyroid tumors. *Oncogene* **5**: 565–570
- Tallini G, Santoro M, Helie M, Carlomagno F, Salvatore G, Chiappetta G, Carcangiu ML, Fusco A (1998) RET/PTC oncogene activation defines a subset of papillary thyroid carcinomas lacking evidence of progression to poorly differentiated or undifferentiated tumor phenotypes. *Clin Cancer Res* **4**: 287–294
- Tanaka J, Ogura T, Sato H, Datano M (1987) Establishment and biological characterization of an *in vitro* human cytomegalovirus latency model. *Virology* **161**: 62–72
- Troncone G, Iaccarino A, Caleo A, Bifano D, Pettinato G, Palombini L (2003) p27 Kip1 protein expression in Hashimoto's thyroiditis. *J Clin Pathol* **56**: 587–591
- Wagner KW, Sapinoso LM, El-Rifai W, Frierson Jr HF, Butz N, Mestan J, Hofmann F, Deveraux QL, Hampton GM (2004) Overexpression, genomic amplification and therapeutic potential of inhibiting the UbcH10 ubiquitin conjugase in human carcinomas of diverse anatomic origin. *Oncogene* **23**: 6621–6629
- Wynford-Thomas D (1997) Origin and progression of thyroid epithelial tumours. Cellular and molecular mechanisms. *Horm Res* **47**: 145–157
- Zeki K, Nakano Y, Inokuchi N, Watanabe K, Morimoto I, Yamashita U, Eto S (1993) Autocrine stimulation of interleukin-1 in the growth of human thyroid carcinoma cell line NIM 1. *J Clin Endocrinol Metab* **76**: 127–133

ONCOGENOMICS

UbcH10 expression may be a useful tool in the prognosis of ovarian carcinomas

MT Berlingieri¹, P Pallante¹, M Guida², C Nappi², V Masciullo³, G Scambia³, A Ferraro⁴, V Leone⁴, A Sboner⁵, M Barbareschi⁶, A Ferro⁶, G Troncone⁷ and A Fusco^{1,4}

¹Dipartimento di Biologia e Patologia Cellulare e Molecolare clo Istituto di Endocrinologia ed Oncologia Sperimentale del CNR, Facoltà di Medicina e Chirurgia di Napoli, Università degli Studi di Napoli 'Federico II', Naples, Italy; ²Dipartimento di Ginecologia e Ostetricia, e Fisiopatologia della Riproduzione Umana, Facoltà di Medicina e Chirurgia di Napoli, Università degli Studi di Napoli 'Federico II', Naples, Italy; ³Istituto di Clinica Ostetrica e Ginecologica, Università Cattolica del S.Cuore, Rome, Italy; ⁴NOGEC (Naples Oncogenomic Center)-CEINGE, Biotecnologie Avanzate-Napoli, & SEMM – European School of Molecular Medicine – Naples Site, Naples, Italy; ⁵Bioinformatics – SRA Division ITC-irst, Centre for Scientific and Technological Research, Povo (Trento), Italy; ⁶U.O. Anatomia Patologica Ospedale S. Chiara Largo Medaglie d'Oro Trento, Italy and ⁷Dipartimento di Anatomia Patologica e Citopatologia, Facoltà di Medicina e Chirurgia, Università di Napoli 'Federico II', Naples, Italy

The UbcH10 gene codes for a protein that belongs to the ubiquitin-conjugating enzyme family. Previous studies of our group suggest UbcH10 expression as a valid indicator of the proliferative and aggressive status of thyroid carcinomas. Therefore, to better understand the process of ovarian carcinogenesis, and to look for possible tools to be used as prognostic markers in these neoplasias, we decided to extend the analysis of the UbcH10 expression to the ovarian neoplastic disease. We found that the UbcH10 gene was upregulated in some ovarian carcinoma cell lines analysed. Then, immunohistochemical studies demonstrate that UbcH10 expression significantly correlates with the tumor grade and the undifferentiated histotype of the ovarian carcinomas. Furthermore, a significant relationship between UbcH10 expression and overall survival was observed. Finally, the block of UbcH10 protein synthesis by RNA interference inhibited the growth of ovarian carcinoma cell lines, suggesting a role of UbcH10 overexpression in ovarian carcinogenesis. Therefore, all these data taken together suggest the possibility to use UbcH10 detection as a marker for the diagnosis and prognosis of these neoplastic diseases and open the perspective of a therapy of some ovarian carcinomas based on the suppression of the UbcH10 synthesis and/or function.

Oncogene advance online publication, 2 October 2006; doi:10.1038/sj.onc.1210010

Keywords: UbcH10; ovarian; carcinomas; immunohistochemistry

Correspondence: Professor A Fusco, Dipartimento di Biologia e Patologia Cellulare e Molecolare, Facoltà di Medicina e Chirurgia, Università degli Studi di Napoli 'Federico II' and NOGEC (Naples Oncogenomic Center)-CEINGE, Biotecnologie Avanzate-Naples, & SEMM – European School of Molecular Medicine – Naples Site, via Pansini 5, 80131 Napoli, Italy.
E-mail: afusco@napoli.com

Received 29 June 2006; revised 27 July 2006; accepted 7 August 2006

Ovarian carcinomas have a great impact in human pathology, in fact ovarian cancer is the leading cause of death from gynecological neoplasias and the fifth most common cancer among women worldwide (Ozols *et al.*, 2004; Jemal *et al.*, 2005).

Research aimed to determine the specific genes involved in the development of ovarian cancers would help to understand how normal ovarian epithelial cells escape regulation of proliferation, apoptosis and senescence. It has been already (Welch and King, 2001) determined that approximately 10% of ovarian cancers arises in women who have inherited mutations in cancer-susceptibility genes such as *BRCA1*, *BRCA2* and other DNA repair genes. Conversely, the vast majority of ovarian cancers are sporadic, presumably resulting from the accumulation of genetic damage over lifetime. Several genes involved in ovarian carcinogenesis have been identified, most notably the *p53* tumor suppressor (Feki and Irminger-Finger, 2004).

Recently in our laboratory, by a microarray gene expression profiling, we found a gene, UbcH10, that was upregulated in thyroid anaplastic carcinoma samples vs the normal thyroid tissues, suggesting a correlation with the malignant progression (Pallante *et al.*, 2005). A high expression of UbcH10 has also been found in carcinomas of different anatomic origin (Wagner *et al.*, 2004).

The UbcH10 gene belongs to the E2 gene family and codes for a protein of 19.6 kDa that is involved in the ubiquitin-dependent proteolysis. In this pathway, ubiquitin-conjugating enzyme (E2), together with ubiquitin ligase (E3), transfers ubiquitin to specific substrate proteins (Hershko and Ciechanover, 1998; Joazeiro and Weissman, 2000).

The aim of our work was to investigate whether the UbcH10 expression might be a new useful indicator for the diagnosis and prognosis of ovarian cancer.

Therefore, we evaluated the expression of UbcH10 by reverse transcription-polymerase chain reaction (RT-PCR) and Western blot in ovarian carcinoma cell lines in comparison with the normal ovarian tissue. All

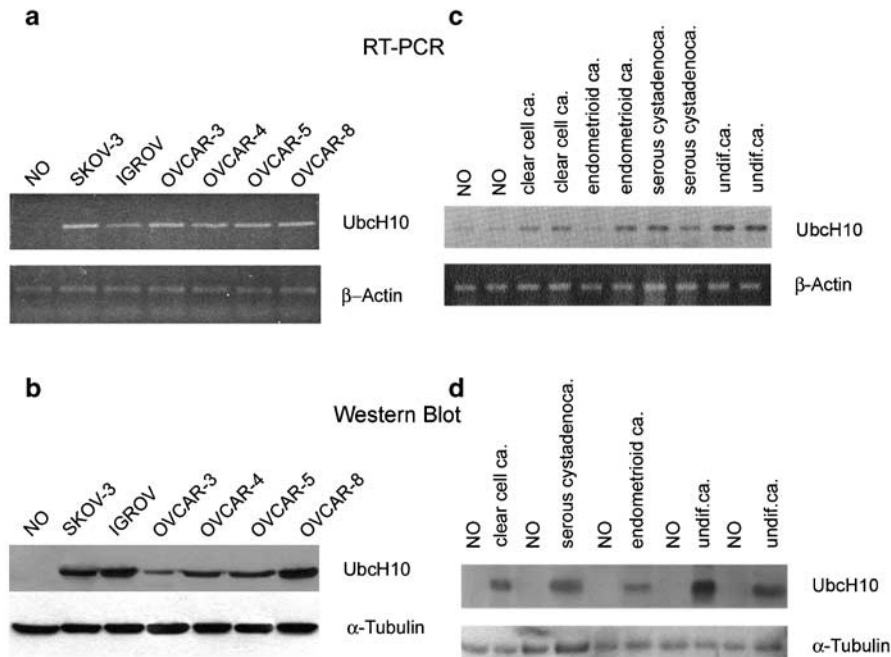


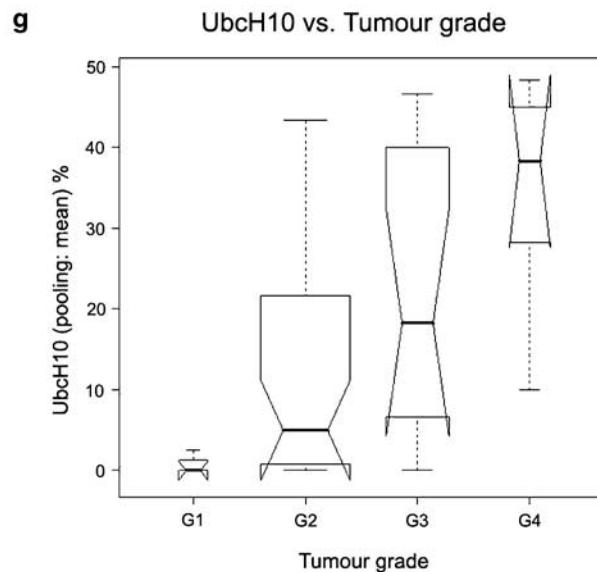
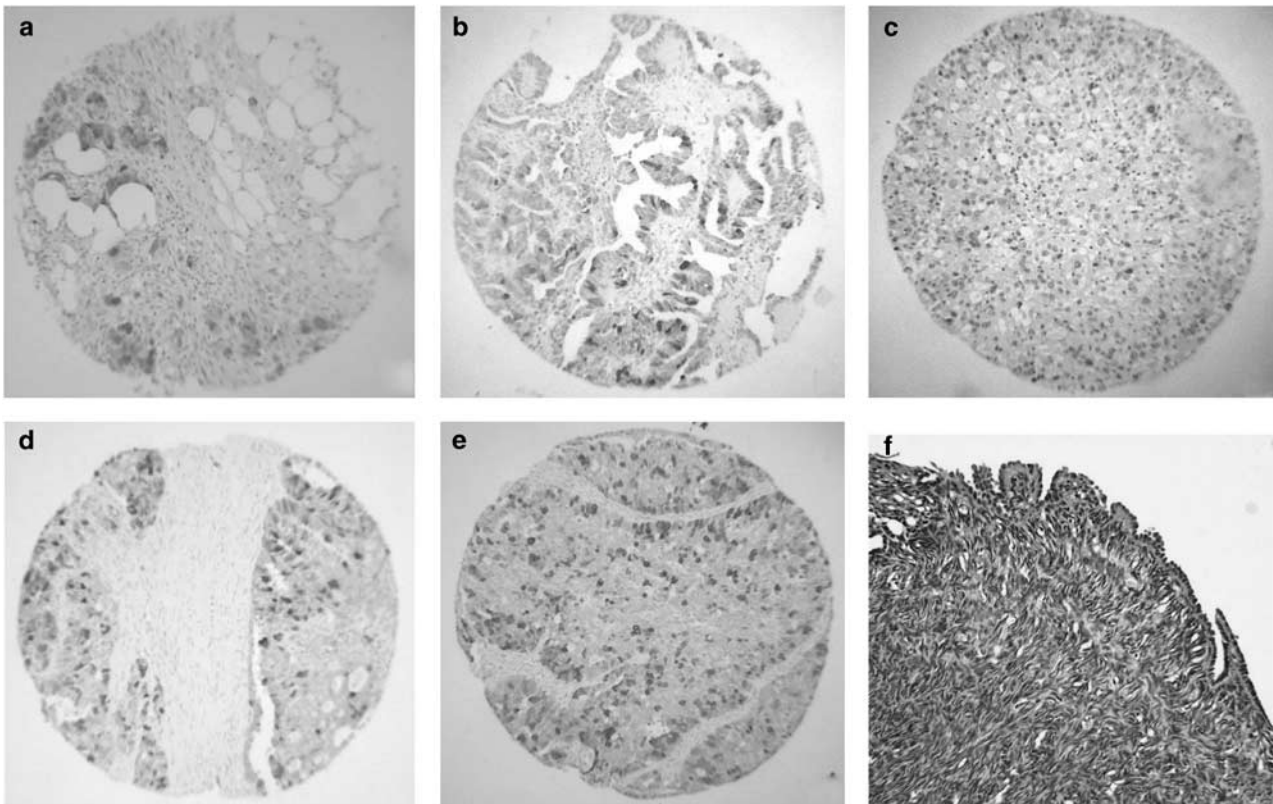
Figure 1 UbcH10 expression in human ovarian carcinoma cell lines and tissues. (a) UbcH10 gene expression analysis by RT-PCR in human ovarian carcinoma cell lines (SKOV-3, IGROV, OVCAR-3, OVCAR-4, OVCAR-5 and OVCAR-8; Masciullo *et al.*, 2003) vs normal tissue. β -Actin gene expression was evaluated as control to normalize the amount of the used RNAs. (b) UbcH10 protein expression analysis by Western blot in the same human ovarian carcinoma cell lines. Blot against α -tubulin has been performed as control for equal protein loading. (c) RT-PCR analysis of UbcH10 expression in human ovarian tumor samples (thirty ovarian carcinoma samples were collected) vs their normal ovarian counterparts. β -Actin expression shows the same amount of RNAs used. NO, normal ovarian tissue. (d) Western blot analysis of UbcH10 protein expression in a panel of ovarian neoplasias. The level of α -tubulin has been used as loading control. NO, normal ovarian tissue. PCR reactions, primers and conditions to amplify UbcH10 and β -actin are as reported elsewhere (Pallante *et al.*, 2005). Protein extraction was performed according to standard procedure as reported by Pierantoni *et al.* (2005).

Figure 2 Immunostaining pattern of UbcH10 expression in ovarian cancer. In all different histotypes of ovarian carcinoma, there was a clear relationship between loss of tumor differentiation and the gain of UbcH10 reactivity. Whereas in differentiated histotypes, as in mucinous (original magnification, $25\times$) (a), serous (original magnification, $25\times$) (b), clear cell (original magnification, $25\times$) (c) and endometrioid (original magnification, $25\times$) (d) carcinomas, there was variability in the levels of UbcH10 expression, all cases of undifferentiated ovarian carcinomas (original magnification, $25\times$) (e) had levels of UbcH10 expression higher than the median value. No immunoreactivity occurred in normal ovarian tissue (original magnification, $25\times$) (f). UbcH10 immunoreactivity has been evaluated in two TMAs (constructed at the Department of Histopathology, S Chiara Hospital, Trento, Italy), as described (Aldovini *et al.*, 2006). TMAs included 60 carcinomas arising from the ovarian surface epithelium, each represented by three different 0.6 mm cores. Pathological data (tumor type, grade and stage), IHC profile (p53, RB245 and ER status) and clinical follow-up data (relapse-free and overall survival rates) were available for analysis. Tumors were typed according to the WHO criteria (Tavassoli and Devilee, 2003), including serous ($n=38$), mucinous ($n=1$), clear cell ($n=4$), endometrioid ($n=6$) and undifferentiated ($n=7$) carcinomas; four cases were excluded for technical reason. Staging was assessed in accordance with the International Federation of Gynecology and Obstetrics (FIGO) (Benedet *et al.*, 2000). Grading informations were derived from the original diagnostic reports. As the tumors composing the TMAs were diagnosed in different years, special care was taken to adopt the same grading system and to grade consistently all cases, by using the same criteria. Consequently, the same four-tier classification system (Vacher-Lavenu *et al.*, 1993), employed in the 1990s and used to diagnose the earlier cases included in the TMAs (with a longer follow-up) was consistently used also to score the cases more recently diagnosed. Thus, tumors were graded into well differentiated (G1), moderately well differentiated without nuclear atypia (G2), moderately well differentiated with nuclear atypia (G3) and poorly differentiated or undifferentiated (G4) (Vacher-Lavenu *et al.*, 1993). Further details on TMAs generation are reported elsewhere (Aldovini *et al.*, 2006). Complete follow-up data were available for all patients from the Departments of Gynecological Surgery and Medical Oncology of the S Chiara Hospital of Trento. Follow-up time was based on patient date of death or the last information in the medical records. As control carried out to assess UbcH10 expression in benign ovary, five samples of normal ovary were also processed. Special care was taken to evaluate UbcH10 expression only on adequately stained TMA slides. Immunostaining was processed by routine methods (Troncone *et al.*, 2003). UbcH10 expression was evaluated by two pathologists in a double-blind fashion and any discordance was resolved after consultation at the double-headed microscope. Values relative to each tumor sample, present in triplicate, were derived by combining the percentage of any single cores. To analyse tissue microarrays, we employed maximum, minimum and mean as pooling methods for the replicates (Liu *et al.*, 2004) and statistical analysis was carried out. We dichotomized biomarker expression against its median values, so as to ease biological interpretation. Finally, to account for the heterogeneity of protein expression across tumor tissues, cases with only one core section with valid staining were excluded by the statistical analysis. This resulted in 56 cases for ovarian data set. Statistical analysis was performed with R statistical package (R Development Core Team, 2004) and SPSS ver. 11.5 for Windows. (g) Correlation between ovarian tumor grade and UbcH10 expression. The correlation of UbcH10 expression vs tumor grade is well established as low levels of UbcH10 expression were recorded in the G1 well-differentiated tumors whereas there was a significant relationship between increasing cytological grading of malignancy and protein expression ($P=0.002$ Kruskal–Wallis test). Comparisons between UbcH10 expression and clinical–pathological data (histotype, grading, T, N), as well as with other biomarkers (p53, RB245, ER) were performed with Wilcoxon’s signed rank test or χ^2 or Kruskal–Wallis test on numerical expression data and with Fisher’s exact test on categorized data.

of the carcinoma cell lines showed a high UbcH10 expression, which was barely detectable in the normal tissue (Figure 1a and b).

The same analyses, performed on ovarian carcinoma tissues, showed a different expression in the different histotypes analysed. In fact, as shown in Figure 1c and d, UbcH10 is expressed at low levels in clear cell carcinomas, endometrioid carcinomas and serous cystadenocarcinomas, whereas the undifferentiated carcinomas express high level of UbcH10.

Immunohistochemistry essentially confirms the data obtained by RT-PCR and Western blot analyses. Whereas benign ovary lacked UbcH10 expression (Figure 2f), the different histotypes of ovarian carcinomas showed certain variability in the range of neoplastic cells expressing UbcH10 (Figure 2a–e). However, there was a clear relationship between the loss of tumor differentiation and the gain of UbcH10 reactivity. This was evident both when examining tumor type and tumor grade: the average levels of UbcH10 expression were low



in tumors belonging to the differentiated histotypes, as in serous (16.6% mean, range: 12.3–19.8%), clear cell (7.1% mean, range: 1.3–10.0%) and endometrioid (9.2% mean, range: 8.3–10.8%) carcinomas. Similarly the only case examined of the mucinous histotype showed a low level of expression (5%). On the contrary, higher levels (33.6% mean, range: 22.9–42.1%) of UbcH10 expression were observed in the undifferentiated histotype of ovarian cancer. All seven cases of undifferentiated ovarian carcinomas had levels of UbcH10 expression higher than the median value ($P=0.015$).

Similarly, UbcH10 expression was also related to the tumor grade, as significant differences were recorded among the different grades ($P=0.002$ Kruskal–Wallis test). In fact, as shown in Figure 2g, low levels of UbcH10 expression were recorded in the G1 well-differentiated tumors (0.8%), whereas there was a significant relationship between increasing cytological grading of malignancy and protein expression. In G2 and in G3 carcinomas, the cells expressing UbcH10 were, respectively, 12.3 and 22%, whereas G4 high-grade tumors showed staining in more than a third of neoplastic cells (34.7%). The correlation with tumor grade is further established if we compare G1 and G2 vs G3 and G4 grades and UbcH10 expression (P -value = 0.023 Fisher's exact test) (data not shown).

As far as the overall survival is concerned, there is a significant relationship with UbcH10 expression

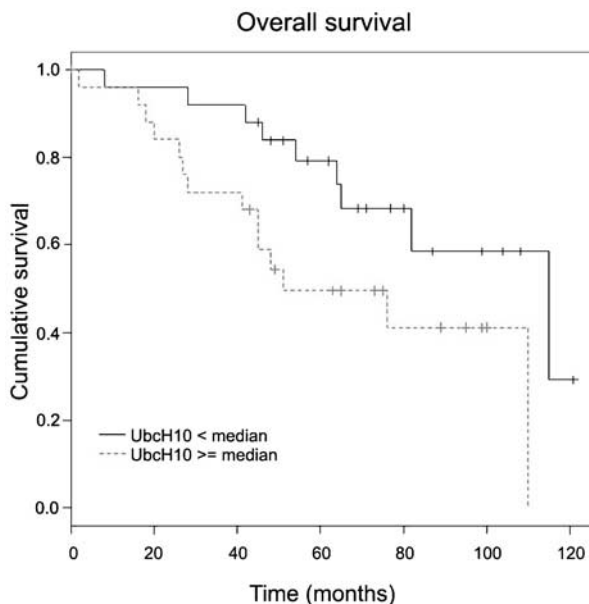


Figure 3 Kaplan–Meier survival analysis with log-rank test was carried out both for overall and relapse-free survival. Fifty-six patients were included in the survival analysis as clinical information was entirely available. The picture shows the results for overall survival analysis. The median age at surgery is 61 years (range 34–84) and the median follow-up time is 62 months (range 0–121 months). A P -value less than 0.05 was considered statistically significant for each analysis. Cases showing higher levels of UbcH10 expression ($> =$ median) were associated with a lower rate of overall survival.

(P -value = 0.044 – log-rank test), as shown in Figure 3, only if we consider the mean as pooling method. Regarding the other pooling methods, as well as for relapse-free survival, no statistical significant correlation was found.

We asked whether UbcH10 overexpression had a role in the process of ovarian carcinogenesis by evaluating the growth rate of one ovarian carcinoma cell line, in which the synthesis of UbcH10 protein was suppressed by RNA interference. The SKOV-3 cell line was treated with siRNA duplexes targeting to the UbcH10 mRNA. After transfection, we observed an efficient knock down of the UbcH10 protein levels at 48 h after treatment (Figure 4a). The cell growth analysis, in the presence or absence of the UbcH10 siRNA duplexes, revealed that the block of the UbcH10 protein synthesis significantly inhibits ovarian carcinoma cell growth. In fact, as shown in Figure 4b, a significant reduction in cell growth rate was observed in SKOV-3 cell line treated with UbcH10 siRNA in comparison with the untreated cells or those treated with the control scrambled siRNA.

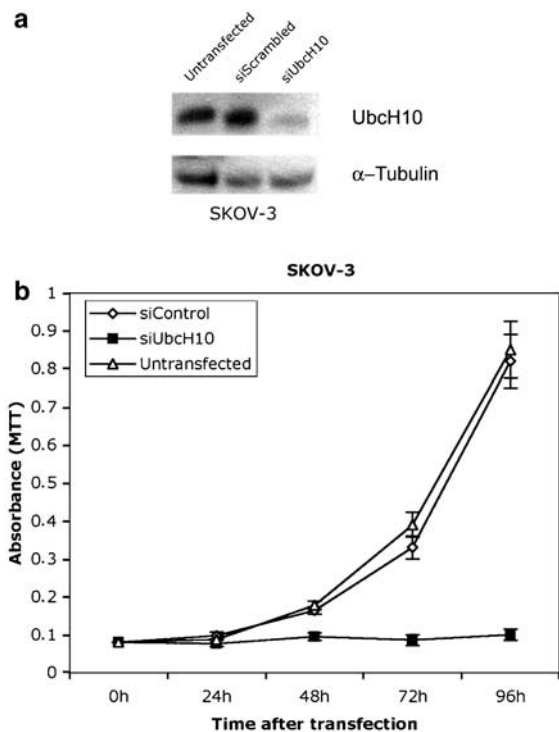


Figure 4 The block of UbcH10 protein synthesis by RNA interference inhibits the proliferation of ovarian carcinoma cells. (a) Inhibition of UbcH10 protein expression by RNAi in SKOV-3 cell line evaluated by Western blot analysis. At 48 h after siRNA transfection, total cell lysates were prepared and normalized for protein concentration. The expression of α -tubulin was used to control equal protein loading (30 μ g). (b) SKOV-3 cell line growth curve after siUbcH10 treatment. SKOV-3 cells were transfected with siUbcH10 duplexes (siUbcH10) and the relative number of viable cells was determined by MTT assay. Cells transfected with a scrambled duplex (siScrambled) and untransfected cells (Untransfected) were used as negative controls. Absorbance was read at 570 nm and the data are the mean of triplicates.

These results indicate a role of UbcH10 in neoplastic ovarian cell proliferation, for this reason we propose the UbcH10 expression as a possible tool to be used in the diagnosis and prognosis of ovarian carcinomas. Abundant expression of UbcH10 was detected in primary ovarian tumors compared with benign ovarian tissues and significantly correlated to tumor grade ($P=0.0008$) and undifferentiated histotype ($P=0.015$). These results are consistent with our previous published data (Pallante *et al.*, 2005) and further support the involvement of UbcH10 in the differentiation process of several human epithelial tissues (Wagner *et al.*, 2004).

UbcH10 is also a negative predictor of clinical outcome in our series, further suggesting its ability to confer a more aggressive phenotype to tumor cells. Studies are ongoing to assess this hypothesis on a larger series of patients with a longer follow-up.

Functional studies also demonstrate that the suppression of the UbcH10 expression by RNA interference reduced the growth of one ovarian carcinoma cell line

indicating a role of UbcH10 overexpression in ovarian carcinogenesis, in particular, in influencing the hyper-proliferative status of the most malignant cells.

In conclusion, all these data taken together suggest the possibility to use this gene as a marker for the diagnosis and prognosis of these neoplastic diseases.

Acknowledgements

This work was supported by grants from the Associazione Italiana Ricerca sul Cancro (AIRC), Progetto Strategico Oncologia Consiglio Nazionale delle Ricerche, the Ministero dell'Università e della Ricerca Scientifica e Tecnologica (MIUR), and 'Piani di Potenziamento della Rete Scientifica e Tecnologica' CLUSTER C-04, the Programma Italia-USA sulla Terapia dei Tumori coordinated by Professor Cesare Peschle and 'Ministero della Salute'. This work was supported from NOGEC-Naples Oncogenomic Center. We thank the Associazione Partenopea per le Ricerche Oncologiche (APRO) for its support.

References

- Aldovini D, Demichelis F, Doglioni C, Di Vizio D, Galligioni E, Brugnara S *et al.* (2006). M-CAM expression as marker of poor prognosis in epithelial ovarian cancer. *Int J Cancer* Jun 27 [Epub ahead of print].
- Benedet JL, Bender H, Jones III H, Ngan HY, Pecorelli S. (2000). FIGO staging classifications and clinical practice guidelines in the management of gynecologic cancers. FIGO Committee on Gynecologic Oncology. *Int J Gynaecol Obstet* **70**: 209–262.
- Feki A, Irminger-Finger I. (2004). Mutational spectrum of p53 mutations in primary breast and ovarian tumors. *Crit Rev Oncol Hematol* **52**: 103–116.
- Hershko A, Ciechanover A. (1998). The ubiquitin system. *Annu Rev Biochem* **67**: 425–479.
- Jemal A, Murray T, Ward E, Samuels A, Tiwari RC, Ghafoor A *et al.* (2005). Cancer statistics, 2005. *CA Cancer J Clin* **55**: 10–30.
- Joazeiro CA, Weissman AM. (2000). Ring finger proteins: mediators of ubiquitin ligase activity. *Cell* **102**: 549–552.
- Liu X, Minin V, Huang Y, Seligson DB, Horvath S. (2004). Statistical methods for analysing tissue microarray data. *J Biopharm Stat* **14**: 671–685.
- Masciullo V, Baldassarre G, Pentimalli F, Berlingieri MT, Boccia A, Chiappetta G *et al.* (2003). HMGA1 protein overexpression is a frequent feature of epithelial ovarian carcinomas. *Carcinogenesis* **24**: 1191–1198.
- Ozols RF, Bookman MA, Connolly DC, Daly MB, Godwin AK, Schilder RJ *et al.* (2004). Focus on epithelial ovarian cancer. *Cancer Cell* **5**: 19–24.
- Pallante P, Berlingieri MT, Troncone G, Kruhoffer M, Orntoft TF, Viglietto G *et al.* (2005). UbcH10 overexpression may represent a marker of anaplastic thyroid carcinomas. *Br J Cancer* **93**: 464–471.
- Pierantoni GM, Rinaldo C, Esposito F, Mottolese M, Soddu S, Fusco A. (2005). High Mobility Group A1 (HMGA1) proteins interact with p53 and inhibit its apoptotic activity. *Cell Death Differ* (9 December): 1–10 (Epub ahead of print).
- R Development Core Team (2004). *A Language and Environment for Statistical Computing*. R Foundation for Statistical Computing: Vienna, Austria.
- Tavassoli FA, Devilee P. (2003). *World Health Organization Classification of Tumours. Tumours of the breast and female genital organs*. IARC Press: Lyon.
- Troncone G, Iaccarino A, Caleo A, Bifano D, Pettinato G, Palombini L. (2003). p27 Kip1 protein expression in Hashimoto's thyroiditis. *J Clin Pathol* **56**: 587–591.
- Vacher-Lavenu MC, Le Tourneau A, Duvillard P, Godefroy N, Pinel MC. (1993). Pathological classification and grading of primary ovarian carcinoma: experience of the ARTAC ovarian study group. *Bull Cancer* **80**: 135–141.
- Wagner KW, Sapinoso LM, El-Rifai W, Frierson HF, Butz N, Mestan J *et al.* (2004). Overexpression, genomic amplification and therapeutic potential of inhibiting the UbcH10 ubiquitin conjugase in human carcinomas of diverse anatomic origin. *Oncogene* **23**: 6621–6629.
- Welsh PL, King MC. (2001). BRCA1 and BRCA2 and the genetics of breast and ovarian cancer. *Hum Mol Genet* **10**: 705–713.

Loss of the CBX7 gene correlates with a more malignant phenotype in thyroid cancer

Pierlorenzo Pallante^{1,2}, Maria Teresa Berlingieri¹, Giancarlo Troncone^{2,3}, Angelo Ferraro², Giovanna Maria Pierantoni¹, Mogens Kruhoffer⁴, Antonino Iaccarino³, Maria Russo³, Nicole Berger⁵, Vincenza Leone², Silvana Sacchetti², Lorenzo Chiariotti², Lucio Palombini³, Massimo Santoro^{1,2} and Alfredo Fusco^{1,2}

¹Dipartimento di Biologia e Patologia Cellulare e Molecolare c/o Istituto di Endocrinologia ed Oncologia Sperimentale del CNR, Facoltà di Medicina e Chirurgia di Napoli, Università degli Studi di Napoli “Federico II”, via Pansini 5, 80131 Naples, Italy.

²NOGEC (Naples Oncogenomic Center)-CEINGE, Biotecnologie Avanzate-Napoli, & SEMM - European School of Molecular Medicine - Naples Site, via Comunale Margherita, 482, 80145 Naples, Italy.

³Dipartimento di Anatomia Patologica e Citopatologia, Facoltà di Medicina e Chirurgia di Napoli, Università di Napoli “Federico II”, via Pansini 5, 80131 Naples, Italy.

⁴Department of Clinical Biochemistry, Aarhus University Hospital, Skejby DK 8200 Aarhus N, Denmark.

⁵Service d'Anatomo-Pathologie, Centre Hospitalier Lyon Sud, Pierre Bénite, France.

Running title: CBX7 in thyroid carcinomas.

Key words: CBX7, thyroid, carcinomas, immunohistochemistry, LOH.

Corresponding author: Alfredo Fusco, Dipartimento di Biologia e Patologia Cellulare e Molecolare, Università di Napoli Federico II and Naples Oncogenomic Center (NOGEC)-CEINGE-Biotecnologie Avanzate, Napoli, & European School of Molecular Medicine (SEMM), via Pansini 5, 80131 Napoli, Italy. Tel: 39-081-3722857 or 7463749; Fax: 39-081-3722808. E mail: afusco@napoli.com or alfusco@unina.it

ABSTRACT

Using gene expression profiling we found that the CBX7 gene was drastically down-regulated in six thyroid carcinoma cell lines versus control cells. This suggested that CBX7 is an oncosuppressor. The aim of this study was to determine whether CBX7 is related to thyroid cancer phenotype, and to try to identify new tools for the diagnosis and prognosis of thyroid cancer. We thus evaluated CBX7 expression in various snap-frozen and paraffin-embedded thyroid carcinoma tissues of different degrees of malignancy by quantitative RT-PCR and immunohistochemistry, respectively. CBX7 expression progressively decreased with malignancy grade and neoplasia stage. Indeed, it decreased in an increasing percentage of cases going from benign adenomas to papillary (PTC), follicular and anaplastic (ATC) thyroid carcinomas. This finding coincides with results obtained in rat and mouse models of thyroid carcinogenesis. CBX7 loss of heterozygosity occurred in 36.8% of PTC and in 68.7% of ATC. Restoration of CBX7 expression in thyroid cancer cells reduced growth rate, which indicates that CBX7 plays a critical role in the regulation of transformed thyroid cell proliferation. In conclusion, loss of CBX7 expression correlates with a highly malignant phenotype in thyroid cancer patients. Consequently, CBX7 monitoring could contribute to thyroid cancer diagnosis and prognosis.

INTRODUCTION

Human tumorigenesis is a multistep process in which the alterations that confer a transformed and malignant phenotype to the normal cells of a tissue reflect several genetic alterations (1). Thyroid tumors originating from follicular cells are a good model with which to investigate the events involved in carcinogenesis because they differ in malignant potential from differentiated to undifferentiated phenotypes (1, 2). Papillary thyroid carcinoma (PTC), which is differentiated and has a good prognosis, is the most frequent malignancy of the thyroid gland (2). The tall cell variant (TCV) of PTC has a worse prognosis than conventional PTC (3). Insular carcinomas have a less differentiated phenotype and a poor 5-year survival rate (2). Finally, anaplastic carcinomas (ATC) are completely undifferentiated, very aggressive and always fatal (2).

Point mutations, rearrangements that activate proto-oncogenes, and loss-of-function in tumor suppressor genes have been identified in thyroid tumors (2). In PTC, activation of the RET/PTC oncogene, caused by rearrangements of the RET proto-oncogene, occurs in about 30% of cases (2), whereas the B-RAF gene is mutated in about 40% of cases (4). These tumors have also been associated with TRK gene rearrangements (5) and MET gene overexpression (6). RAS gene mutations (7) and PAX8-PPAR- γ rearrangements (8) are frequent in follicular thyroid carcinomas (FTC), whereas impaired function of the p53 tumor suppressor gene is typical of ATC (9-11). Other genes, including CBX7, have been implicated in thyroid neoplasias.

Within the context of a microarray study, we found that the CBX7 gene was down-regulated in thyroid carcinoma-derived cell lines and thyroid fresh tumors. CBX7, which

is located on chromosome 22q13.1, encodes a novel Polycomb protein (Pc) of 28.4 kDa of 251 amino acids that contains a “chromodomain” between amino acids 10 and 46. The chromodomain was originally defined as a 37-amino-acid region of homology shared by heterochromatin protein 1 (HP1) and Pc proteins from *Drosophila melanogaster* (12, 13). The CBX7 protein appears to be involved in the control of normal cell growth (13, 14). Moreover, mouse CBX7 associates with facultative heterochromatin and with the inactive X chromosome, which indicates that CBX7 is involved in the repression of gene transcription (15).

Thyroid cancer is the most prevalent endocrine neoplasia. About 20,000 new cases are diagnosed in the United States each year, and more than 1,500 patients die of thyroid cancer annually. Given the poor prognosis associated with the less differentiated histologic types, namely TCV PTC and Hurthle variants, and the undifferentiated ATC, there is a need for molecular markers that can help to predict prognosis, so that patients with a dismal prognosis can be offered different, perhaps, innovative therapy.

In an attempt to determine whether CBX7 is related to thyroid cancer phenotype, and to find new tools for the diagnosis and prognosis of thyroid cancer, we have evaluated its expression in a large number of thyroid carcinoma tissues, and in rat and mouse models of thyroid carcinogenesis.

RESULTS

CBX7 gene expression is down-regulated in human thyroid carcinoma cell lines. In a first step, we looked for genes potentially involved in the neoplastic transformation of the thyroid gland. To this aim, we extracted RNAs from normal human thyroid primary cells and six human thyroid carcinoma cell lines (the follicular carcinoma WRO cell line, the PTC TPC-1 and FB-2 cell lines, the NPA cell line that originates from a poorly differentiated PTC, and the ATC ARO and FRO cell lines) and hybridized them to U95Av2 Affymetrix oligonucleotide arrays (Affymetrix, Santa Clara, CA) containing 12.625 transcripts (16). We looked for genes whose expression was drastically (at least 10 fold) up- or down-regulated in all the six thyroid carcinoma cell lines versus normal thyroid primary cell culture, on the assumption that genes whose expression was altered in all carcinoma cell lines could be involved in thyroid cell transformation. Thus, genes that were decreased in all the carcinoma cell lines were considered candidate tumor suppressor genes. Among the down-regulated genes, CBX7 was the only gene drastically down-regulated in all the cell lines tested with the cDNA microarray (Figure 1A). This result was confirmed by RT-PCR analysis in a large panel of thyroid carcinoma cell lines with normal thyroid primary culture cells as control (Figure 1B).

The loss of CBX7 expression correlates with a more aggressive phenotype of thyroid carcinomas. To determine whether the loss of CBX7 expression is a feature of thyroid tumors and not only of cultured thyroid carcinoma cell lines, we carried out an immunohistochemical analysis of paraffin-embedded tissues using polyclonal antibodies

raised against the carboxy-terminal region of human CBX7 protein (see Methods). As shown in Table 1, all 20 samples of normal thyroid parenchyma expressed CBX7 at a very high level, which coincides with the strong CBX7 staining in all follicles (Figure 2A). The intensity of nuclear labeling of epithelial thyroid cells in FA was similar to that of the internal control stromal and endothelial cells (Figure 2B). Conversely, CBX7 expression was reduced in malignant lesions. As shown in Table 1, and in Figure 2C and D, the percent of low expressors was high in well-differentiated tumors, namely FTC (66%; 21/32 samples) and PTC (57%; 17/30 samples). It was even higher in the less differentiated tumors, namely poorly differentiated carcinomas (83%; 10/12) (Table 1, and Figure 2F and G) and TCV PTC (5/6; 83%) (Table 1, and Figure 2E). In the latter, neoplastic cells were almost devoid of CBX7 expression, which sharply contrasted with the intense staining of the infiltrating lymphocytes and stromal cells. Similarly, CBX7 expression was completely lost in all cases of anaplastic carcinoma (12/12) (Table 1, Figure 2H). No staining was observed when normal thyroid gland samples were stained with antibodies pre-incubated with CBX7 recombinant protein (Figure 2I) or in the absence of the primary antibodies (data not shown). Therefore, CBX7 was expressed in normal thyroid and in benign neoplastic lesions, decreased in well-differentiated carcinomas and was drastically reduced in aggressive thyroid tumors.

Analysis of CBX7 expression in normal and neoplastic thyroid tissues by semiquantitative RT-PCR and quantitative Real-Time PCR. We also evaluated CBX7 expression by semiquantitative RT-PCR in a panel of matched normal/tumor tissues. The results confirmed the immunohistochemical data. In fact, there was an amplified band

corresponding to CBX7 in normal thyroid tissues (Figure 3A). The amplified band decreased in PTC samples and almost disappeared in ATC. qRT-PCR analysis of a large number of human thyroid carcinoma samples of different histotypes confirmed a correlation between the reduction of CBX7 expression and a more malignant phenotype of thyroid neoplasias. In fact, as reported in Figure 3B, there was a negative fold change in CBX7 expression from -2.1 to -13 (average, -4.8) in the PTC samples versus normal counterpart tissue. The reduction was even more pronounced in the anaplastic carcinoma samples, with a fold change ranging from -10.8 to -24.5 (average, -14.6). These data are well correlated with the immunohistochemical data, and suggest that CBX7 expression is controlled at transcriptional level.

Analysis of human thyroid fine-needle aspiration biopsy. Fine-needle aspiration biopsy has become an integral part of the preoperative evaluation of thyroid nodules. To evaluate whether CBX7 gene expression analysis can be applied to FNAB samples, we studied 15 cases of thyroid papillary carcinoma by immunohistochemistry and qRT-PCR. In 8 cases out of 15, CBX7 expression was lower in FNABs from patients affected by a carcinoma than in FNABs from thyroid goiter as evaluated by immunohistochemistry (Figure 4A) and qRT-PCR (Figure 4B).

LOH at CBX7 locus (22q13.1). In some types of cancers, LOH of tumor suppressor genes at region 22q is believed to be a key step in carcinogenesis (17-19). We there used several SNP markers to evaluate LOH on chromosome 22q13.1, at the CBX7 locus in 60 cases of thyroid carcinomas of different histotypes. As shown in Table 2, LOH at CBX7 locus occurred in 36.8% of the informative PTC (7 out of 19 cases), whereas in 68.7%

(11/16 cases) of informative ATC. The percentage of LOH was much higher in the TCV variant of PTC (3/4 cases; 75%) than in classical PTC (7/19 cases; 36.8%). Again, LOH of CBX7 was well correlated with tumor phenotype, TCV being more aggressive than classical PTC (3). We next looked for CBX7 gene mutations in human thyroid carcinoma samples. We analyzed 20 PTC samples and 6 ATC samples and found no mutations (data not shown).

Methylation status of the CBX7 gene. To investigate the mechanisms underlying CBX7 downregulation in thyroid tumors, we evaluated DNA methylation of the CBX7 gene in normal and tumor tissues. An analysis of CBX7, carried out with the CpG plot program (see Methods), revealed two CpG islands. The first extended about 1000 nucleotides around the transcription initiation site and the second was located at the distal part of intron 2 (Figure 5). We analyzed the putative promoter region (between -83 and +154) of genomic DNA extracted from five PTC and corresponding adjacent normal tissues, from 5 ATC, and from the thyroid papillary carcinoma cell line TPC-1 (Figure 5, upper panel). We found no methylation in any of the 42 CpGs present in this region (data not shown). By contrast, methylation of the last part of this CpG island (from +187 to +502, Figure 5, upper panel), which contains 21 CpGs, was much higher in ATC than in PTC and normal tissues (Figure 5, lower panel). No significant methylation was found in the second CpG island.

CBX7 expression in rat thyroid cells transformed by viral oncogenes. The infection of two rat thyroid differentiated cell lines, PC Cl 3 (20) and FRTL-5 (21), with several

murine retroviruses induces different effects on the differentiated and transformed phenotype (22-24). PC MPSV and PC PyMLV cells are dedifferentiated and tumorigenic, whereas PC *v-raf*, PC KiMSV and PC E1A cells are dedifferentiated but not tumorigenic when injected into nude mice. PC E1A cells are transformed to an irrefutable neoplastic phenotype after introducing a second oncogene such as the polyoma middle-T antigen or *v-raf* genes (23). Conversely, FRTL-5 cells become tumorigenic after infection with the Kirsten murina sarcoma virus carrying the *v-ras-Ki* oncogene (25). We evaluated CBX7 expression in these cell lines. As shown in Figure 6A, the gene was abundantly expressed in normal thyroid cells and in all cells that did not show the malignant phenotype, whereas its expression was abolished in the malignantly transformed cells FRTL-5 KiMSV and PC MPSV, and in PC E1A cells infected with a virus carrying the *v-raf* oncogene. Interestingly, CBX7 expression was retained in FRTL-5 KiMSV-HMGA1 and in PC MPSV-HMGA2, cells previously transfected with a vector carrying respectively HMGA1 and HMGA2 gene in an antisense orientation, able to prevent the malignant transformation of FRTL-5 and PC Cl 3 cells (26, 27), and then with the relative oncogene. In fact, although these cells undergo morphological changes and lose the thyroid differentiation markers, they are unable to grow in soft agar and to induce tumors after injection into athymic mice (26, 27). In conclusion, also the analysis of rat thyroid cells transformed *in vitro* confirms that the loss of CBX7 expression is associated with the expression of a highly malignant phenotype.

CBX7 expression in experimental mouse models of thyroid carcinogenesis. We used qRT-PCR analysis to evaluate CBX7 expression in thyroid neoplasias in transgenic

animal lines expressing TRK (Tg-TRK) (28), RET/PTC3 (Tg-RET/PTC3) (29), N-ras (Tg-N-ras) (30) and large T SV40 (Tg-SV40) (31) oncogenes under the transcriptional control of the thyroglobulin promoter. Transgenic mice carrying TRK and RET/PTC3 oncogenes develop PTC (28, 29), whereas N-ras mice develop thyroid follicular neoplasms that undergo de-differentiation, predominantly FTC (30). ATC were obtained from Tg-SV40 mice (31). As shown in Figure 6B, CBX7 expression was much lower in ATC from large T SV40 transgenic mice compared with mouse normal thyroid tissue. CBX7 mRNA expression was significantly, albeit not greatly, reduced in PTC from TRK and RET/PTC3 mice. CBX7 expression was also reduced in the FTC from N-ras mice. In summary, the analysis of the experimental models of thyroid carcinogenesis confirms that the loss of CBX7 expression is related to the undifferentiated histotype.

Restoration of CBX7 gene expression inhibits the growth of thyroid carcinoma cell lines.

To determine whether loss of CBX7 gene expression affects thyroid carcinogenesis, we evaluated the growth rate of thyroid carcinoma cell lines in which CBX7 expression had been restored. To this aim we carried out a colony forming assay with cell lines obtained from human thyroid carcinomas (NPA, TPC-1 and FB-2) after transfection with the vector carrying the CBX7 gene or the empty backbone vector. The colonies were scored after two weeks. As shown in Figure 7, cells transfected with the CBX7 gene generated a lower number of colonies than did cells transfected with the backbone vector: for the NPA cells the inhibition was about 48% (representative experiment: empty vector, 296 colonies; CBX7, 154 colonies) while for FB-2 and TPC-1 cells the inhibition was even much higher.

Generation of an adenovirus carrying the CBX7 gene. We generated a replication-defective adenovirus carrying the CBX7 gene in the sense (Ad-CBX7) orientation. We then infected thyroid carcinoma cell lines with the Ad-CBX7 virus, and measured protein levels in cell lysates collected at different time points after adenovirus infection. No CBX7 protein was detected in carcinoma cells infected with the control virus (Ad-GFP). We then constructed growth curves of cells infected with Ad-CBX7 and control adenovirus (Ad-GFP). As shown in Figure 8, cell growth rate was significantly lower in ARO and NPA cell lines infected with Ad-CBX7 than in the same cells infected with the control virus. The percentage of growth inhibition five days after infection was 38.5% in ARO cells and 54% in NPA cells.

DISCUSSION

The results of this study show that CBX7 is abundantly expressed in normal thyroid gland, but is drastically down-regulated or absent in all the thyroid carcinoma cell lines. Interestingly, CBX7 expression decreased with malignancy grade and neoplasia stage. In fact, CBX7 expression was comparable to normal thyroid tissue in FA, which is benign, slightly reduced in PTC displaying the classical histotype, and drastically reduced, and in most cases absent, in FTC, in the TCV of PTC, in poorly differentiated carcinomas and in ATC. Based on these findings, it is feasible that CBX7 levels could serve to differentiate between benign and malignant thyroid neoplasms. Indeed, in clinical practice, it is difficult to distinguish between FTC and the benign FA (32, 33). In the perspective of diagnosis/prognosis, CBX7 expression level in FNAB may be used to identify PTC by immunohistochemistry and by qRT-PCR. Interestingly, a recent paper concerning the cytogenetics of Chernobyl thyroid tumors identified a correlation between the deletion of the chromosomal region 22q13.1, where the CBX7 gene is located, and a worse prognosis (34).

Our finding of a decrease in CBX7 levels in relation to malignancy was supported by our model of rat thyroid cells transformed by several oncogenes and in transgenic mice carrying thyroglobulin promoter-driven oncogenes. CBX7 expression was absent from thyroid cells that show a highly malignant phenotype and in ATC that develop in large T SV40 transgenic mice. Differently, CBX7 expression was retained, albeit at a low level, in transformed rat thyroid cells that are not yet tumorigenic and in PTC developing in RET/PTC and TRK mice. Therefore, our data indicate that loss of CBX7 expression

correlates with a more aggressive phenotype of thyroid carcinomas and perhaps with a worst prognosis. This result is consistent with our preliminary finding of a correlation between low CBX7 expression and reduced survival in colon carcinoma (Pallante and Terracciano, manuscript in preparation). Moreover, the association between lack of CBX7 expression and a more aggressive histotype seems to apply also to breast, ovary and prostate carcinomas (Pallante and Troncone, manuscript in preparation).

In an attempt to unravel the mechanism underlying loss of CBX7 gene expression in malignant thyroid neoplasias, we analyzed LOH at the CBX7 locus (22q13.1). We detected LOH in 36.8% and 68.7% of the PTC and ATC, respectively. However, no mutations were found in thyroid carcinomas. Conversely, there was a hypermethylation status in ATC, which are practically devoid of CBX7 expression. Therefore, we suggest that gene methylation, associated in most cases with LOH, might account for the block of CBX7 expression in ATC, whereas the decreased expression in PTC may be due to an allelic loss plus other epigenetic mechanism.

The biological characteristics of the CBX7 protein suggests that it acts as a tumor suppressor. In fact, like other Pc proteins that exert their effects through transcriptional repression, CBX7 is involved in the mechanism of transcriptional repression. Moreover, the expression of a fusion protein between CBX7 and the DNA-binding domain of Gal4 (Gal4/CBX7) caused a dose-response repression of the reporter gene versus the control (13). These studies suggest that the CBX7 protein could be involved in maintaining the transcriptionally repressive state of genes by modifying chromatin and rendering it heritably changed in its expressibility. To determine whether CBX7 plays an important role in thyroid carcinogenesis, we restored the CBX7 function in human thyroid cancer

cell lines and examined cell growth rate. CBX7 expression clearly reduced cell growth rate, which indicates that the gene plays a critical role in thyroid carcinogenesis. One may speculate that restoration of CBX7 function by adenovirus-mediated delivery could be applied in the most highly aggressive thyroid tumors.

In conclusion, our data suggest that low CBX7 gene expression is associated with a malignant phenotype of thyroid neoplasias, and that loss of CBX7 could play a critical role in thyroid cancer progression.

METHODS

Cell Culture and Transfections. We used the following human thyroid carcinoma cell lines in this study: TPC-1, WRO, NPA, ARO, FRO, NIM 1, B-CPAP, FB-1, FB-2, Kat-4 and Kat-18, which are described elsewhere (16). They were grown in DMEM (Gibco Laboratories, Carlsbad, CA) containing 10% fetal calf serum (Gibco Laboratories), glutamine (Gibco Laboratories) and ampicillin/streptomycin (Gibco Laboratories) in a 5% CO₂ atmosphere. Normal human thyroid primary culture cells have been established and grown as already described (35). PC Cl 3 (20) and FRTL-5 (21) cell lines were cultured in modified F12 medium supplemented with 5% calf serum (Gibco Laboratories) and six growth factors (thyrotropic hormone, hydrocortisone, insulin, transferrin, somatostatin and glycyl-histidyl-lysine) (Sigma, St. Louis, MO). PC CL 3 and FRTL-5 infected with several oncogenes PC KiMSV, PC HaMSV, PC *v-raf*, PC MPSV (20), PC PyMLV (22), PC E1A, PC E1A+*v-raf* (23), PC RET/PTC, PC HaMSV+RET/PTC1 (24), PC MPSV-HMGA2 (27), FRTL-5 KiMSV (25), FRTL-5 KiMSV-HMGA1 (26) cells were cultured in the same medium as PC CL 3 and FRTL-5 cells but without the six growth factors. Thyroid cells were transfected using Lipofectamine reagent (Invitrogen, Carlsbad, CA) according to the manufacturer's instructions. The transfected cells were selected in a medium containing geneticin (G418) (Life Technologies, Milan, Italy). For each transfection, several G418 resistant clones and the mass cell population were isolated and expanded for further analysis.

Human Thyroid Tissue Samples. Neoplastic human thyroid tissues and normal adjacent tissue or the contralateral normal thyroid lobe were obtained from surgical specimens and immediately frozen in liquid nitrogen. Thyroid tumors were collected at the Service d'Anatomo-Pathologie, Centre Hospitalier Lyon Sud, Pierre Bénite, France. The tumor samples were stored frozen until required for RNA or protein extraction.

RNA Isolation. Total RNA was extracted from tissues and cell cultures using the RNAeasy Mini Kit (Qiagen, Valencia, CA) according to the manufacturer's instructions. The integrity of the RNA was assessed by denaturing agarose gel electrophoresis.

Reverse Transcriptase and PCR Analysis

Reverse Transcription. 1 µg of total RNA from each sample was reverse-transcribed with QuantiTect[®] Reverse Transcription Kit (Qiagen) using an optimized blend of oligo-dT and random primers according to the manufacturer's instructions.

Semiquantitative RT-PCR. PCR was carried out on cDNA using the GeneAmp PCR System 9600 (Applied Biosystems, Foster City, CA). The RNA PCR Core Kit (Applied Biosystems) was used to perform amplifications. After a first denaturing step (94°C for 3 min), PCR amplification was performed for 25 cycles (94°C for 30 s, 60°C for 30 s, 72°C for 30 s).

The primers used are:

Human CBX7 forward 5'-CATGGAGCTGTCAGCCATC-3'

Human CBX7 reverse 5'-CTGTACTTTGGGGGCCATC-3'

Human β-actin forward 5'-TCGTGCGTGACATTAAGGAG-3'

Human β -actin reverse 5'-GTCAGGCAGCTCGTAGCTCT-3'

Rat CBX7 forward 5'-GTCATGGCCTACGAGGAGAA-3',

Rat CBX7 reverse 5'-CTTGGGTTTCGGACCTCTCT-3';

Rat GAPDH forward 5'-TGATTCTACCCACGGCAAGTT-3'

Rat GAPDH reverse 5'-TGATGGGTTTCCCATTGATGA-3'

To ensure that RNA samples were not contaminated with DNA, negative controls were obtained by carrying out the PCR on samples that were not reverse-transcribed, but otherwise identically processed. The PCR products were separated on a 2% agarose gel, stained with ethidium bromide and scanned with a Typhoon 9200 scanner (GE Healthcare, Piscataway, NJ).

Selection of primers and probes for qRT-PCR. To design a qRT-PCR assay we used the Human ProbeLibrary™ system (Exiqon, Vedbaek, Denmark). Briefly, using locked nucleic acid (LNA™) technology (36, 37), Exiqon provides 90 human prevalidated TaqMan probes of only 8-9 nucleotides that recognize 99% of human transcripts in the RefSeq database at NCBI (38, 39). Using the ProbeFinder assay design software (freely accessed on the web site www.probelibrary.com) we chose the best probe and primers pair. To amplify a fragment for Real-Time PCR of CBX7 mRNA, we entered its accession number (NM_175709.2) on the assay design page of the ProbeFinder software and we chose an amplicon of 71 nucleotides that spanned the 3rd and 4th exons. The probe number was “human 63” (according to the numbering of Exiqon’s Human ProbeLibrary kit) and the primer sequences were: CBX7 forward 5'-CGTCATGGCCTACGAGGA-3'; CBX7 reverse 5'-TGGGTTTCGGACCTCTCTT-3'.

The same procedure was used to choose the probe and primers for the housekeeping gene G6PD (accession number X03674). We opted for an amplicon of 106 nucleotides that spanned the 3rd and 4th exons. The probe number was “human 05” (according to the numbering of Exiqon’s Human ProbeLibry kit) and the primer sequences were: G6PD forward 5’-ACAGAGTGAGCCCTTCTTCAA-3’; G6PD reverse 5’-GGAGGCTGCATCATCGTACT-3’. All fluorogenic probes were dual-labeled with FAM at 5’-end and with a black quencher at the 3’-end.

qRT-PCR. Real-Time Quantitative TaqMan PCR was carried out with the Chromo4 Detector (MJ Research, Waltham, MA) in 96-well plates using a final volume of 20 μ l. For PCR we used 8 μ l of 2.5x RealMasterMixTM Probe ROX (Eppendorf AG, Hamburg, Germany) 200 nM of each primer, 100 nM probe and cDNA generated from 50 ng of total RNA. The conditions used for PCR were 2 min at 95°C and then 45 cycles of 20 sec at 95°C and 1 min a 60°C. Each reaction was carried out in duplicate. We used the $2^{-\Delta\Delta CT}$ method to calculate relative expression levels (40).

We also carried out qRT-PCR reactions with mouse cDNA in a final volume of 20 μ l using 10 μ l of 2x Power SYBR Green PCR Master Mix (Applied Biosystems), 200 nM of each primer and cDNA generated from 50 ng of total RNA. The conditions used for PCR were 10 min at 95°C and then 45 cycles of 30 sec at 95°C and 1 min a 60°C. Each reaction was carried out in duplicate, and at the end of the PCR run, a dissociation curve was constructed using a ramping temperature of 0.2°C per sec from 65°C to 95°C. A single melting point was obtained for CBX7 and β -actin amplicons (data not shown). The mouse β -actin gene served as control. We used the following primers: mouse CBX7

forward 5'-AATGGCATGGCTAAGGATGG-3' and mouse CBX7 reverse 5'-ACATAGGTTCGTATGGTAGCA-3'; mouse β -actin forward 5'-TCAGAAGGACTCCTATGTGG-3' and mouse β -actin reverse 5'-CGCAGCTCATTGTAGAAGGT-3'.

Protein Extraction, Western Blotting and Antibodies. Protein extraction and western blotting procedure were carried out as reported elsewhere (16). Membranes were incubated with a primary antibody raised against the C-terminus of the human CBX7 protein (Neosystem, Strasbourg, France) for 60 min (at room temperature). To ascertain that equal amounts of protein were loaded, the western blots were incubated with antibodies against the γ -tubulin protein (Sigma). Membranes were then incubated with the horseradish peroxidase-conjugated secondary antibody (1:3000) for 60 min (at room temperature) and the reaction was detected with a western blotting detection system (ECL) (GE Healthcare).

Immunostaining: Technique. The cell distribution of the CBX7 protein was assessed by immunostaining formalin-fixed, paraffin-embedded thyroid tumor blocks retrieved from the files of the Dipartimento di Scienze Biomorfologiche e Funzionali at the University of Naples Federico II and selected to represent a wide range of thyroid neoplastic diseases. Briefly, xylene-dewaxed and alcohol-rehydrated paraffin sections were placed in Coplin jars filled with a 0.01 M tri-sodium citrate solution, and heated for 3 min in a conventional pressure cooker (16). After heating, slides were thoroughly rinsed in cool running water for 5 min. They were washed in Tris-buffered saline pH 7.4 and then incubated overnight with the specific rabbit polyclonal primary antibody. Subsequently,

tissue sections were stained with biotinylated anti-rabbit immunoglobulins, and then with peroxidase-labelled streptavidine (Dako, Carpinteria, CA). The signal was developed by using diaminobenzidine chromogen as substrate. Incubations both omitting and pre-adsorbing the specific antibody, were used as negative controls.

Immunohistochemistry: Evaluation. To ensure that we evaluated CBX7 expression only on technically adequate slides, we discarded slides that lacked a convincing internal control, namely labeling of stromal, endothelial or lymphoid cell, shown to be positive in a preliminary normal tissue micro-array analysis (data not shown). Based on these criteria, we scored paraffin-embedded stained slides from 20 cases of FA, 30 cases of classical PTC, 6 cases of TCV PTC, 32 cases of FTC, 12 cases of poorly differentiated carcinoma, and 12 cases of ATC. As controls, we selected areas of normal thyroid parenchyma from the lobe contralateral to the tumor in 20 surgical specimens of PTC. Individual cells were scored for the expression of CBX7 by quantitative analysis performed with a computerized analyzer system (Ibas 2000, Kontron, Zeiss), as described previously (16), and tumors were subdivided in low-expressors (less than 50% of positive cells) and in high-expressors (more than 50% of positive cells).

Thyroid Fine-Needle Aspiration Biopsies (FNAB). The FNAB were carried out at the Dipartimento di Anatomia Patologica e Citopatologia (University of Naples Federico II) as described elsewhere (41, 42). Samples were obtained from 15 patients with thyroid neoplasias who subsequently underwent surgery because the FNAB cytology indicated a diagnosis of cancer. Normal thyroid cells, used as controls, were obtained from FNAB of

thyroids carrying non-neoplastic nodules. FNAB samples were washed twice with 1x PBS and then processed for RNA extraction using the procedure detailed in a previous section.

Loss-of-heterozygosity (LOH) analysis. We used several SNP markers to evaluate LOH at the CBX7 locus on chromosome 22q13.1. We selected the SNP markers (<http://www.ncbi.nih.gov/SNP/>) that showed high average heterozygosity levels in order to obtain the highest number of informative cases. Briefly, genomic DNA was PCR-amplified in a region spanning about 200 bp around the SNP analyzed, then the purified PCR product was sequenced. We measured the height of the two peaks on the chromatogram and calculated the ratio of the two alleles in the matched tumor/normal samples: LOH was defined if the ratio in the carcinoma sample was less than 50%. SNPs and relative primers used to amplify them are as follows:

rs710190 (LOH1-L 5'-TGAATCCACAGACCCACAGA-3', LOH1-R 5'-GGTTCAGAGGGGACTCTTCC-3'); *rs5750753* (LOH2-L 5'-GACAGCCAAGGAAAGACAGG-3', LOH2-R 5'-GTGTGATGGGCAGGCTTT-3');
rs713841 (LOH3-L 5'-CCAGACGTCTCAAAGCCTGT-3', LOH3-R 5'-CAGCACAAAAGACCTCACCA-3'); *rs2076476* (LOH4-L 5'-ACAGGGCATCTTTGTGAAGC-3', LOH4-R 5'-GTGAAAATGGTGGGCACTG-3');
rs2281258 (LOH5-L 5'-AGAACCATTACAAGTGGGG-3', LOH5-R 5'-TCTGGAAAGCACAGCAAATG-3'); *rs2235686* (LOH6-L 5'-TGGCCTCAGCATGTTAAGAA-3', LOH6-R 5'-GTTCCCTCCCCCACTTTGAT-3');
rs714016 (LOH7-L 5'-TGGCTGCACTGTAAGGACAC-3', LOH7-R 5'-CTTCTGGGGGTCAGGAATTT-3'); *rs139390* (LOH8-L 5'-

CACCTGCCCTGTAGGCTTAG-3', LOH8-R 5'-GCAGGATATTGGAAGCCAGA-3');
rs139393 (LOH9-L 5'-CCTTCACCCTGTCCTGGTAA-3', LOH9-R 5'-
TTCATCCTCTCTTGCCTGGT-3').

Methylation analysis using bisulphite genomic sequencing. The promoter region and the entire coding sequence of the human CBX7 gene were analyzed for CG content; CpG islands were determined based on a 200-bp length of DNA with a CG content of >50% and a CpG/GpC ratio of >0.5, using the CpGplot program, available at <http://www.ebi.ac.uk/emboss/cpgplot/>. Bisulphite genomic sequencing was used to analyze the methylation patterns of individual DNA molecules. Sodium bisulphite conversion of genomic DNA (about 200 ng for each conversion) was obtained using the EZ DNA Methylation Kit™ (Zymo Research, Orange, CA) following the manufacturer's instructions. The CpG islands identified were then PCR-amplified using the following primers:

1F: -440 -407 5'-TTC/GGGTTTTTGGTAGTTATTGGGAGGTTATGAGG-3'

1Fn: -114 -84 5'-AGGAAAAC/GGTTGC/GGTAGGTTTAAAAATGGAA-3'

1R: +211+178 5'- AAAACG/AAAAAAAAACCCCACTAAAATCCTAAAAAC -3'

1Rn: +186 +155 5'-CCTAAAAACCG/ACCCCG/AAACAACCTCACCTTC-3'

2F:+155 +186 5'-GAAGGTGAGGTTGTTC/GGGGGGC/GGGTTTTTAGG-3'

2R:+593 +560 5'- CCG/AAAAAAAACTTTTCCAAAACCTCACTTACAAC-3'

2Rn:+535 +503 5'- CCAAATCCCG/AAATTCAAACCCAACTCTAACC-3'

3Fn:+7005 +7031 5'-GGTGTGGGAAGGGTGTTTTGGGATTTG-3'

3R: +7259 +7230 5'-CACCAACATCTTAATTATTTAAACCCAACC-3'

3Rn: +7196 +7170 5'-CCCTCCG/ACAATACAAAAACCCA AAAAC-3'

PCR reactions were carried out using FastStart Taq DNA polymerase (Roche, Basel, Switzerland) under the following conditions: 1) Pre-nested PCRs were normally carried out on 10 ng of bisulphite-treated DNA in a final reaction volume of 50 μ l, using standard conditions with 5 min at 95°C, 2 min at 70°C, followed by 5 cycles of 1 min at 95°C, 2 min at 57-60°C, and 1.5 min at 72°C, then 25 cycles of 30 sec at 95°C, 1.5 min at 50-55°C, and 1.5 min at 72°C, then a final elongation of 5 min at 72°C before holding at 4°C; 2) Nested PCRs were carried out under the same conditions using 5 μ l of the corresponding pre-nested PCRs in a final reaction volume of 50 μ l. The PCR final products were cloned into the pGEM[®]-T Easy Vector System II (Promega, Madison, WI) following the supplier's procedures. The positive screened colonies contained the sequence of one individual DNA molecule. The plasmid DNA from the selected positive colonies containing vectors with the insert was purified using the Qiagen plasmid Mini Kit. The purified plasmids were sequenced in both directions using T7 and Sp6 primers. Twenty independent clones for each genomic preparation and fragment of interest were sequenced to determine the methylation pattern of individual molecules. Sequencing was carried out at the CEINGE Sequencing Core Facility (Naples, Italy).

Plasmid constructs and cell colony-forming assay. CBX7 expression plasmid was constructed by cloning the human cDNA sequence in a pCR[™]II TA Cloning[®] vector

(Invitrogen). The primers used were: CBX7 forward 5'-ATGGAGCTGTCAGCCATC-3' and CBX7 reverse 5'-TCAGAACTTCCCCTGCG-3'. The inserted cDNA was then subcloned into the *BamHI/XhoI* sites of the mammalian expression vector pcDNA 3.1 (Invitrogen). The expression of CBX7 was assessed by Western blotting. Cells, plated at a density of 90% in 100-mm dishes, were transfected with 5 µg pcDNA3.1 or pCBX7 and supplemented with geneticin (G418) 24 h later. Two weeks after the onset of drug selection, the cells were fixed and stained with crystal violet (0.1% crystal violet in 20% methanol).

Preparation of recombinant adenovirus and infection protocol. The recombinant adenovirus was constructed using AdEasyTM Vector System (Quantum Biotechnologies, Montreal, Quebec). The cDNA fragment was inserted in the sense orientation into the *NotI* and *HindIII* sites of the pShuttle-CMV vector to generate the recombinant pShuttle-CBX7-CMV construct. It was linearized and co-transformed through electroporation with pAdEasy-1, which carries the adenovirus genome, in BJ5183 electrocompetent cells. After homologous recombination, a recombinant AdEasy-CMV-CBX7 plasmid was generated (Ad-CBX7), which was then extracted and linearized. QBI-293A cells were transfected with different clones to produce different viral particles, and the infectivity of each clone was tested. Viral stocks were expanded in QBI-293A cells, which were harvested 36-40 h after infection and lysed. The virus titer of the 293 cells was determined. The adenovirus AdCMV-GFP (Quantum Biotechnologies) was used as control. Cells (5×10^4) were seeded in a six-well plate. After 24 h, cells were infected at MOI 100 with Ad-CBX7 or Ad-GFP for 90 min using 500 µl of infection medium (DMEM supplemented with 2%

FBS) at 37°C in a 5% CO₂ incubator. Pilot experiments with Ad-GFP were carried out to determine the optimal MOI for each cell line. At MOI 100, the cell lines became GFP-positive without manifesting toxicity. Infected cells were harvested and counted daily in a hemacytometric chamber.

ACKNOWLEDGEMENTS

This work was supported by grants from the Associazione Italiana Ricerca sul Cancro (AIRC), Progetto Strategico Oncologia Consiglio Nazionale delle Ricerche, the Ministero dell'Università e della Ricerca Scientifica e Tecnologica (MIUR), and “Piani di Potenziamento della Rete Scientifica e Tecnologica” CLUSTER C-04, the Programma Italia-USA sulla Terapia dei Tumori coordinated by Prof. Cesare Peschle, and “Ministero della Salute”. This work was supported from NOGEC-Naples Oncogenomic Center. We thank the Associazione Partenopea per le Ricerche Oncologiche (APRO) for its support. We are grateful to Jean Ann Gilder (Scientific Communication) for editing the text.

CONFLICT OF INTEREST

The authors have declared that no conflict of interest exists.

NONSTANDARD ABBREVIATIONS USED

ATC, anaplastic thyroid carcinoma; FNAB, fine-needle aspiration biopsy; FA, follicular adenoma; FTC, follicular thyroid carcinoma; G6PD, glucose-6-phosphate dehydrogenase; LOH, loss of heterozygosity; PTC, papillary thyroid carcinoma; qRT-PCR, quantitative RT-PCR; SNP, single nucleotide polymorphism; TCV, tall cell variant; Tg, thyroglobulin.

REFERENCES

1. Hedinger, C., Williams, E.D., and Sobin, L.H. 1989. The WHO Histological classification of thyroid tumours: a commentary on the second edition. *Cancer*. **63**:908-911.
2. Kondo, T., Ezzat, S., and Asa, S.L. 2006. Pathogenetic mechanisms in thyroid follicular-cell neoplasia. *Nat. Rev. Cancer*. **6**:292-306.
3. Nardone, H.C., et al. 2003. c-Met expression in tall cell variant papillary carcinoma of the thyroid. *Cancer*. **98**:1386-1393.
4. Xing, M. 2005. BRAF mutation in thyroid cancer. *Endocr. Relat. Cancer*. **12**:245-262.
5. Pierotti, M.A., and Greco, A. 2006. Oncogenic rearrangements of the NTRK1/NGF receptor. *Cancer Lett*. 2006. **232**:90-98.
6. Di Renzo, M.F., et al. 1992. Overexpression of the c-MET/HGF receptor gene in human thyroid carcinomas. *Oncogene*. **7**:2549-2553.
7. Suarez, H.G., et al. 1990. Presence of mutations in all three ras genes in human thyroid tumors. *Oncogene*. **5**:565-570.
8. Kroll, T.G., et al. 2000. PAX-8-PPARgamma1 fusion oncogene in human thyroid carcinoma. *Science*. **289**:1357-1360.
9. Ito, T., et al. 1992. Unique association of p53 mutations with undifferentiated but not differentiated carcinomas of the thyroid gland. *Cancer. Res*. **52**:1369-1371.
10. Donghi, R., et al. 1993. Gene p53 mutations are restricted to poorly differentiated and undifferentiated carcinomas of the thyroid gland. *J. Clin. Invest*. **91**:1753-1760.

11. Fagin, J.A., et al. 1993. High prevalence of mutations of p53 gene in poorly differentiated human thyroid carcinomas. *J. Clin. Invest.* **91**:179-184.
12. Paro, R., and Hogness, D.S. 1991. The Polycomb protein shares a homologous domain with a heterochromatin-associated protein of *Drosophila*. *Proc. Natl. Acad. Sci. U. S. A.* **88**: 263-267.
13. Gil, J., Bernard, D., Martinez, D., and Beach, D. 2004. Polycomb CBX7 has a unifying role in cellular lifespan. *Nat. Cell. Biol.* **6**:67-72.
14. Bernard, D., et al. 2005. CBX7 controls the growth of normal and tumor-derived prostate cells by repressing the Ink4a/Arf locus. *Oncogene.* **24**:5543-5551.
15. Bernstein, E., et al. 2006. Mouse polycomb proteins bind differentially to methylated histone H3 and RNA and are enriched in facultative heterochromatin. *Mol. Cell. Biol.* **26**:2560-2569.
16. Pallante, P., et al. 2005. UbcH10 overexpression may represent a marker of anaplastic thyroid carcinomas. *Br. J. Cancer.* **93**:464-471.
17. Wild, A., et al. 2002. Chromosome 22q in pancreatic endocrine tumors: identification of a homozygous deletion and potential prognostic associations of allelic deletions. *Eur. J. Endocrinol.* **147**:507-513.
18. Iida, A., et al. 1998. Mapping of a new target region of allelic loss to a 2-cM interval at 22q13.1 in primary breast cancer. *Genes Chromosomes Cancer.* **21**:108-112.
19. Allione, F., et al. 1998. Loss of heterozygosity at loci from chromosome arm 22Q in human sporadic breast carcinomas. *Int. J. Cancer.* **75**:181-186.
20. Fusco, A., et al. 1987. One- and two-step transformations of rat thyroid epithelial cells by retroviral oncogenes. *Mol. Cell. Biol.* **7**:3365-3370.

21. Ambesi-Impiombato, F.S., Parks, L.A., and Coon, H.G. 1980. Culture of hormonedependent functional epithelial cells from rat thyroids. *Proc. Natl. Acad. Sci. U. S. A.* **77**:3455-3459.
22. Berlingieri, M.T., et al. 1988. Cooperation between the polyomavirus middle-T-antigen gene and the human c-myc oncogene in a rat thyroid epithelial differentiated cell line: model of in vitro progression. *Mol. Cell. Biol.* **8**:2261-2266.
23. Berlingieri, M.T., et al. 1993. The Adenovirus E1A gene blocks the differentiation of a thyroid epithelial cell line, however the neoplastic phenotype is achieved only after cooperation with other oncogenes. *Oncogene.* **8**:249-255.
24. Santoro, M., et al. 1993. The TRK and RET tyrosine kinase oncogenes cooperate with ras in the neoplastic transformation of a rat thyroid epithelial cell line. *Cell. Growth. Differ.* **4**:77-84.
25. Fusco, A., et al. 1985. A mos oncogene-containing retrovirus, myeloproliferative sarcoma virus, transforms rat thyroid epithelial cells and irreversibly blocks their differentiation pattern. *J. Virol.* **56**:284-292.
26. Berlingieri, M.T., et al. 2002. Thyroid cell transformation requires the expression of the HMGA1 proteins. *Oncogene.* **21**:2971-2980.
27. Berlingieri, M.T., et al. 1995. Inhibition of HMGI-C protein synthesis suppresses retrovirally induced neoplastic transformation of rat thyroid cells. *Mol. Cell. Biol.* **15**:1545-1553.
28. Russell, J.P., et al. 2000. The TRK-T1 fusion protein induces neoplastic transformation of thyroid epithelium. *Oncogene.* **19**:5729-5735.

29. Powell, D.J. Jr., et al. 1998. The RET/PTC3 oncogene: metastatic solid-type papillary carcinomas in murine thyroids. *Cancer Res.* **58**:5523-5528.
30. Vitagliano, D., et al. 2006. Thyroid targeting of the N-ras(Gln61Lys)oncogene in transgenic mice results in follicular tumors that progress to poorly differentiated carcinomas. *Oncogene*. In press.
31. Ledent, C., Dumont, J., Vassart, G., and Parmentier, M. 1991. Thyroid adenocarcinomas secondary to tissue-specific expression of simian virus-40 large T-antigen in transgenic mice. *Endocrinology*. **129**:1391-1401.
32. Yeh, M.W., Demircan, O., Ituarte, P., and Clark, O.H. 2004. False-negative fine-needle aspiration cytology results delay treatment and adversely affect outcome in patients with thyroid carcinoma. *Thyroid*. **14**:207-215.
33. Segev, D.L., Clark, D.P., Zeiger, M.A., and Umbricht, C. 2003. Beyond the suspicious thyroid fine needle aspirate. A review. *Acta Cytol.* **47**:709-722.
34. Richter, H., et al. 2004. Chromosomal imbalances in post-chernobyl thyroid tumors. *Thyroid*. **14**:1061-1064.
35. Curcio, F., Ambesi-Impiombato, F.S., Perrella, G., and Coon, H.G. 1994. Long-term culture and functional characterization of follicular cells from adult normal human thyroids. *Proc. Natl. Acad. Sci. U. S. A.* **91**:9004-9008.
36. Obika, S., et al. 1997. Synthesis of 2'-O,4'-C methyleneuridine and cytidine. Novel bicyclic Nucleosides Having a Fixed C3-endo Sugar Puckering. *Tetrahedron Lett.* **38**:8735-8738.
37. Koshkin, A.A., et al. 1998. LNA (Locked nucleic acids): synthesis of the adenine, cytosine, guanine, 5-methylcytosine, thymine and uracil bicyclonucleoside monomers,

- oligomerisation and unprecedented nucleic acid recognition. *Tetrahedron*. **54**:3607–3630.
38. Mouritzen, P., et al. 2004. The ProbeLibrary™ - Expression profiling 99% of all human genes using only 90 dual-labeled real-time PCR Probes. *Biotechniques*, **37**:492-495.
39. Mouritzen, P., et al. 2005. ProbeLibrary™ - Expression profiling 99% of all human genes using only 90 dual-labeled 2005. ProbeLibrary: A new method for faster design and execution of quantitative real-time PCR. *Nat. Methods*. **2**:313-317.
40. Livak, K.J., and Schmittgen, T.D. 2001. Analysis of relative gene expression data using real-time quantitative PCR and the $2^{-\Delta\Delta CT}$ method. *Methods*. **25**:402-408.
41. Zeppa, P., et al. 1990. Fine needle aspiration of medullary thyroid carcinoma: a review of 18 cases. *Cytopathology*. **1**:35-44.
42. Troncone, G., et al. 2000. Cyclin-dependent kinase inhibitor p27(Kip1) expression in thyroid cells obtained by fineneedle aspiration biopsy: a preliminary report. *Diagn. Cytopathol*. **23**:77-81.

FIGURE LEGENDS

Figure 1. CBX7 expression in human thyroid carcinoma cell lines. (A) CBX7 gene expression by microarray analysis in human thyroid carcinoma cell lines vs normal human thyroid primary culture cells (NTPC). Avg. Diff, average difference: it is a quantitative relative indicator of a transcript expression level ($\sum(\text{PM-MM})/\text{pairs}$ on average). (B) CBX7 gene expression analysis by RT-PCR in human thyroid carcinoma cell lines vs the normal human thyroid primary culture cells (NTPC). β -actin gene expression served as loading control.

Figure 2. CBX7 staining in normal and neoplastic thyroid tissues. CBX7 nuclear staining was intense in benign follicular epithelial cells of normal thyroid (A) and of follicular adenoma (B), whereas it was weak in follicular carcinoma (C). CBX7 progressively decreased going from well-differentiated “classic variant” papillary (D) carcinomas to the “tall cell variant” of PTC (E), to poorly differentiated (F, G) and anaplastic (H) carcinomas. The signal disappeared after incubation of the sample with antigen (I). Sample showed in the G panel is the same of F, but magnified, to better show cell nuclei. Arrows with letters indicate the following sample features: (*P*→) nuclei showing cytological features of PTC negative for CBX7 expression; (*F*→) FTC nuclei negative for CBX7 expression; (*L*→) lymphocyte showing CBX7 expression and providing positive internal control; (*E*→) endothelial cells showing CBX7 expression and providing positive internal control.

Figure 3. CBX7 expression in fresh thyroid tumor samples from patients. (A) RT-PCR analysis of CBX7 expression in human thyroid tumor samples vs their normal thyroid counterparts. β -actin expression served as loading control. NT, normal thyroid tissue; PTC1 to PTC6, papillary thyroid carcinomas from different patients; ATC1 to ATC5, anaplastic thyroid carcinomas from different patients. (B) qRT-PCR analysis of human thyroid tumor samples of different histotypes. The fold change indicates the relative change in expression levels between tumor samples and normal samples, assuming that the value of each normal sample is equal to 1.

Figure 4. Immunocytochemistry (A, B) and qRT-PCR (C) analyses of CBX7 of fine needle aspiration biopsies (FNAB), whose PTC pre-operative cytological diagnosis was histologically proven. FNAB goiter samples were used as controls. The fold change indicates the relative change in expression levels between tumor and goiter samples, assuming that the value of the normal sample was equal to 1. FNAB 1 to 8, from different patients.

Figure 5. Methylation analysis of the CBX7 gene. The structure of CBX7 is shown in the upper panel. The transcriptional start site is indicated as +1. The positions of the CpG islands and of the primers used for bisulfate analysis are indicated. The first part of the upstream portion of CpG island 1 (-84 to +155) and the CpG island 2 (+7031 to +7170) were unmethylated in normal, tumor tissues and in the tumoral cell line TPC1. Lower panel, methylation of the first intron (21 CpG sites): two anaplastic tumors (43T and 107T), one papillary tumor (10T) and its corresponding normal tissue (10N) are shown. The

degree of methylation is reported as the percentage of m-C obtained for each CpG dimer on a total of 20 independent clones analyzed (see Methods).

Figure 6. CBX7 expression in experimental models of thyroid carcinogenesis. (A) CBX7 expression by RT-PCR in rat thyroid cells transformed by several oncogenes. GAPDH gene expression was evaluated as control to normalize the amount of the used RNAs. (B) CBX7 expression by qRT-PCR in thyroid carcinomas developing in transgenic mice expressing RET-PTC-3, TRK, N-ras and large T SV40 oncogenes. The fold change indicates the relative change in expression levels between tumor samples and normal samples, assuming that the value of each normal sample is equal to 1.

Figure 7. Colony-forming assay with CBX7 transfection in several thyroid carcinoma cell lines. NPA, FB-2 and TPC-1 cells were transfected with a vector expressing CBX7 cDNA and its corresponding empty vector pcDNA3.1. Cells were selected for resistance to G418 and clones were stained and counted after 14 days.

Figure 8. Inhibitory effects of Ad-CBX7 infection on the growth of human thyroid carcinoma cell lines. (A) The cell lines indicated were infected with Ad-CBX7 or Ad-GFP (control adenovirus) at MOI 100 and counted daily. Representative curves of three independent experiments are reported. (B) CBX7 protein expression was assessed 48 h after infection with Ad-CBX7 at MOI 100 by western blot with an anti CBX7 antibody. Blot against γ -tubulin is to demonstrate an equal protein loading.

Table 1. CBX7 expression in normal and neoplastic thyroid tissues by IHC.

<i>Histotype</i>	<i>Cases</i>	<i>CBX7 expression</i> ^a			
		<i>High</i>		<i>Low</i>	
Normal Thyroid Parenchyma	n=20	100%	(20/20)	0%	(0/20)
Follicular Adenomas	n=20	100%	(20/20)	0%	(0/20)
Follicular Carcinomas	n=32	34%	(11/32)	66%	(21/32)
Papillary Carcinomas - Classic Variant	n=30	43%	(13/30)	57%	(17/30)
Papillary Carcinomas - Tall Cell Variant	n=6	17%	(1/6)	83%	(5/6)
Poorly Differentiated Carcinomas	n=12	17%	(2/12)	83%	(10/12)
Anaplastic Carcinomas	n=12	0%	(0/12)	100%	(12/12)

^a*High* : cases with more than 50% of neoplastic cells showing CBX7 staining; *Low* : cases with less than 50% of neoplastic cells showing CBX7 staining.

Table 2. Loh frequency statistics at CBX7 locus (22q13.1) by SNP sequencing method.

<i>Histotype</i>	<i>Cases</i>	<i>(Inf^a)</i>	<i>LOH^b</i>
Papillary Carcinoma- Classic Variant	n=36	(19)	36.8% (7/19)
Papillary Carcinoma- Tall Cell Variant	n=6	(4)	75% (3/4)
Follicular Carcinomas	n=5	(3)	66.6% (2/3)
Anaplastic Carcinomas	n=20	(16)	68.7% (11/16)

^a*Inf*: informative cases are samples showing SNP heterozygosity corresponding to two peaks (two alleles) on the sequencing chromatogram.

^bThe LOH frequency is equal to the ratio between allelic loss and informative cases.

Figure 1

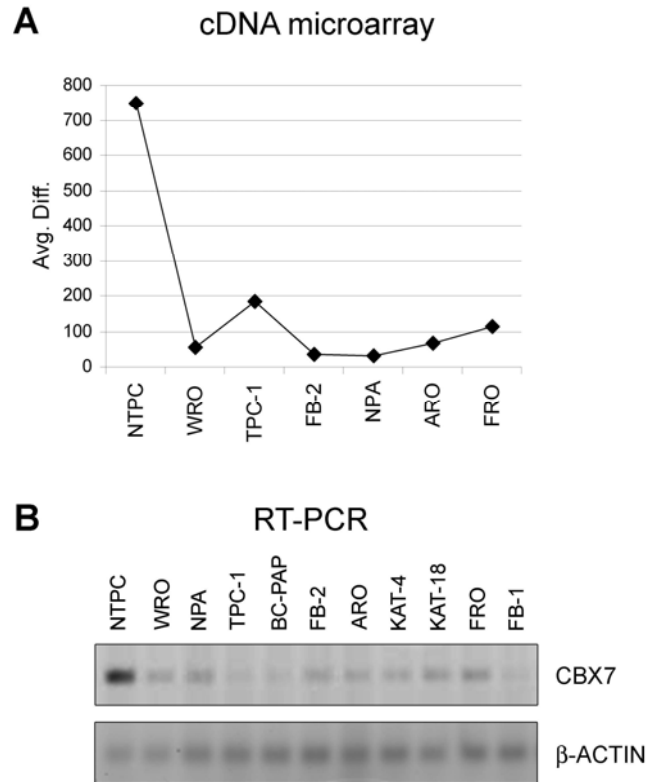


Figure 2

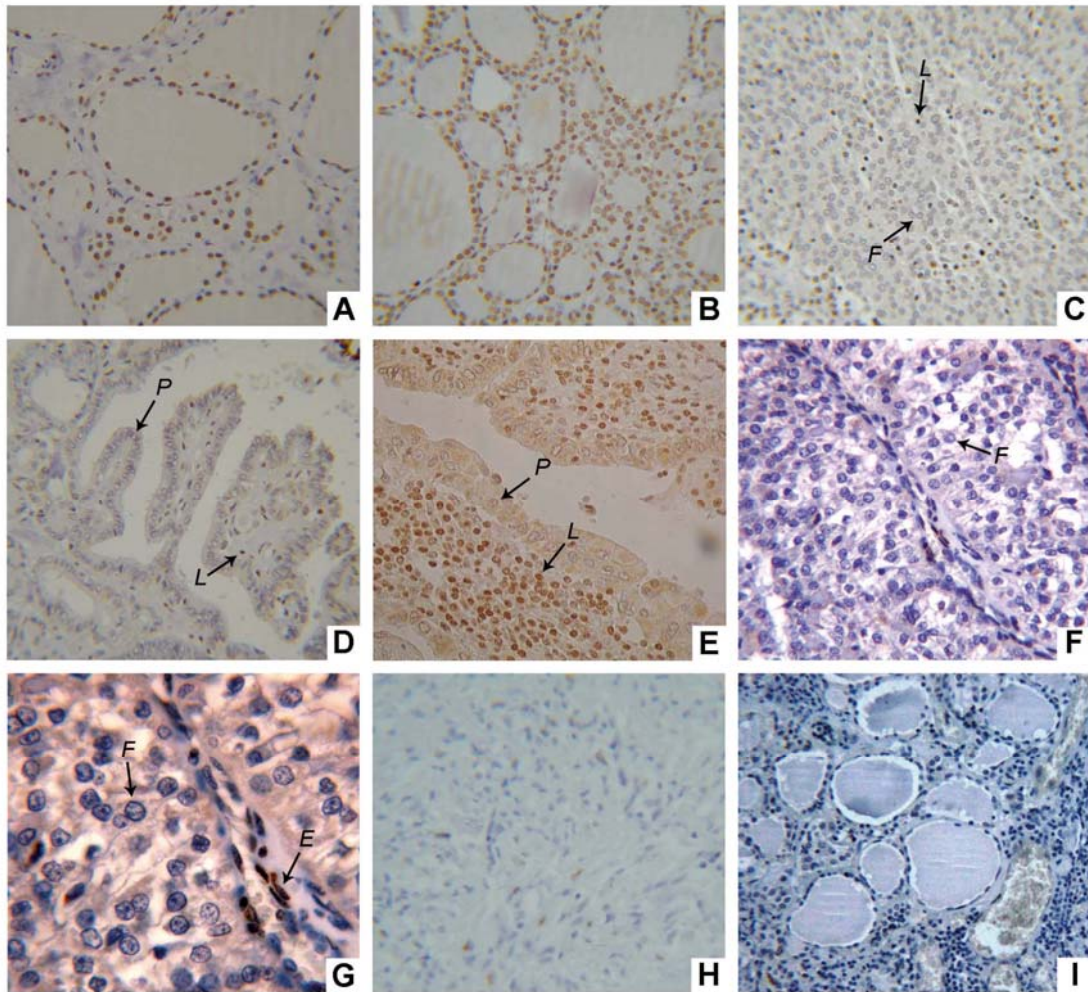


Figure 4

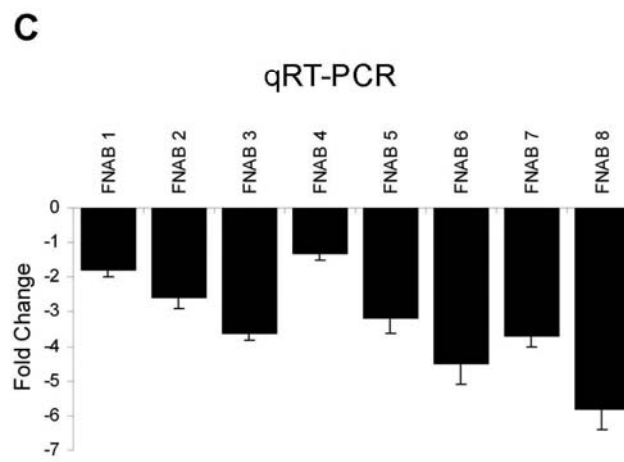
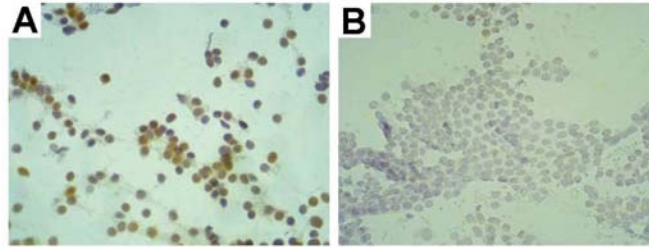


Figure 5

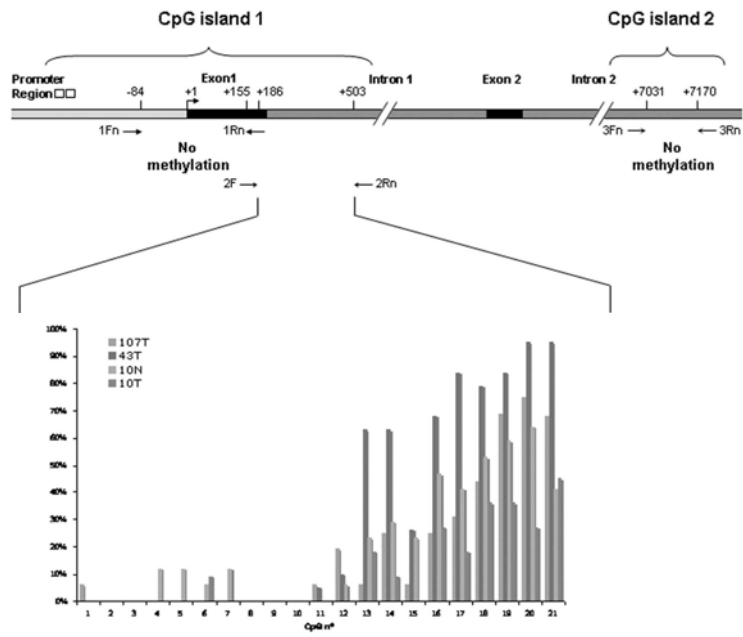
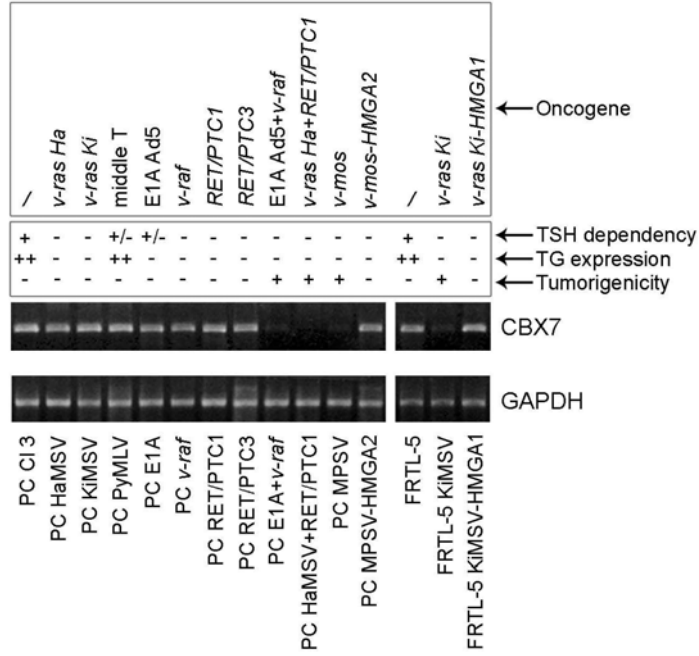


Figure 6

A



B

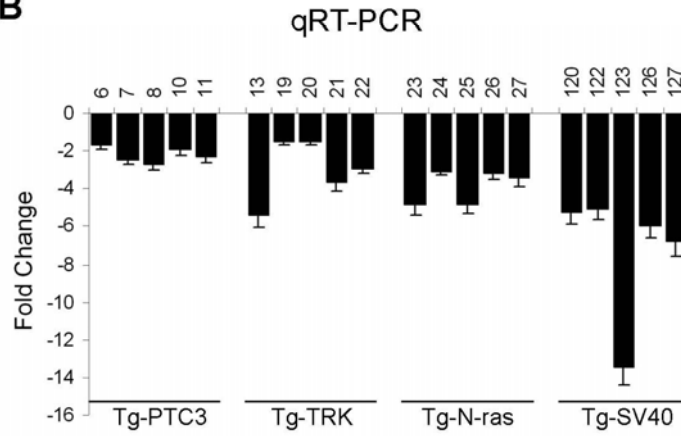


Figure 7

Colony Assay

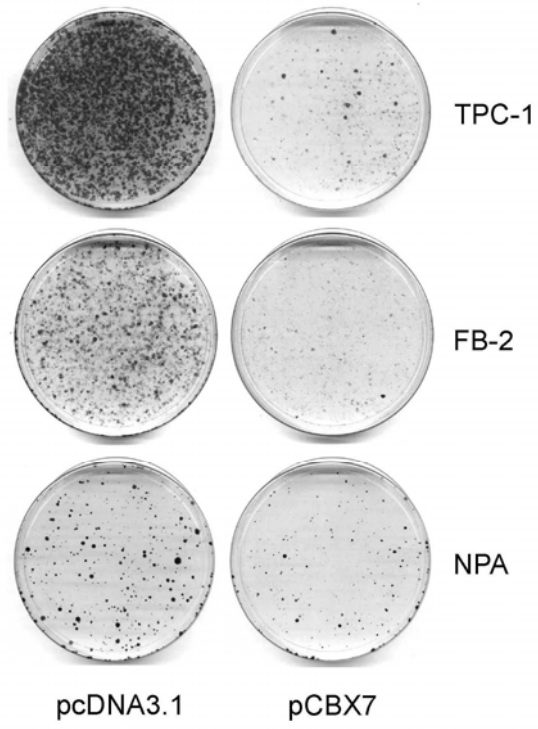
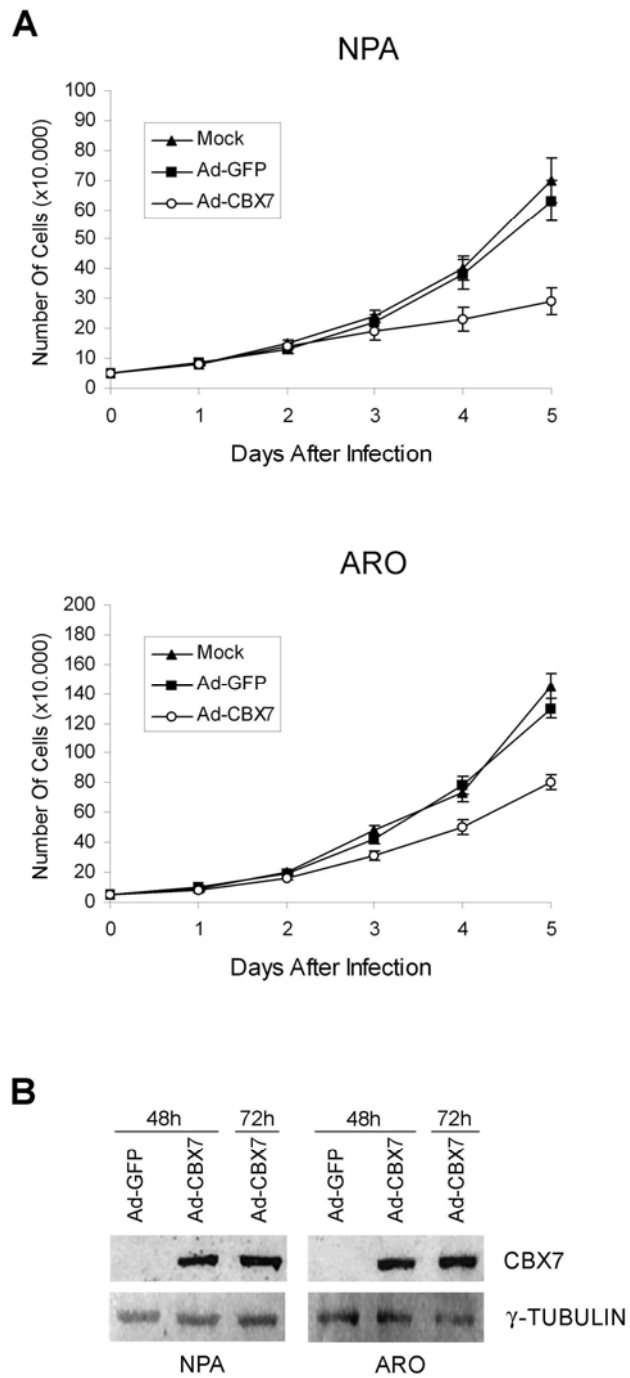


Figure 8



Transcriptional profile of Ki-Ras-induced transformation of thyroid cells

Roberta Visconti¹, Antonella Federico^{1,2}, Valeria Coppola¹, Francesca Pentimalli¹, Maria Teresa Berlingieri¹, Pierlorenzo Pallante¹, Mogens Kruhoffer³, Torben F. Orntoft³ and Alfredo Fusco^{1,2}.

¹Dipartimento di Biologia e Patologia Cellulare e Molecolare “L. Califano”, Università degli Studi di Napoli “Federico II” e/o Istituto di Endocrinologia e Oncologia Sperimentale “G. Salvatore” del CNR, Napoli, Italy; ²NOGEC (Naples Oncogenomic Center) - CEINGE, Biotecnologie Avanzate S.C.ar.l., Napoli, Italy; ³Department of Clinical Biochemistry, Aarhus University Hospital, Aarhus, Denmark.

Abbreviated title= Ki-Ras-regulated genes in thyroid tumors

Key words= Ras, thyroid, cancer

Word count= 3335

Number of figures= 5

Corresponding author: Alfredo Fusco, CEINGE, Biotecnologie Avanzate S.C.ar.l., Via Comunale Margherita 482, 80145 Napoli, Italy. Tel.: +39 (081) 3722857; Fax +39 (081) 3722808; E-mail: afusco@napoli.com

Reprint requests to: Alfredo Fusco, CEINGE, Biotecnologie Avanzate S.C.ar.l., Via Comunale Margherita 482, 80145 Napoli, Italy.

This study was supported by AIRC (Associazione Italiana per la Ricerca sul Cancro) and by MIUR (Ministero dell'Istruzione, dell'Università e della Ricerca). We thank APRO (Associazione Partenopea per le Ricerche Oncologiche) for its support.

ABSTRACT

In the last years, an increasing number of experiments has provided compelling evidence for a casual role of Ras protein mutations, resulting in their constitutive activation, in thyroid carcinogenesis. However, despite the clear involvement of Ras proteins in thyroid carcinogenesis, the nature of most of the target genes, whose expression is modulated by the Ras-induced signaling pathways and that are ultimately responsible for Ras-induced cellular transformation, remains largely unknown. To analyze Ras-dependent modulation of gene expression in thyroid cells we took advantage of a differentiated rat thyroid cell line, FRTL-5. As a model for Ras-dependent thyroid transformation, we used FRTL-5 cells infected with the Kirsten murine sarcoma virus, carrying the *v-Ki-Ras* oncogene. The infected cells (FRTL-5 *v-Ki-Ras*) have lost expression of the thyroid differentiation markers and are also completely transformed. We hybridized two different Affimetrix chips containing probe sets interrogating both known rat genes and ESTs for a total of more than 17,000 sequences using mRNA extracted from FRTL-5 and FRTL-5 *v-Ki-Ras* cell lines. We identified about 1,000 genes whose expression was induced and about 1,500 genes whose expression was downregulated more than two fold by Ras. We confirmed the differential expression of many of these genes in FRTL-5 *v-Ki-Ras* as compared to parental cells by using alternative techniques. Remarkably, we investigated the expression of some of the Ras-regulated genes in human thyroid carcinoma cell lines and tumor samples, our results, therefore, providing a new molecular profile of the genes involved in thyroid neoplastic transformation.

INTRODUCTION

Thyroid cancer is the most common form of endocrine malignancy, causing significant morbidity and mortality (1). Still, risk factors for this form of tumor are relatively debated; however, exposure to ionizing radiation, especially in childhood, is a well-established cause of thyroid carcinogenesis in humans (2). In fact, head, neck, or thorax irradiation administered in childhood to treat diseases such as lymphoid hyperplasia of the tonsils or enlarged thymus gland or radiation exposure during the atomic explosions in Japan increased the risk of developing thyroid tumors (3, 4). Finally, in the last fifteen years, the frequency of thyroid carcinomas is dramatically increased in the population exposed to the massive release of radionuclides that followed the explosion of the nuclear reactor in Chernobyl (2).

Besides their clinical relevance, thyroid tumors have been deeply investigated also because they represent an excellent multi-stage model for epithelial tumor progression. In fact, thyroid neoplasms comprise a broad spectrum of malignancies with different phenotypic characteristics and a variable biological and clinical behavior: from the benign adenomas through the slowly progressive differentiated papillary and follicular carcinomas to the invariably fatal anaplastic carcinomas (1). The several studies on thyroid tumors have allowed the identification of many genetic alterations. Thus, mutations of the TSH receptor and of the α subunit of the adenylate cyclase stimulatory protein $G\alpha_s$ have been described in hyperfunctioning adenomas (5, 6). Studies on papillary thyroid carcinomas revealed that the prevalence of chromosomal rearrangements leading to oncogene formations is quite high in tumors of such histotype, the rearrangements being, indeed, more common in tumors associated with radiation exposure (7). In about 40% of papillary thyroid carcinomas the kinase domain of the tyrosine kinase receptor c-Ret is fused with the N-terminal

region of heterologous genes (8). Moreover, rearrangements of the NTRK1 gene, coding for the nerve growth factor receptor, have been described in about 10% of papillary carcinomas (9). Furthermore, a common feature of both sporadic and radiation-induced papillary thyroid carcinomas is the activation of the serine-threonine kinase BRAF. Interestingly, the molecular mechanisms causing activation of the BRAF kinase activity is different in sporadic versus post-Chernobyl tumors, BRAF being activated by point mutation in sporadic tumors and by rearrangements in radiation-induced tumors (10, 11). In addition, p53 mutations have been frequently observed in undifferentiated thyroid carcinomas (12-14). Finally, mutations of the Ras proteins, resulting in their constitutive activation, have been found in a high percentage of follicular and anaplastic carcinomas (15, 16). Of note, such Ras mutations have been found in very early malignancies and in benign tumors (17), thereby suggesting a very high sensitivity of the thyroid to Ras-induced transformation. Indeed, besides epidemiological data, *in vitro* gene transfer experiments have provided compelling evidence for a casual role of Ras mutations in thyroid carcinogenesis. Introduction of mutated Ras into normal adult human thyroid follicular cells results in fact in a dramatic stimulation of cell proliferation (18). Moreover, it has been demonstrated that infection of normal rat thyroid cells with the Kirsten murine sarcoma virus carrying the *v-Ki-Ras* oncogene results in the loss of the differentiated functions and in the acquisition of a completely transformed phenotype, the cells being able to grow in soft agar and to cause tumors when injected in athymic mice (19). A role for Ras mutations in thyroid carcinogenesis has been demonstrated also *in vivo*. It has been in fact shown that the injection of the Kirsten murine sarcoma virus into the thyroid gland of adult Fischer rats induces thyroid carcinomas when the

animals are treated with a goitrogenic agent (20). Finally, transgenic mice expressing the Ki-Ras oncogene in the thyroid do develop tumors (21).

Mutations in Ras proteins have been described not only in thyroid neoplasias but also in a wide variety of tumors, Ras being, indeed, one of the dominantly acting oncogenes most frequently implicated in human cancer (22). The evidences for a causative role of Ras mutations in the process of carcinogenesis are persuasive in all the cell types and tissues examined so far. Still, the molecular mechanisms of Ras-dependent cellular transformation have remained elusive.

The four human Ras genes (R-, Ha-, Ki- and N-Ras) code for 21-kD proteins that function as GDP/GTP molecular switches (23). They are located at the inner surface of the plasma membrane downstream of growth factor receptors and, upon activation, control a cytoplasmic cascade of kinases, including the extracellular-regulated protein kinases (Erks) (23). In turn, the kinases regulate the activity of several nuclear transcription factors, ultimately controlling the expression of specific target genes (24). Thus, Ras proteins are crucial for converting growth-promoting signals into specific changes in gene expression. Indeed, activation of the Ras-induced signaling pathways appears to be central for the proliferative response to many growth factors, and, upon Ras mutation, the persistent activation of most of these signaling routes is sufficient for transformation. However, the nature of most of the target genes, whose expression is modulated by the Ras downstream effectors and that are ultimately responsible for Ras-induced cellular transformation, remains largely unknown. Thus, we have used the powerful oligonucleotide microarray hybridization technique to analyze Ras-dependent modulation of gene expression in thyroid cells. We identified about 1,000 genes whose expression is induced and about 1,500 genes whose expression is downregulated more than twofold by Ras. We confirmed the expression

of some of the Ras-regulated genes in human thyroid carcinoma cell lines and tumor samples, these data providing new molecular basis for understanding the biological properties of thyroid cancer and the mechanisms of Ras-induced cellular transformation.

MATERIALS AND METHODS

Cell culture. FRTL-5 and PC C13 are thyroid epithelial cell lines derived from 3- to 4-weeks and from 18-month-old Fisher rats, respectively (25, 26). FRTL-5 *v-Ki-Ras*, PC C13 *v-mos*, PC C13 *v-raf*, PC C13 E1A, PC C13 E1A *v-raf* cell lines have been described (26, 19, 27). All rat thyroid cell lines were cultured in Coon's modified Ham's F12 medium supplemented with 5% calf serum (Gibco Laboratories). Normal, but not virally infected, FRTL-5 and PC C13 cells required six growth factors (1×10^{-10} M TSH, 10 μ g/ml insulin, 1×10^{-8} M hydrocortisone, 5 μ g/ml human transferrin, 10ng/ml somatostatin, 10ng/ml glycyl-L-histidyl-L-lysine acetate).

The human thyroid carcinoma cell lines studied were: WRO (28), FB-2 (29), NPA (30), TPC-1 (31), B-CPAP (32), FRO (14) and ARO (30). They were grown in Dulbecco's Modified Eagle's Medium containing 10% fetal bovine serum (Gibco Laboratories).

Tissue samples and RNA preparation. Samples of thyroid cancer tissues and of the corresponding adjacent noncancerous thyroid tissues were obtained from patients that underwent thyroidectomy. Samples were immediately snap-frozen in liquid nitrogen. A pathologist determined histological classification according to WHO's classification. Total RNAs were extracted from tissues and cell culture using TRI REAGENT method, following the instructions of Molecular Research Center, Inc.

High-density oligonucleotide microarray analysis. cRNA was prepared from total RNA, hybridized to Affimetrix oligonucleotide arrays (containing rat transcripts), scanned and analyzed according to Affimetrix (Santa Clara, CA) protocols. Scanned

image files were visually inspected for artifacts and normalized by using GENECHIP3.3 software (Affimetrix). Comparisons were made for the transformed sample versus the wild-type sample, taking the wild type as baseline, by using GENECHIP3.3. The fold-change values, indicating the relative change in the expression levels between the Ras-transformed sample and the wild-type sample, were used to identify genes differentially expressed between these conditions.

Semiquantitative RT-PCR. RT-PCR was performed with Applied Biosystems reagents. 500ng of DNase I (Invitrogen)-treated total RNA from FRTL-5 and FRTL-5 *v-Ki-Ras* were reverse-transcribed in single-stranded cDNA in a 20 μ l reaction containing 5mM MgCl₂, PCR buffer 1X (500mM KCl, 100mM Tris-HCl, pH 8.3), dNTPs 1mM each, a mixture of 2.5mM random examers, 1U/ μ l RNase Inhibitor, 2.5U/ μ l Murine Leukemia Virus Reverse Transcriptase. To ensure that RNA samples were not contaminated with DNA, negative controls were obtained by performing PCR on samples that were not reverse-transcribed but otherwise identically processed. The cDNAs were then amplified by PCR in a 25 μ l reaction tube containing 1mM MgCl₂, PCR buffer 0.8X, 100ng of each primer, 0.25U/ μ l AmpliTaq DNA Polymerase. In the co-amplification experiments, the gene of interest and the β -actin gene were amplified using a 6:1 ratio of the respective primers. The PCR products were separated on a 2% agarose gel, stained with ethidium bromide and scanned using a Typhoon 9200 scanner. Digitized data were analyzed using Imagequant (Molecular Dynamics). The primers sequences are available upon request.

RESULTS

Identification of genes regulated by Ki-Ras in thyroid cells. To identify the genes regulated by Ras oncogenes in thyroid cells, we took advantage of a rat thyroid cell line, FRTL-5, expressing all the markers of thyroid differentiation (i.e., they express thyroglobulin and TSH-R, they trap iodide and are dependent on TSH for growth). We have previously demonstrated that the same cells infected with a retrovirus carrying the *v-Ki-Ras* oncogene (FRTL-5 *v-Ki-Ras*) not only lost all the markers of thyroid differentiation but were also completely transformed as they were able to grow in soft agar and to cause tumors when injected in nude mice (19). To identify genes regulated by *v-Ki-Ras* in thyroid cells, RNA was extracted from FRTL-5 and FRTL-5 *v-Ki-Ras* and utilized for hybridizing a set of high-density synthetic oligonucleotide array capable of analyzing about 17,000 rat genes and expressed sequence tags (ESTs). The expression profile of the Ras-transformed cells was compared with that of the wild-type FRTL-5 cells that were used as a common reference (33). We applied an arbitrary filter level of twofold change in the ratios of gene expression. Figure 1A shows the number of transcripts increased or decreased in the Ras-transformed cells. For practical reasons, we downsized the list to those genes that showed a tenfold change of expression and ended up with a list of about 100 genes. Figure 1B shows a list of these genes and their accession numbers. To assess the predictive value of the microarray analysis, we first looked at the genes already known to be differentially regulated in FRTL-5 *v-Ki-Ras* versus wild type cells. As expected, all the markers of thyroid differentiation resulted to be highly downregulated in FRTL-5 *v-Ki-Ras* versus FRTL-5 (data not shown). Remarkably, Ki-Ras gene expression resulted highly upregulated in FRTL-5 *v-Ki-Ras* cells

compared to FRTL-5 (data not shown), further confirming the high quality of the gene expression profile analysis.

Validation of the microarray analysis. To validate the expression changes detected by the oligonucleotide array, we analyzed the mRNA levels of some of the genes more significantly regulated in FRTL5 *v-Ki-Ras* cells using an alternative technique, i.e. semiquantitative RT-PCR. All the genes that resulted highly up or downregulated in the microarray analysis were confirmed to be expressed at higher or lower levels, respectively, in FTL5 *v-Ki-Ras* cells versus the wild type cells by RT-PCR. Although the precise magnitude of change in expression was not always recapitulated, both the direction and the order of magnitude of change predicted by the array were confirmed by the RT-PCR experiments. Some representative RT-PCR analyses are shown in figures 2A and 2B.

Analysis of the Ras-dependent genes in different rat transformed cell systems. To investigate the expression of the Ras-dependent genes in another cellular system, we took advantage of a different rat thyroid cell line, PC Cl3, expressing the thyroid differentiation markers (i.e. thyrotropin-dependency, ability to trap iodide, thyroglobulin synthesis and secretion) (19). We have previously demonstrated that infection with the *v-mos* oncogene confer to the PC Cl3 cells the typical markers of neoplastic transformation, the PC Cl3 *v-mos* cells being able to grow in soft agar and to induce tumors after injection into athymic mice. We analyzed, by semiquantitative RT-PCR, the expression of a Ras-dependent gene, RalA, in PC Cl3 and PC Cl3 *v-mos* cells. As shown in figure 3A, RalA gene was highly upregulated in transformed cells as compared to the wild-type PC Cl3 cells. To further investigate the expression of the RalA gene, we took advantage of other cell lines available in our laboratory, 10

representing a good model of multistep malignant progression. In fact, we have previously demonstrated that the infection with the E1A or the *v-raf* oncogenes completely de-differentiated PC Cl3 cells but still the cells were unable to grow in soft agar or to induce tumors in athymic mice (19). On the other hand, the cooperation of the two oncogenes completely transformed the PC Cl3 cells (27). As shown in figure 3B, RalA was not induced in PC Cl3 E1A cells compared to the parental PC Cl3 cells. Interestingly, however, it was induced in both PC Cl3 *v-raf* and in PC Cl3 E1A *v-raf* cells, this strongly suggesting that RalA expression is upregulated not only by Ras but also by its downstream effector Raf.

Analysis of the Ras-dependent genes in human thyroid carcinoma cell lines. Next, we investigate by RT-PCR the expression of the identified Ras-regulated genes in seven thyroid carcinoma cell lines. These cell lines are representative of human thyroid tumors of different histotypes: in fact, one (WRO) is derived from a follicular carcinoma, four (FB-2, NPA, TPC-1 and B-CPAP) are derived from papillary carcinomas and two (FRO and ARO) are derived from anaplastic carcinomas. Figure 4A shows the levels of five different Ras-induced genes. Annexin A2 and RalA, two genes whose expression was induced by Ras in rat thyroid cells, were, as expected, upregulated in all seven carcinoma cell lines. Ehd4 and Ler3 were induced in all but two carcinomas cell lines while Prxx1 was induced only in the NPA cell line. We next verified in the human thyroid carcinoma cell lines the expression of Dusp1 and CD24, two genes whose expression was downregulated by Ras in rat thyroid cells. As shown in figure 4B, both genes were significantly downregulated in all the human thyroid carcinoma cell lines analyzed. Remarkably, the expression of CD24 was completely undetectable in four out of the seven carcinoma cell lines.

Analysis of the Ras-dependent genes in human thyroid carcinomas. To further analyze the expression of Ras-regulated genes in human thyroid tumors, we analyzed by RT-PCR human carcinomas of different histotypes. In all the experiments the expression of the Ras-regulated genes in the carcinoma samples was compared to the expression of the same gene in the normal tissue obtained from the same patient. As shown in figure 5A, Annexin A2, RalA and Ler3, three Ras-induced genes, were significantly upregulated in the vast majority of the tumor samples. Accordingly, as shown in figure 5B, the expression of Dusp1, whose expression was reduced in the tumoral cell lines analyzed, was downregulated in a great fraction of the thyroid carcinomas analyzed when compared with normal tissue. Remarkably, the expression of CD24, whose expression was undetectable in most of the thyroid carcinoma cell lines analyzed, resulted strongly downregulated in all the anaplastic thyroid tumor samples investigated.

DISCUSSION

In this study, we have globally analyzed gene expression of Ras transformed thyroid cells to reveal characteristic changes in gene expression associated with carcinogenesis in thyroid cells. We have focused our attention on thyroid cells transformed by Ras as several data provided by us as well by other laboratories have shown the clear involvement of this protein in thyroid neoplastic transformation.

To begin the analysis of our data, it should be observed that all the established marker genes of normal thyroid cells, such as thyroglobulin and TSH receptor, were found to be severely downregulated in *v-Ki-Ras* transformed cells, reflecting their less differentiated state.

Moreover, as described previously, even by setting a tenfold threshold of induction or downregulation in transformed versus wild type cells, the number of genes whose expression is modulated by Ras is quite high. Most of these genes could be sort out in two main groups: 1) genes already correlated to a tumor phenotype, even though not always in the thyroid, or, conversely, 2) novel or known genes never correlated to any tumor phenotype. Among the genes already described as modulated in cancer and found by our analysis as regulated by Ras, CD24, coding for a small heavily glycosylated glycosylphosphatidylinositol-linked cell surface protein, appears to be particularly interesting. We have, in fact data showing that CD24 expression is undetectable in most of the carcinoma cell lines analyzed and is greatly downregulated only and in all the anaplastic carcinomas we have analyzed. This data is not in accordance with most of the literature about CD24 expression in cancer. In fact, high levels of CD24 expression detected by immunohistochemistry have been found in epithelial ovarian, breast, non-small cell lung, prostate and pancreatic cancer (34). With the exception of pancreatic cancer, high rates of CD24 are significantly

associated with a bad prognosis (34). As CD24 is a ligand of the adhesion receptor P-selectin (35), it has been hypothesized that its overexpression on cancer cells might enhance their metastatic potential. Thus, our finding that CD24 is downregulated only in thyroid carcinomas of anaplastic histotype is in conflict with the other data available in literature suggesting CD24 as marker for the most aggressive forms of cancer. Hence, studies aimed at the evaluation of CD24 expression in a larger tumor collection of anaplastic thyroid carcinomas are currently ongoing in our laboratory.

As discussed above, among the genes found as Ras-regulated in our screening, many have never been globally analyzed in human tumor samples. Among them, the interferon-induced mRNA, a gene whose expression is downregulated in FRTL-5 *v-Ki-Ras* cells when compared to the parental cells, is particularly of interest. Although not shown in this paper, we have preliminary results demonstrating that the human homolog of interferon-induced mRNA is severely downregulated in many thyroid tumors. This is particularly intriguing: as the gene has been cloned because greatly induced by the interferons, potent antiproliferative cytokines (36), it could be hypothesized a role for the interferon-induced mRNA as tumor suppressor. Remarkably, interferon-induced mRNA has been found as severely downregulated also in mouse fibroblasts and rat ovarian cells transformed by Ras (37, 38). The physiological function of this gene as well as its role in Ras-mediated transformation will warrant further investigations.

Despite the key role in tumorigenesis, few studies have assessed the gene expression profile of cells transformed by mutated Ras proteins. It has been reported the gene expression pattern of mast cells expressing a Ras oncogene (39) and of transformed fibroblasts expressing mutant H-Ras, Ki-Ras and N-Ras genes (37). However, both mast cells and fibroblasts are not the ideal cell systems to investigate the effects of

Ras genetic alterations, as the epithelial cells are predominantly affected by Ras mutations that cause in this case carcinomas. Only recently a study addressing the transcriptome profiling of a rat cell culture model of ovarian epithelial cells transformed by the Ki-Ras oncogene has been published (38). By subtractive suppression hybridizations the authors recovered genes encoding negative and positive regulators of cellular transformation, survival, angiogenesis and invasiveness, not verifying, however, the expression of the genes modulated by Ras in human tumors. Conversely, in this study, we have shown that some of the genes identified by the microarray analysis as modulated by Ras in cell lines are overexpressed or downregulated in human tumors as well. Moreover, relevantly, the expression of the Ras modulated genes was verified in thyroid tumors, where the prevalence of Ras mutations is quite high. Thus, we expect that some of these genes, once systematically analyzed in a large spectrum of thyroid tumors, could provide useful markers for the diagnosis and prognosis of the thyroid tumors as well potential targets for the development of new, improved therapeutic drugs.

In summary, using a microarray approach, we have detected more than 100 genes whose expression is modulated more than tenfold by Ki-Ras in rat thyroid cells. More relevantly, we have shown that there is complete concordance among the results obtained in rat thyroid cells, in human thyroid carcinoma cell lines and in human tumor samples. Thus, the genes identified as modulated by Ras in rat cells provide a wealth of data that will be opportune to investigate further in human tumors.

REFERENCES

1. **Hedinger C, Williams ED, Sobin LH** 1989 The WHO histological classification of thyroid tumors: a commentary on the second edition. *Cancer* 63:908-911
2. **Williams D** 2002 Cancer after nuclear fallout: lessons from the Chernobyl accident. *Nat Rev Cancer* 2:543-549
3. **Maxon HR, Thomas SR, Saenger EL, Buncher CR, Kereiakes JG** 1977 Ionizing irradiation and the induction of clinically significant disease in the human thyroid gland. *Am J Med* 63:967-978
4. **Takeichi N, Ezaki H, Dohi K** 1991 A review of forty-five years study of Hiroshima and Nagasaki atomic bomb survivors. Thyroid cancer: reports up to date and a review. *J Radiat Res* 32 Suppl:180-188
5. **Parma J, Duprez L, Van Sande J, Cochaux P, Gervy C, Mockel J, Dumont J, Vassart G** 1993 Somatic mutations in the thyrotropin receptor gene cause hyperfunctioning thyroid adenomas. *Nature* 365:649-651
6. **O'Sullivan C, Barton CM, Staddon SL, Brown CL, Lemoine NR** 1991 Activating point mutations of the *gsp* oncogene in human thyroid adenomas. *Mol Carcinog* 4:345-349

7. **Nikiforov YE** 2002 RET/PTC rearrangement in thyroid tumors. *Endocr Pathol* 13:3-16
8. **Santoro M, Melillo RM, Carlomagno F, Fusco A, Vecchio G** 2002 Molecular mechanisms of RET activation in human cancer. *Ann N Y Acad Sci* 963:116-121
9. **Pierotti MA, Bongarzone I, Borrello MG, Mariani C, Miranda C, Sozzi G, Greco A** 1995 Rearrangements of TRK proto-oncogene in papillary thyroid carcinomas. *J Endocrinol Invest* 18:130-133
10. **Kimura ET, Nikiforova MN, Zhu Z, Knauf JA, Nikiforov YE, Fagin JA** 2003 High prevalence of BRAF mutations in thyroid cancer: genetic evidence for constitutive activation of the RET/PTC-RAS-BRAF signaling pathway in papillary thyroid carcinoma. *Cancer Res* 63:1454-1457
11. **Ciampi R, Knauf JA, Kerler R, Gandhi M, Zhu Z, Nikiforova MN, Rabes HM, Fagin JA, Nikiforov YE** 2005 Oncogenic AKAP9-BRAF fusion is a novel mechanism of MAPK pathway activation in thyroid cancer. *J Clin Invest* 115:94-101
12. **Ito T, Seyama T, Mizuno T, Tsuyama N, Hayashi T, Hayashi Y, Dohi K, Nakamura N, Akiyama M** 1992 Unique association of p53 mutations with undifferentiated but not with differentiated carcinomas of the thyroid gland. *Cancer Res* 52:1369-1371

13. **Donghi R, Longoni A, Pilotti S, Michieli P, Della Porta G, Pierotti MA**
1993 Gene p53 mutations are restricted to poorly differentiated and undifferentiated carcinomas of the thyroid gland. *J Clin Invest* 91:1753-1760

14. **Fagin JA, Matsuo K, Karmakar A, Chen DL, Tang SH, Koeffler HP** 1993
High prevalence of mutations of the p53 gene in poorly differentiated human thyroid carcinomas. *J Clin Invest* 91:179-184

15. **Lemoine NR, Mayall ES, Wyllie FS, Williams ED, Goyns M, Stringer B, Wynford-Thomas D** 1989 High frequency of ras oncogene activation in all stages of human thyroid tumorigenesis. *Oncogene* 4:159-164

16. **Namba H, Rubin SA, Fagin JA** 1990 Point mutations of ras oncogenes are an early event in thyroid tumorigenesis. *Mol Endocrinol* 4:1474-1479

17. **Vasko V, Ferrand M, Di Cristofaro J, Carayon P, Henry JF, de Micco C**
2003 Specific pattern of RAS oncogene mutations in follicular thyroid tumors. *J Clin Endocrinol Metab* 88:2745-2752

18. **Lemoine NR, Staddon S, Bond J, Wyllie FS, Shaw JJ, Wynford-Thomas D** 1990 Partial transformation of human thyroid epithelial cells by mutant Ha-ras oncogene. *Oncogene* 5:1833-1837

19. **Fusco A, Berlingieri MT, Di Fiore PP, Portella G, Grieco M, Vecchio G** 1987 One- and two-step transformations of rat thyroid epithelial cells by retroviral oncogenes. *Mol Cell Biol* 7:3365-3370

20. **Portella G, Ferulano G, Santoro M, Grieco M, Fusco A, Vecchio G** 1989 The Kirsten murine sarcoma virus induces rat thyroid carcinomas in vivo. *Oncogene* 4:181-188

21. **Santelli G, de Franciscis V, Portella G, Chiappetta G, D'Alessio A, Califano D, Rosati R, Mineo A, Monaco C, Manzo G et al** 1993 Production of transgenic mice expressing the Ki-ras oncogene under the control of a thyroglobulin promoter. *Cancer Res* 53:5523-5527

22. **Bos JL** 1990 ras oncogenes in human cancer: a review. *Cancer Res* 49:4682-4689. Erratum in: 1990 *Cancer Res* 50:1352

23. **Campbell SL, Khosravi-Far R, Rossman KL, Clark GJ, Der CJ** 1998 Increasing complexity of Ras signaling. *Oncogene* 17:1395-1413

24. **Treisman R** 1996 Regulation of transcription by MAP kinase cascades. *Curr Opin Cell Biol* 8:205-215

25. **Ambesi-Impiombato FS, Parks LA, Coon HG** 1980 Culture of hormone-dependent functional epithelial cells from rat thyroids. *Proc Natl Acad Sci USA* 77:3455-3459

26. **Fusco A, Portella G, Di Fiore PP, Berlingieri MT, Di Lauro R, Schneider AB, Vecchio G** 1985 A mouse oncogene-containing retrovirus, myeloproliferative sarcoma virus, transforms rat thyroid epithelial cells and irreversibly blocks their differentiation pattern. *J Virol* 56:284-292
27. **Berlingieri MT, Santoro M, Battaglia C, Grieco M, Fusco A** 1993 The Adenovirus E1A gene blocks the differentiation of a thyroid epithelial cell line, however the neoplastic phenotype is achieved only after cooperation with other oncogenes. *Oncogene* 8:249-255
28. **Estour B, Van Herle AJ, Juillard GJ, Totanes TL, Sparkes RS, Giuliano AE, Klandorf H** 1989 Characterization of a human follicular thyroid carcinoma cell line (UCLA RO 82 W-1). *Virchows Arch B Cell Pathol Incl Mol Pathol* 57:167-174
29. **Basolo F, Giannini R, Toniolo A, Casalone R, Nikiforova M, Pacini F, Elisei R, Miccoli P, Berti P, Faviana P, Fiore L, Monaco C, Pierantoni GM, Fedele M, Nikiforov YE, Santoro M, Fusco A** 2002 Establishment of a non-tumorigenic papillary thyroid cell line (FB-2) carrying the RET/PTC1 rearrangement. *Int J Cancer* 97:608-614
30. **Pang XP, Hershman JM, Chung M, Pekary AE** 1989 Characterization of tumor necrosis factor-alpha receptors in human and rat thyroid cells and regulation of the receptors by thyrotropin. *Endocrinology* 125:1783-1788

31. **Tanaka J, Ogura T, Sato H, Hatano M** 1987 Establishment and biological characterization of an in vitro human cytomegalovirus latency model. *Virology* 161:62-72

32. **Fabien N, Fusco A, Santoro M, Barbier Y, Dubois PM, Paulin C** 1994 Description of a human papillary thyroid carcinoma cell line. Morphologic study and expression of tumoral markers. *Cancer* 73:2206-2212

33. **Grewal A, Conway A** 2000 Tools for analyzing microarray expression data. *Journal of Lab Automation* 5:62-64

34. **Kristiansen G, Sammar M, Altevogt P** 2004 Tumour biological aspects of CD24, a mucin-like adhesion molecule. *J Mol Histol* 35:255-262

35. **Aigner S, Sthoeger ZM, Fogel M, Weber E, Zarn J, Ruppert M, Zeller Y, Vestweber D, Stahel R, Sammar M, Altevogt P** 1997 CD24, a mucin-type glycoprotein, is a ligand for P-selectin on human tumor cells. *Blood* 89:3385-3395

36. **Deblandre GA, Marinx OP, Evans SS, Majjaj S, Leo O, Caput D, Huez GA, Wathelet MG** 1995 Expression cloning of an interferon-inducible 17-kDa membrane protein implicated in the control of cell growth. *J Biol Chem* 270:23860-23866

37. **Zuber J, Tchernitsa OI, Hinzmann B, Schmitz AC, Grips M, Hellriegel M, Sers C, Rosenthal A, Schafer R** 2000 A genome-wide survey of RAS transformation targets. *Nat Genet* 24:144-152
38. **Tchernitsa OI, Sers C, Zuber J, Hinzmann B, Grips M, Schramme A, Lund P, Schwendel A, Rosenthal A, Schafer R** 2004 Transcriptional basis of KRAS oncogene-mediated cellular transformation in ovarian epithelial cells. *Oncogene* 23:4536-4555
39. **Brem R, Certa U, Neeb M, Nair AP, Moroni C** 2001 Global analysis of differential gene expression after transformation with the v-H-ras oncogene in a murine tumor model. *Oncogene* 20:2854-2858. Erratum in: 2001 *Oncogene* 20:4916

LEGENDS TO FIGURES

Figure 1: Changes of gene expression in FRTL-5 and FRTL-5 *v-Ki-Ras* cells.

A) Scatter plot of changes of gene expression in FRTL-5 and FRTL-5 *v-Ki-Ras* cells. For each gene, the RNA expression level in the wild type cells is given on the X axis and the expression level for the same gene in the transformed cells is plotted on the Y axis. The upper and lower boundaries represent a twofold difference.

B) List of the genes, identified by their accession numbers, up and downregulated more than tenfold in FRTL-5 *v-Ki-Ras* vs. FRTL-5 cells.

Figure 2: RT-PCR verification of genes differentially expressed in FRTL-5 *v-Ki-Ras* transformed cells compared to wild type cells.

A) RT-PCR verification of genes upregulated in FRTL-5 *v-Ki-Ras* cells. Total RNA isolated from the indicated cell lines was retrotranscribed in presence or absence of the reverse transcriptase enzyme (RT). The cDNAs were analyzed for the expression of the designated genes by PCR. The reaction products were electrophoresed and images of the ethidium bromide stained gels are shown. β -actin was used as a control for the amount of RNAs. β -actin was either amplified at the same time and in the same conditions of the investigated genes (upper panel) or co-amplified with the RNA of interest (lower panel). In the last two lanes the negative control, lacking RNA, is showed.

B) RT-PCR verification of genes downregulated in FRTL-5 *v-Ki-Ras* cells. Total RNA isolated from the indicated cell lines was retrotranscribed in presence or absence of the reverse transcriptase enzyme (RT). The cDNAs were analyzed for the expression of the designated genes by PCR. The reaction products were electrophoresed and images of the ethidium bromide stained gels are shown. β -actin

was used as a control for the amount of RNAs. In the last two lanes the negative control, lacking RNA, is showed.

Figure 3: RalA gene expression is upregulated in thyroid cells infected with retroviruses carrying the *v-mos* and *v-raf* oncogenes.

A and B) Total RNA isolated from the indicated cell lines was retrotranscribed in presence or absence of the reverse transcriptase enzyme (RT). The cDNAs were analyzed for the expression of RalA by PCR. The reaction products were electrophoresed and images of the ethidium bromide stained gels are shown. β -actin, co-amplificated in the same reaction tube with RalA, was used as a control for the amount of RNAs. In the last two lanes the negative control, lacking RNA, is showed.

Figure 4: RNA levels of selected genes in human thyroid cell lines.

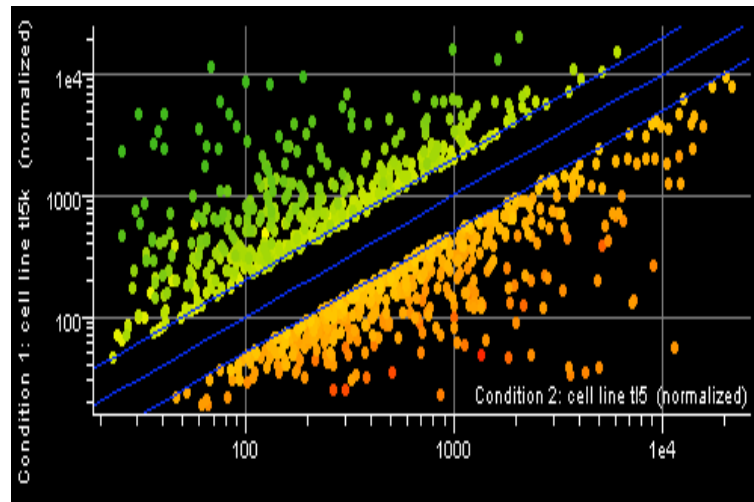
A and B) Total RNA isolated from the indicated cell lines was retrotranscribed in presence or absence of the reverse transcriptase enzyme (RT). The cDNAs were analyzed for the expression of the designated genes by PCR. The reaction products were electrophoresed and images of the ethidium bromide stained gels are shown. β -actin, co-amplificated in the same reaction tube with the genes of interest, was used as a control for the amount of RNAs. In the last two lanes the negative controls, lacking RNA, are showed.

The bar-graph quantification is showed under each ethidium bromide gel, with the exception of Ler-3 gene which levels of expression were undetectable in the normal thyroid. The expression levels of the genes of interest were normalized with respect to that of normal thyroid, whose value was arbitrarily taken as 1. β -actin levels were used to normalize the expression of the genes of interest to the RNA levels.

Figure 5: RNA levels of selected genes in human thyroid tumors.

A and B) Bar-graph quantification of the expression of selected genes verified by RT-PCR as described previously. The expression levels of the genes of interest in the tumor samples were normalized with respect to that of normal tissue. On each bar is indicated the histotype of the tumor sample: Ad= follicular adenoma; P= papillary carcinoma; A= anaplastic carcinoma.

A



B

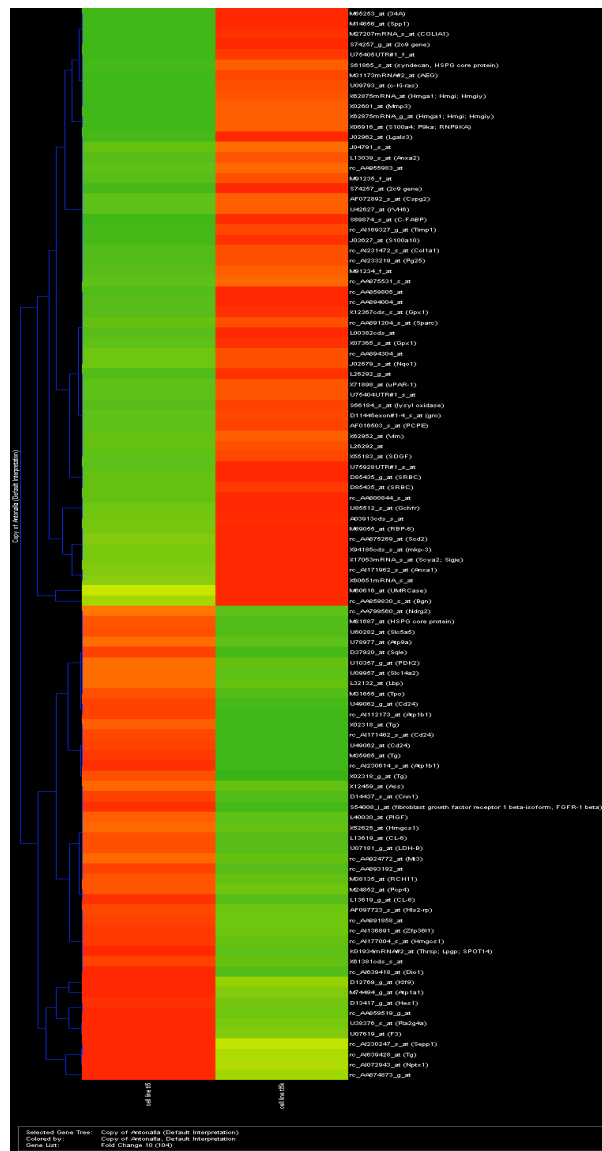


Figure 1

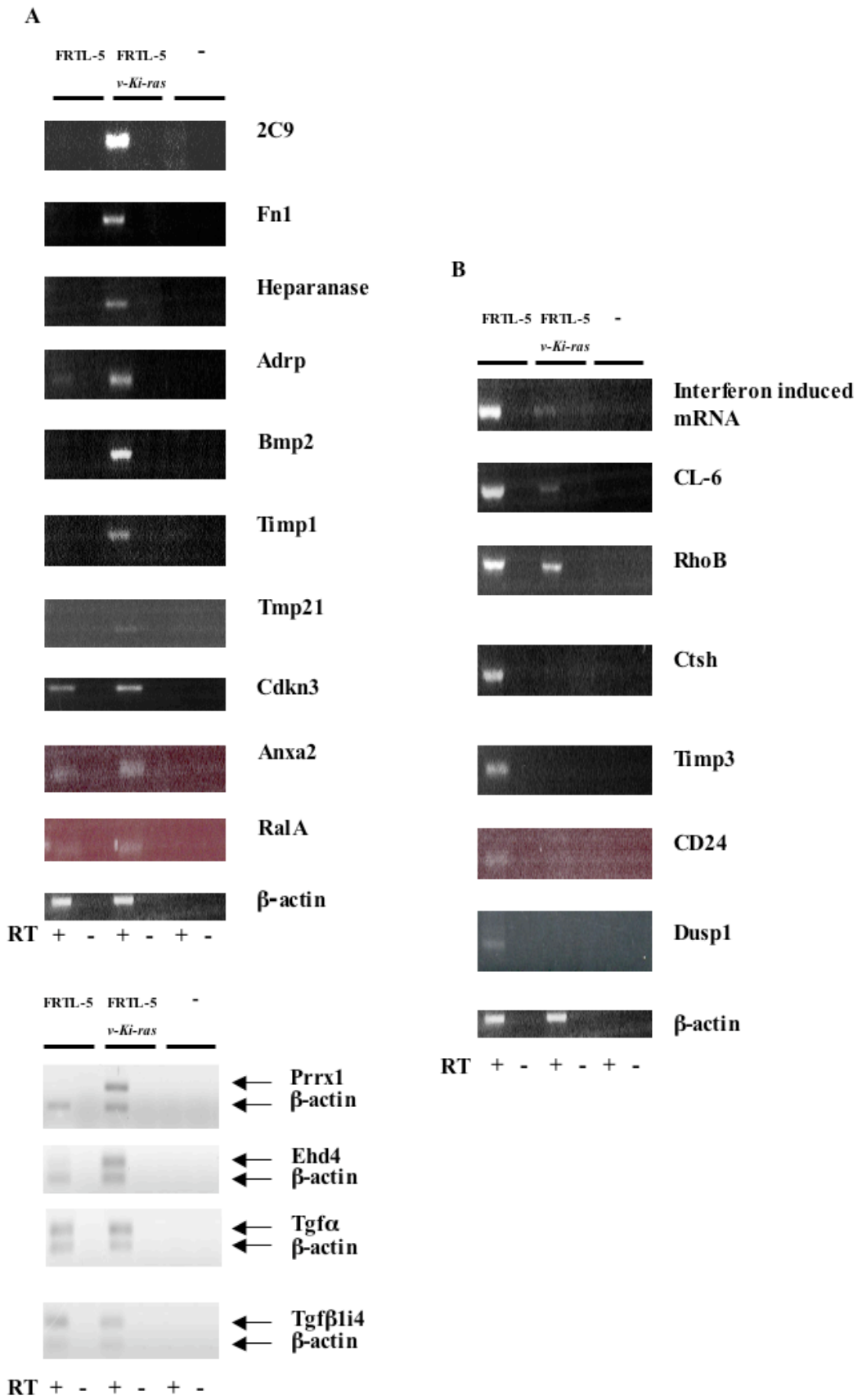
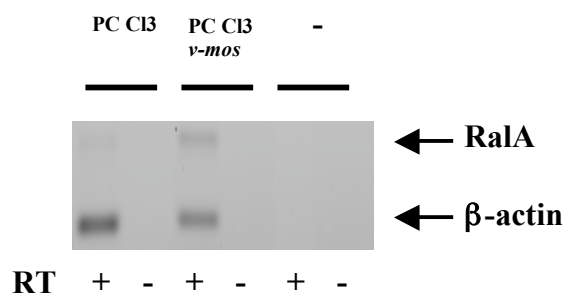


Figure 2
27

A



B

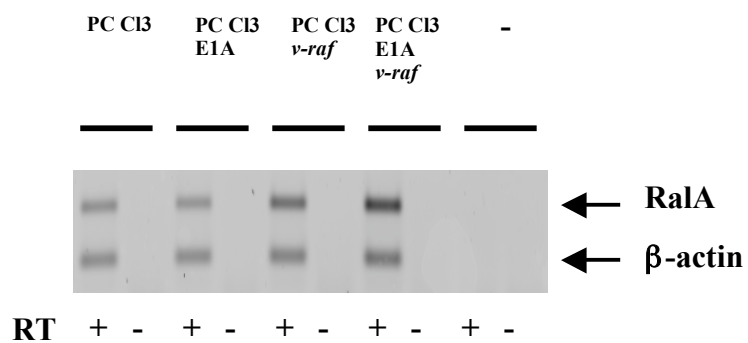


Figure 3

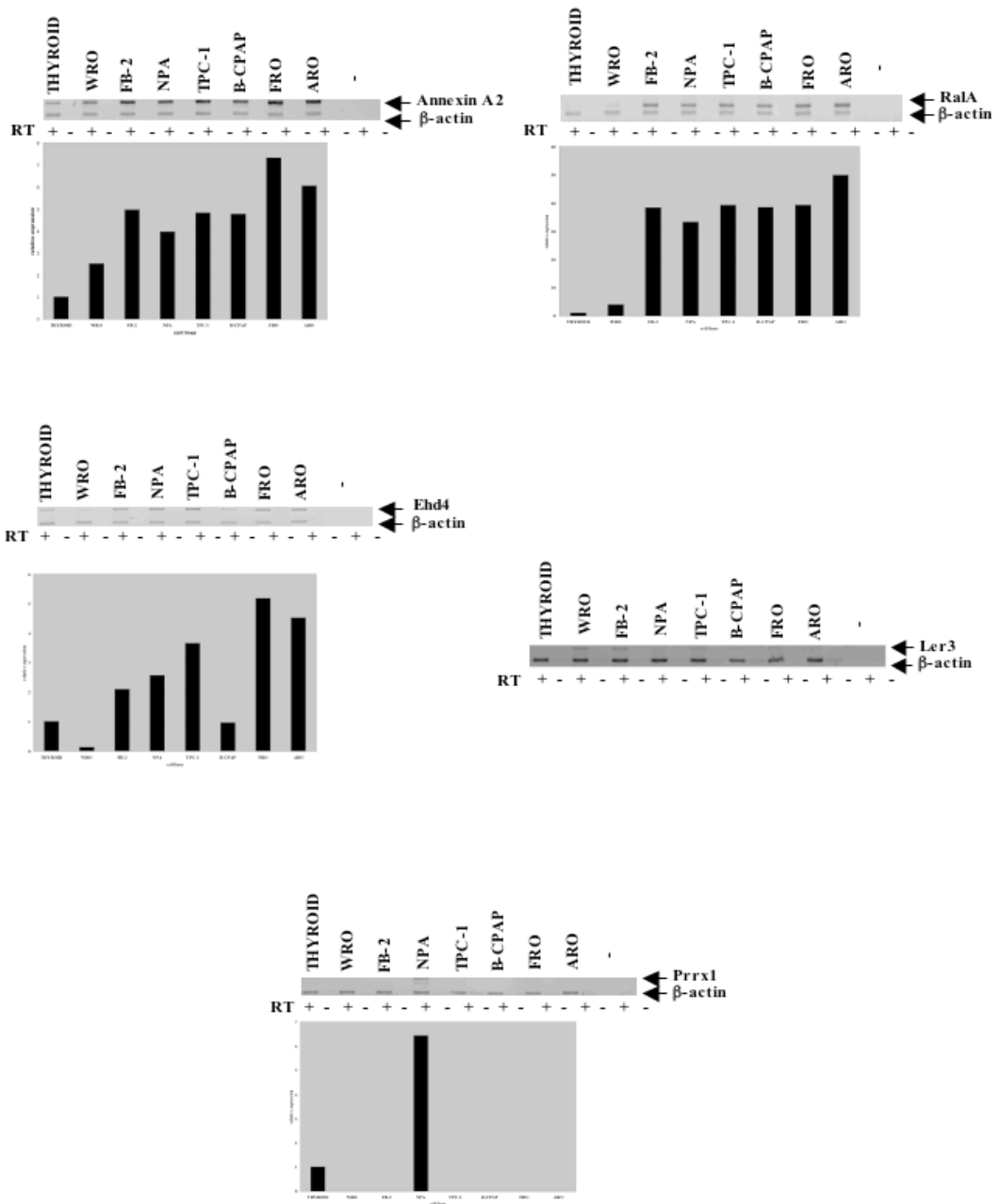


Figure 4A

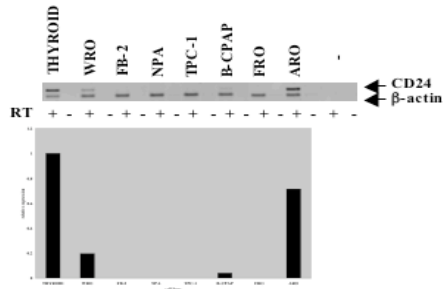
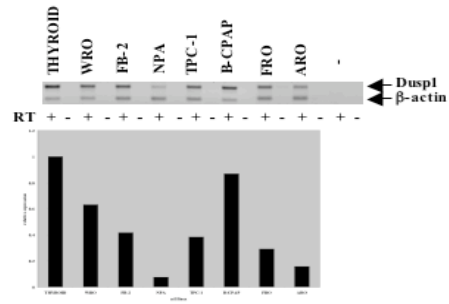
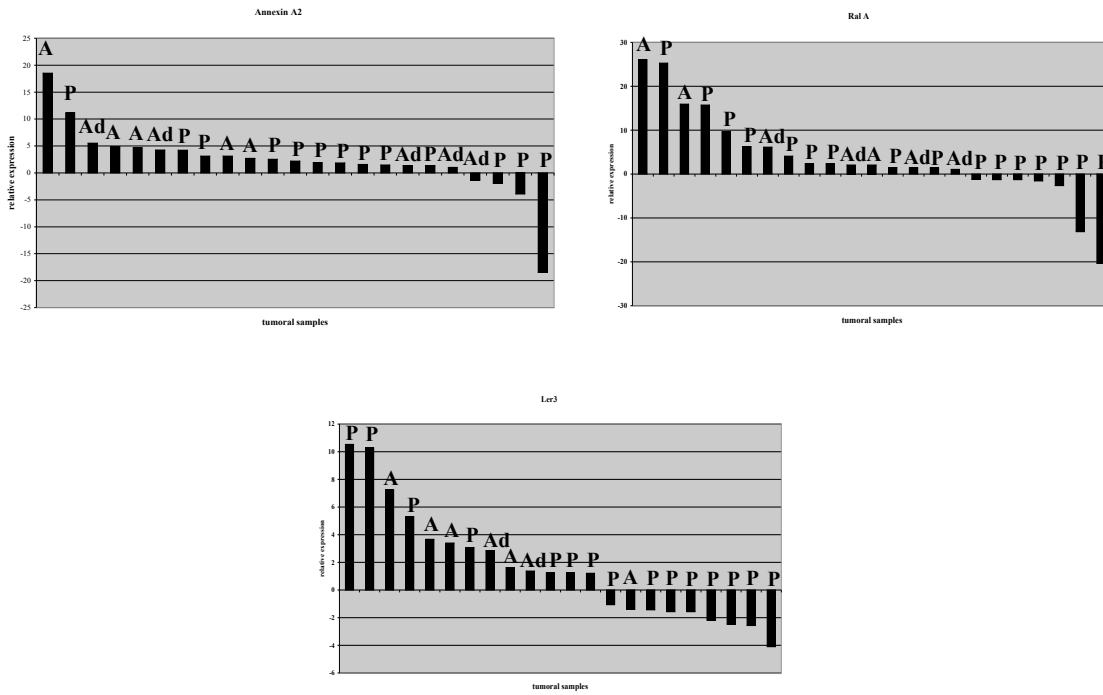


Figure 4B

A



B

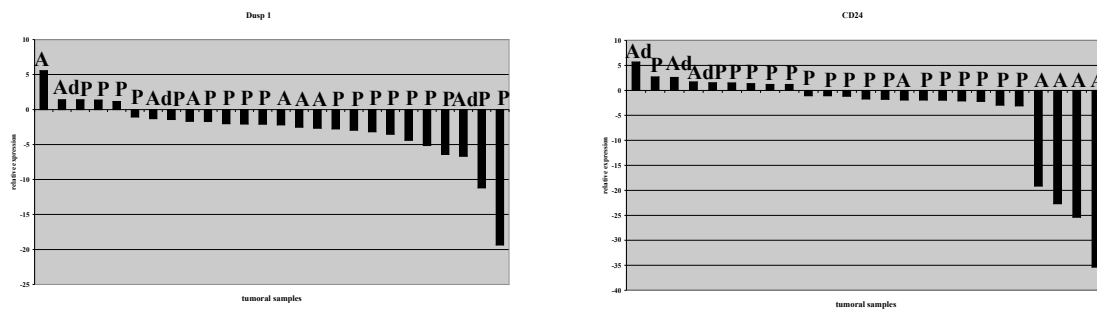


Figure 5